**Fibroblast Growth Factor-21 (FGF21) in Domestic Cats**

by

Emily Jeanne Brinker

A dissertation submitted to the Graduate Faculty of
Auburn University
in partial fulfillment of the
requirements for the Degree of
Doctor of Philosophy

Auburn, Alabama
May 6, 2023

Keywords: cats, fibroblast growth factor 21, insulin resistance, dyslipidemias, animals, body weight



Approved by

Emily Graff, Chair, Associate Professor of Pathobiology
Robert Judd, Department Head and Professor of Anatomy, Physiology and Pharmacology
Russell Cattley, Professor Emeritus of Pathobiology
Maninder Sandey, Assistant Professor of Pathology
Jey Koehler, Associate Professor of Pathobiology

Abstract

Fibroblast growth factors (FGFs) are a group of structurally homologous yet functionally pleiotropic proteins. Unlike canonical and intracellular FGFs, the FGF19 subfamily, which includes FGF15/19, FGF21, and FGF23, act as endocrine hormones that regulate phosphate, bile acid, and metabolic homeostasis, respectively. Research in human and rodent models demonstrates the potential of these endocrine FGFs to treat various diseases. Data from studies evaluating the metabolic effects of FGF21 pathway activation show improved lipid homeostasis and insulin sensitivity, decreased severity of non-alcoholic steatohepatitis, and potential use as a therapeutic for pancreatitis. Even though cats commonly suffer from metabolic diseases, including obesity, pancreatitis and hepatic lipidosis, there are no studies evaluating FGF21 in cats and only rare studies in other non-laboratory domestic species. This dissertation serves as the first exploration of FGF21 in domestic cats and probes how the FGF21 pathway can be utilized as a future therapy in veterinary medicine.

Chapter 1 of this dissertation reviews the endocrine FGF family, focusing on the physiology and current research. FGF19/FGF15 serves as a mechanism of bile homeostasis. FGF23, a bone-derived hormone, regulates urinary phosphate retention and active vitamin D levels. FGF21, the main focus of this dissertation, is an endocrine link between the liver and adipose tissue, regulating metabolic homeostasis. This literature review further discusses what is known about FGF21 within domestic animals and veterinary medicine.

Chapter 2 is a prospective preliminary cross-sectional study utilizing purpose-bred, male-neutered, 6-year-old, obese and overweight cats administered either a recombinant human FGF21 mimetic modified for increased thermal and confirmational stability or saline control over a 14-day treatment period. Treatment with FGF21 resulted in significant weight loss

(~5.93%) compared to control and a trend toward decreased intrahepatic triglyceride content. Cats treated with FGF21 had reduced serum alkaline phosphatase. No significant changes were noted in liver elasticity, serum, liver, metabolic parameters, or gut microbiome composition. This chapter demonstrates that in obese and overweight cats, activation of the FGF21 pathway can safely induce weight loss with trends to improve liver lipid content. Manipulation of the FGF21 pathway has promising potential as a therapeutic for feline obesity. Further studies are needed to see if FGF21 pathway manipulation can be therapeutic for feline metabolic disease.

Chapter 3 explores the FGF21 pathway utilizing banked feline tissues in clinically normal and selected diseased cats. This study evaluated the distribution of transcript and protein expression of FGF21, and its co-receptors, Fibroblast Growth Factor Receptor 1c and β-klotho in key tissues. Relative to the lowest expressing tissue, the highest expression of FGF21 was in the liver, with strong and consistent immunohistochemical reactivity in formalin-fixed paraffin-embedded liver sections. Contrary to other species, FGF21 is not highly expressed in adipose tissues despite the presence of FGF21 co-receptors. This chapter proposes that the retention of the FGF21 endocrine pathway and the loss of the FGF21 autocrine/paracrine pathway in the adipose tissues may be responsible for the unique differences in the feline response to FGF21 mimetics. Additionally, the immunohistochemical expression of FGF21 in cases of spontaneous feline pancreatitis was examined, with strong FGF21 immunoreactivity within macrophages, which may represent M2 polarity.

This dissertation provides a starting point for evaluating the FGF21 pathway within domestic animals, including cats. These findings suggest that there are unique signaling pathways and therapeutic potential to target the FGF21 pathway, and further studies are needed to determine if FGF21 therapies will be a viable option in a clinical setting.

Acknowledgments

I want to thank my committee chair, Dr. Emily Graff and my committee members, Drs. Jey Koehler, Maninder Sandey, Russell Cattley, and Robert Judd for their constant guidance and mentorship. Thank you to Dr. Doug Martin for his careful review and service as my University Reader. I would also be remiss not to thank the numerous people who helped me through a combined residency and Ph.D. program. Moreover, I would like to thank Dr. Rie Watanabe, Leah Hoffman, Cynthia Hutchinson, and Lisa Jolly for their technical support, general life advice, and friendship and for dealing with all of my small crises, for which there have been many.

Table of Contents

List of Tables

List of Figures

Chapter 1



Chapter 2



Chapter 3

List of Abbreviations

| | |
|---|---|
| 1H-MRS | Proton Magnetic Resonance Spectroscopy |
| AAALAC | American Associated for the Accreditation of Laboratory Animal Care |
| Adipo-IR | Adipose Tissue Insulin Resistance |
| ALKP | Alkaline Phosphatase |
| ALT | Alanine Aminotransferase |
| ARIF | Acoustic Radiation Impulse Force |
| ASRAM | Acidic Serine Aspartate-Rich MEPE-Associated |
| AST | Aspartate Aminotransferase |
| ATF2 | Activating Transcription Factor 2 |
| AUC | Area Under the Curve |
| BAT | Brown Adipose Tissue |
| BWA | Burrows-Wheeler Aligner |
| CREBH | cAMP-Responsive Element Binding protein - Hepatocyte-Specific |
| CRI | Continuous Rate Infusion |
| CT | Computed Tomography |
| CYP27A1 | Sterol 27-Hydroxylase |
| CYP7A1 | Cholesterol 7α-Hydroxylase |
| DAB | 3,3'-Diaminobenzidine |
| DI | Deionized |
| DIO | Diet-Induced Obese |
| DIO2 | Type II Iodothyronine Deiodinase |
| DMP1 | Dentin Matrix Protein-1 |
| FFPE | Foramalin-Fixed Paraffin Embedded |

| | |
|---|---|
| FGF | Fibroblast Growth Factor |
| FGFR | Fibroblast Growth Factor Receptor |
| FGFRL1 | Fibroblast Growth Factor Receptor-like 1 |
| FXR | Farsenoid X Receptor |
| GALNT3 | N-acetylgalactosaminyltransferase 3 |
| GCN2 | General Control Nonderepressible 2 |
| H&E | Hematoxylin and Eosin |
| HBS | Heparin Sulfate Glycosaminoglycan Binding Site |
| HCC | Hepatocellular Carcinoma |
| HOMA-IR | Homeostatic Model Assessment for Insulin Resistance |
| HSGAG | Heparin Sulfate Glycosaminoglycan |
| IACUC | Institutional Animal Care and Use Committee |
| IBA1 | Ionized Calcium Binding Adaptor Molecule 1 |
| Ig | Immunoglobulin |
| IHC | Immunohistochemistry |
| ISR | Integrated Stress Response |
| KL | α-klotho |
| KLB | β-klotho |
| KO | Knockout |
| LTCL | Lactase-like protein |
| MAPK | Mitogen-Activated Protein Kinase |
| MEPE | Matrix Extracellular Phospho-Glycoprotein |
| NCBI | National Center for Biotechnology Information |
| NCC | Sodium-Chloride Cotransporter |

| | |
|---|---|
| NEFA | Non-Esterified Fatty Acid |
| NPT2A/C | Type II Sodium Phosphate Cotransporter A/C |
| NRVM | Neonatal Rat Ventricular Cardiomyocytes |
| PcoA | Principal Coordinates Analysis |
| PGC-1α | Peroxisome Proliferator-Activated Receptor γ Coactivator Protein-1 |
| PHEX | Phosphate-Regulating Gene with Homologies to Endopeptidases on X Chromosome |
| PI3K | Phosphoinositide 3-Kinases |
| PPAR | Peroxisome Proliferator-Activated Receptor |
| PTH | Parathyroid Hormone |
| rh- | Recombinant Human |
| RXR | Retinoid X Receptor |
| SHP | Small Heterodimer Partner |
| Sirt1 | Sirtuin 1 |
| STZ | Streptozotocin |
| T1DM | Type 1 Diabetes Mellitus |
| T2DM | Type 2 Diabetes Mellitus |
| TBS | Tris-Buffered Saline |
| TRPV5 | Transient Receptor Potential Cation Channel Subfamily V Member 5 |
| UCP-1 | Uncoupling Protein-1 |
| USDA | United States Department of Agriculture |
| WNK4 | With-no-lysine Kinase 4 |
| WT | Wild Type |
| XLH | X-linked Hypophosphatemia |

# Chapter 1: Literature Review: The Fibroblast Growth Factors, the Endocrine Fibroblasts Growth Factors, and the Signaling Pathway: Focus on Domestic Animals

## *1 Introduction*

There are three major fibroblastic growth factors (FGFs) groups: the intracellular, the canonical, and the endocrine. The non-secreted intracellular FGFs bind the C-termini of voltage-gated sodium channels to regulate their function (1, 2). The secreted canonical and endocrine fibroblast growth factors signal to the four high-affinity tyrosine kinase fibroblast growth factor receptors (FGFRs) and fibroblast growth factor receptor-like 1 (FGFRL1) (3). Structurally, the FGFRs are composed of three immunoglobulin-like (Ig-like) domains, conferring ligand binding specificity. FGFRs1-3 have 'a,' 'b,' and 'c' isoforms corresponding to an alternate exon splicing form of the third Ig-like domain (4). The endocrine FGF19 subfamily has binding affinity for the 'c' isoforms of FGFRs (*e.g.*, FGFR1c) and FGFR4, rather than the 'b' isoforms (the 'a' isoform has no known signal capability) (5).

Both the canonical and endocrine FGFs contain a heparin sulfate glycosaminoglycan (HSGAG) binding site (HBS), which serves as the co-receptor binding site for the paracrine FGFs (3). However, due to structural differences, the FGF19 subfamily has an HBS that negligibly binds HSGAG. Due to this low-affinity binding, FGF19 subfamily members can transmigrate through an HSGAG-rich extracellular matrix on the cell surface and circulate in an endocrine fashion rather than remain in an autocrine and paracrine pathway (Figure 1) (3, 6). The endocrine fibroblast growth factors signal through an FGFR, typically dimerized with a klotho family member co-receptor. Most notably, the klotho family member α-klotho binds FGF23 and β-klotho binds FGF19 and FGF21 (Figure 2) (7, 8). A third member of the klotho family, LCTL (lactase-like protein), may be involved in the FGF19 signaling pathway, especially considering

its high expression in the mouse brown adipose tissue (BAT), but its function in the endocrine system is overall unknown (9).

*2 Fibroblast Growth Factor 23 (FGF23)*

The primary function of Fibroblast Growth Factor 23 (FGF23) is to regulate phosphorous homeostasis along with vitamin D and parathyroid hormone (PTH) in the body, creating cross-talk with the kidney, parathyroid gland, and bone stores (10). FGF23 is produced in the bone and secreted into circulation by osteoblasts and osteocytes in response to a poorly described mechanism of impaired extracellular matrix mineralization (11-13). Based on what we know from mutations in diseases of hypophosphatemic rickets, the release of FGF23 in the osteocyte is regulated by autocrine and paracrine signaling of the phosphate-regulating gene with homologies to endopeptidases on X chromosome (PHEX), dentin matrix protein-1 (DMP1), matrix extracellular phospho-glycoprotein (MEPE), and acidic serine aspartate-rich MEPE-associated (ASRAM) motifs (14, 15). Before secretion, O-glycosylation is promoted by polypeptide N-acetylgalactosaminyltransferase 3 (GALNT3), enhancing the function of active FGF23 by preventing proteolysis (10, 16). Proteolysis is an important regulatory mechanism to prevent the activation of FGF23. To initiate this mechanism, a non-activated and non-glycosylated FGF23 is phosphorylated on serine 180 by Fam20C. This phosphorylation marks a cleavage site for substillin-like proprotein convertase FURIN to fragment the FGF23 amino acid sequence. The FGF23 fragments are then ubiquitinated and degraded (17).

Once in circulation, FGF23 signals via the dimerization of co-receptors α-klotho and an FGFR, primarily FGFR1c, with the downstream signaling stimulating the MAPK-Erk1/2 pathways (11, 18, 19). The initial effects of FGF23 occur in the epithelial cells of the distal renal

convoluted tubule, where FGF23 stimulates the retention of Na+ and Ca2+ from the urine by activating the sodium-chloride cotransporter (NCC) and Transient Receptor Potential Cation Channel Subfamily V Member 5 (TRPV5) channels, respectively, via activation of with-no-lysine kinase 4 (WNK4) (11, 20, 21). The cells of the renal proximal convoluted tubule downregulate 1α-hydroxylase to reduce 1,25-dihydroxyvitamin D3 synthesis, or the active form of vitamin D, thereby reducing circulating levels of phosphorous and calcium. Additionally, FGF23 downregulates the membranous expression of NPT2A/C via the Erk1/2-SGK pathway through phosphorylation of Na+/H+ exchange regulatory factor-1 (NHERF-1). With phosphorylation of the scaffolding protein NHERF-1, NPT2A/C is degraded, preventing phosphate reabsorption and promoting phosphate excretion in the urine (12, 22).

In the parathyroid gland, the effect of FGF23 on levels of PTH is controversial. This controversy is evident by conflicting results in studies on bovine parathyroid cell culture versus mouse parathyroid cell culture. For example, in a study on bovine parathyroid cell culture, recombinant human FGF23 (rhFGF23) dose-dependently downregulated both PTH mRNA and protein secretion after 12-48 hours of treatment and upregulated mRNA levels of 1α-hydrolase after 3-24 hours of treatment (23). Additionally, there was some small mitogenic effect of rhFGF23, as bovine parathyroid cells had a minor but still significant increase in proliferation than the control with no differences in percent total apoptosis or percent viability (23). In a different study examining C57BL/6 mouse parathyroid gland culture, PTH secretion and parathyroid proliferation, as measured by a $Ki67^{+}$ cell index, were shown to be dependent on the FGF23 incubation duration (24). After 1 hour of incubation with FGF23, PTH secretion was slightly reduced, but after four days of incubation with FGF23, PTH secretion and Ki67+ cell index were markedly increased compared to the vehicle-treated cells. The effect of FGF23 on

PTH secretion seems to depend on many factors, including time, dose, and species. It should be noted that there are protein differences between bovine, mouse, and human FGF23, which may have contributed to the varying effects of rhFGF23 on bovine and mouse parathyroid cells. The chain sequence of bovine FGF23 (Uniprot identifier E1BJU2[20-245]) has 78.9% identity and 86.0% similarity to the chain sequence of human FGF23 (Q9GZV9[25-251]), and the chain sequence of mouse FGF23 (Q9EPC2[25-251]) has 71.8% identity and 81.9% similarity to the chain sequence of human FGF23 (25).

The discovery of FGF23's actions has expanded our understanding of the bone-heart link in cases of chronic kidney disease. In humans with chronic kidney disease, elevated serum FGF23 is independently associated with a higher risk of developing new-onset left ventricular hypertrophy (26). This group replicated their findings linking FGF23 elevations in chronic kidney disease to developing left ventricular hypertrophy in isolated neonatal rat ventricular cardiomyocytes (NRVMs) and rodent models. This pathway is mediated by FGFR4 and reversible with FGF4 blockade *in vitro* in neonatal rat ventricular myocytes and *in vivo* in C57BL/6J mice (27). This deleterious effect of left ventricular hypertrophy with increased FGF23 has precluded potential uses of FGF23 analog therapy. Instead, therapies target FGF23 to prevent it from binding with FGFRs. Several studies link high circulating levels of FGF23 and chronic kidney disease in dogs and cats (28-30), but what this means for the physiology of cardiac hypertrophy in veterinary cases of kidney disease or of FGF23 targeting therapy in veterinary clinics is unknown.

One significant disease that FGF23 targeting therapy is used for is X-linked hypophosphatemia (XLH). XLH results from a mutation in the PHEX gene, leading to a lack of FGF23 regulation. Subsequent increased levels of FGF23 lead to hypophosphatemia, decreased

1α-hydroxylase activity, and rickets (28). In a phase 2 clinical trial of children with XLH, burosamab, an anti-FGF23 monoclonal antibody, led to overall clinical improvement with an increase in physical function, reduced pain, and improved renal tubular phosphate reabsorption and serum phosphorous (29). In a phase 3 clinical trial of adults with XLH treated with burosamab, most treated patients had a serum phosphate concentration above the lower reference interval, along with an improvement in stiffness but not a significant improvement in physical function or pain (30). Burosamab is currently an FDA-approved drug to treat X-linked hypophosphatemia.

### *3 Fibroblast Growth Factor 15/19 (FGF15/19)*

Bile acid synthesis is a significant regulatory function of cholesterol homeostasis, as bile acids are synthesized de novo within the hepatocyte from cholesterol through two major pathways, the classical and alternative pathways, initiated by cholesterol 7α-hydroxylase (CYP7A1) and sterol 27-hydroxylase (CYP27A1), respectively (31). Most bile is secreted into the small intestine through the biliary tree. Bile acid stimulates the farnesoid X receptor (FXR ) in the liver, kidney, gut, and adrenal cortex (32), with the distal ileum being the primary site of FXR bile-binding activity (33). FXR is a nuclear receptor family member and binds DNA in a heterodimer with the retinoid X receptor (RXR), acting simultaneously as a receptor and a transcription factor (34, 35). This heterodimerization of FXR and RXR induces the production of FGF15/19 (32).

FGF15/19 is a regulator of the liver-intestinal axis that is diurnally controlled and produced postprandial as negative feedback of biliary acid synthesis in conjunction with hepatic orphan nuclear receptor SHP (small heterodimer partner) (36-39). FGF15 is the rodent family

ortholog of FGF19, and the signal chain of mouse FGF15 (Uniprot identifier O35622[26-218]) has only 49.0% protein sequence identity and 65.0% similarity with human FGF19 (O95750[25-216]) (25). FGF15 is an enterokine with the highest expression in the ileum, followed by a more marginal expression in the jejunum and no detectable expression in the liver (9). In contrast, FGF19 in humans is produced primarily in the gallbladder and common bile duct for secretion through the biliary system into the intestine with less mRNA production in the ileum (36, 40), and minimal FGF19 mRNA expression is found in non-cholestatic livers (41). Similarly to FXR (33), FGF19 has increased hepatic expression with cholestasis (41, 42).

FGF15/19 signals through all four canonical FGFRs in heterodimerization with co-receptor β-klotho (5). The main metabolic effects are through FGFR1c and FGFR4 (43, 44), and poorly described effects in health through FGFR2c and FGFR3c (45). In the liver, FGF15/19 binds with FGFR4 to inhibit cholesterol 7α-hydroxylase (CYP7A1), the rate-limiting enzyme in the classical bile acid synthesis pathway, inhibiting bile acid synthesis (37). FGF15 expression was absent in the ileum in mice with bile duct ligation, and there was no repression of CYP7A1. When these mice were given an FXR synthetic agonist, there was a marked increase in ileal FGF15 mRNA and a decrease in hepatic CYP7A1 mRNA, consistent with induction of FGF15 by FXR agonism by bile acids, and regulation of CYP7A1 by FGF15 (37). To confirm that this effect on CYP7A1 was mediated through FGF15-FGFR4 interaction, $FGFR4^{-/-}$ 129/Sv mice infected with FGF15-expressing adenovirus lacked repression of CYP7A1 mRNA.

In addition to its regulation of bile synthesis, FGF15/19 has metabolic actions driven primarily by binding with FGFR1c instead of FGFR4. Mouse studies have shown that FGFR4 activation by FGF19 does not drive improvements in glucose homeostasis (44). Supporting this, an FGF19 variant that preferentially activates FGFR1c and does not activate FGFR4 has similar

metabolic activity as wild-type FGF19, suggesting that β-klotho/FGFR1c receptor binding is the primary metabolic driver of FGF19 (46). Notably, FGF19 increases the BAT's energy expenditure by upregulating uncoupling protein-1 and browning white adipose tissue (47). FGF19 modulation of glucose homeostasis is due to the inhibition of hepatic gluconeogenesis (48) and increases in glycogenesis through the regulation of glycogen synthase kinase 3α (49). FGF19 regulates hepatic protein metabolism and stimulates hepatic protein synthesis (49).

FGF19-β-klotho/FGFR4 binding is unique in that it only occurs in the liver (50), and activation of this pathway is heavily implicated in the pathogenesis of hepatocellular carcinoma. In human hepatocellular carcinoma (HCC) cell lines, FGF19 increases proliferation and invasion and inhibits apoptosis (51). The *in vitro* work translates *in vivo* to mouse models where exogenous FGF19 administration of mice induces centrilobular hepatocyte proliferation (52) and hepatic expression of the proliferation marker alpha-fetoprotein and the proto-oncogenes Egr-1 and c-Fos (53, 54). Transgenic mice overexpressing FGF19 in skeletal muscle are an animal model of HCC, as 80% of female mice develop HCC by 10 - 12 months (54). FGF19, and not FGFR4, is overexpressed in human HCCs compared to non-neoplastic human liver tissue, and high expression of FGF19 mRNA is an independent predictor of poor prognosis (51). As a proof of concept that FGF19-β-klotho/FGFR4 binding is carcinogenic, FGF19 transgenic mouse models of HCC that were administered anti-FGFR4 monoclonal antibodies to prevent the binding of FGF19 to FGFR4 had inhibited tumor growth (55). Additionally, anti-FGF19 antibodies prevent the development of HCC in FGF19 transgenic mice (56). Pan-FGFR and FGFR4-specific inhibitors are under investigation in clinical trials in patients with HCC (57). However, FGF19-β-klotho/FGFR4 targeted therapies cause dysregulation of bile acid homeostasis. In cynomolgus monkeys, administration of > 3 mg/kg of an anti-FGF19 antibody

led to the expected increase in bile acid synthesis through upregulation of CYP7A1 and altered bile transporter expression with impaired ileal bile acid reabsorption, causing diarrhea (58). In a phase 1/2 clinical trial of utilizing a selective FGFR4 inhibitor, FGF401, in humans with β-klotho/FGFR4-expressing tumors, diarrhea and increases in serum alanine aminotransferase and aspartate aminotransferases and total bile acid were seen, indicating potential bile hepatotoxicity (59). In an attempt to reduce side effects of bile acid dysregulation while maintaining the antitumor effects of anti-FGF19, preclinical trials of antibodies targeting the N-terminus of FGF19 have been developed. These antibodies show suppressed HCC growth in xenograft mouse models and did not lead to adverse biliary acid-related events in cynomolgus monkeys (60). FGFR4 inhibitors are not well investigated in veterinary medicine for hepatocellular carcinoma, but in Beagle preclinical studies, FGF401 has been associated with increased serum aminotransferases, particularly alanine aminotransferase, which was reversible with the bile acid sequestrant cholestyramine, indicating bile acid homeostasis dysregulation similarly to the human phase 1/2 clinical trial (61).

Despite the tumorigenic potential of FGF19, FGF19-β-klotho/FGFR1c signaling is being investigated for clinical use for its positive metabolic effects. In mouse models of obesity, FGF19 induces weight loss without a change in food intake and improves glucose homeostasis (62). FGF19 analogs have made it to phase 2 clinical trials, where patients had significantly reduced hepatic fat content and improved fibrosis (63, 64). There is some evidence that FGF19 analog use can be expanded to other liver disorders beyond non-alcoholic steatohepatitis. In a clinical trial of cholestatic liver disease, FGF19 analogs were demonstrated to cause improved hydrophobic serum bile acids in patients with various chronic liver disease etiologies (65). Due to these promising findings in clinical trials and concern for increased risk of tumors like

hepatocellular carcinoma, FGF19 analogs are being developed to retain the beneficial metabolic and hepatic effects with minimal to absent tumorigenic potential (66). Non-tumorigenic FGF19 agonists may be beneficial to look at in veterinary medicine in animals to treat intrahepatic and extrahepatic cholestasis, particularly a subset of patients with concurrent hepatocellular triglyceride accumulation, to decrease bile hepatotoxicity.

### *4 Fibroblast Growth Factor 21 (FGF21)*

FGF21 binds to its co-receptors, FGFR1c and β-klotho, via its N-terminus and C-terminus, respectively (67). FGF21 binding to FGFR1c and β-klotho is responsible for many of the beneficial effects described for FGF21, such as weight loss and improvements in glucose, insulin, lipid homeostasis, and cardioprotection (68, 69). Specifically, transgenic mice with overexpression of FGF21 have lower body weight despite increases in caloric intake, lower fasted plasma glucose without hypoglycemia, lower triglycerides, retained BAT stores, smaller subcutaneous adipocytes, and improved glucose clearance and insulin sensitivity with oral glucose tolerance tests (70). Downstream actions of FGF21 are primarily due to the major energy homeostasis regulator, peroxisome proliferator-activated receptor γ coactivator protein-1 (PGC-1α) (71, 72). Importantly, as FGF21 does not activate FGFR4, it does not promote mitogenicity as observed with FGF19 (52, 70).

FGF21 pathway physiology is inherently complex as several different transcription factors mediate production in multiple organ systems (Figure 3). Increases in circulating FGF21 are associated with various dietary modifications and are predominantly linked to FGF21 as a starvation hormone but FGF21 concentrations can also be increased with ketogenic diets, amino acid-restricted diets, alcohol consumption, and high carbohydrate diets (73-76) (Figure 4). With

starvation, ketogenic diets, and alcohol consumption, glucocorticoids and catecholamines induce lipolysis in the adipose tissue via the cAMP-dependent protein kinase A pathway, converting triglycerides into free fatty acids and releasing free fatty acids into circulation (77-79). Circulating fatty acids are sensed by the peroxisome proliferator-activated receptor (PPAR) family. This family of nuclear transcription factors is implicated in numerous metabolic pathways, including peroxisomal β-oxidation, ketogenesis, and FGF21 (80, 81).

In the liver, the primary site of circulating FGF21 production, peroxisome proliferator-activated receptor α (PPARα) is the principal regulator of FGF21 production (80, 82-84), with the potential interaction of many other transcription elements, such as cAMP-responsive element binding protein- hepatocyte-specific (CREBH), RXR, and thyroid receptor β (85, 86). Carbohydrate-rich diets induce the hepatic expression of the carbohydrate-responsive element-binding protein (ChREBP), a transcription factor that mediates carbohydrate metabolism and related metabolic effects (87). ChREBP and PPARα together bind to FGF21's promoter region to induce FGF21 expression (88). In response to amino acid starvation, hepatic FGF21 is induced by ATF4. ATF4 is a downstream target of general control nonderepressible 2 (GCN2) kinase and is activated during amino acid restriction (89).

Hepatic-produced FGF21 is responsible for many beneficial endocrine and autocrine/paracrine metabolic effects. From PGC-1α activation, hepatic FGF21 is implicated in the reduction in hepatic lipid accumulation, brown fat thermogenesis, triglyceride clearance, hepatic gluconeogenesis without glycogenolysis, tricarboxylic acid cycle flux, and ketogenesis (72, 83). C57Bl/6 diet induced obese (DIO) mice with liver-specific knockout (KO) of FGF21 have increased insulin resistance compared to wild-type DIO mice, while there was no change in insulin sensitivity with the DIO adipose-specific KO mice. The liver FGF21 KO mice also had

increased hepatocellular lipid accumulation, epididymal white adipose tissue fibrosis, and impaired glucose uptake in the BAT (83). Hepatic FGF21 signals for thermogenesis in neonatal mice during the fetal-to-neonatal transition. In conjunction with increasing PPARα-dependent hepatic mRNA expression and circulating FGF21, the BAT in neonatal suckling mice with a high lipid milk diet undergoes thermogenic activation with increased mRNA expression of adaptive thermogenesis-promoting proteins PGC-1α, uncoupling protein-1 (UCP-1), and type II iodothyronine deiodinase (DIO2) (90). Supporting the role of FGF21 in triglyceride clearance and ketogenesis, mice on a ketogenic diet with adenoviral knockdown of hepatic FGF21 were lipemic, characterized by elevations in triglycerides, cholesterol, and fatty acids, along with increased hepatic triglycerides, and decreased serum β-hydroxybutyrate compared to control mice (82). Systemic FGF21 signals to regions of β-klotho expressing neurons, particularly in the paraventricular nucleus and the suprachiasmatic nucleus, to control sweetness and alcohol preference, promote glucose homeostasis, control fertility, modulate energy expenditure through sympathetic nerve activity, and control circadian rhythm (91).

FGF21 is not only a hepatokine but also an adipokine, myokine, and cardiomyokine (69, 71, 92). Mice with adipose tissue-specific knockout of FGF21 do not have significant changes in circulating FGF21, suggesting that adipose-derived FGF21 remains localized as an autocrine/paracrine mediator (83). With cold exposure, FGF21 produced within the BAT mediates thermogenesis (93). During cold exposure, catecholamine release stimulates β-adrenergic receptors, which activate the cAMP-dependent protein kinase A pathway, which leads to downstream activation of the transcription factor ATF2 (94). In the brown adipose tissue, ATF2 mediates FGF21 expression (95). Supporting the autocrine/paracrine role of FGF21 in thermogenic activation of brown adipose tissue in wild-type C57Bl/6J mice, cold exposure

upregulates FGF21 and PGC-1α mRNA levels in the BAT without concurrent changes in plasma FGF21 (93). In the murine white adipose tissue, FGF21 is locally regulated by PPARγ and not PPARα, as in the liver (84, 96). Interestingly FGF21 also regulates PPARγ (84), suggesting a positive feedback cycle. Autocrine/paracrine FGF21 in the white adipose tissue is responsible for cold-exposure-induced browning by increasing PGC-1α protein levels and expression of UCP-1 and DIO2 (71). FGF21 incubation stimulates adiponectin secretion, a glucose-lowering and insulin-sensitizing adipokine *in vivo* and *in vitro* (97). FGF21 lowers plasma ceramides (98), a sphingolipid implicated in inducing multisystemic lipotoxicity of metabolic disorders (99). The glucose and ceramide lowering effects of FGF21 are lost in adiponectin KO mice, showing that FGF21's stimulation of adiponectin is essential for glucose homeostasis and amelioration of lipotoxicity (97, 98).

In skeletal myocytes, expression of FGF21 is induced by insulin through a PI3K-Akt1-dependent pathway. Transgenic mice with skeletal muscle-specific Akt1 overexpression and cultured Akt1-overexpressing myocytes have upregulated FGF21 mRNA and protein expression, particularly with the addition of insulin, which is diminished with a PI3K inhibitor (92). In skeletal myocytes, FGF21 promotes glucose uptake and mediates muscle loss and mitophagy during starvation in a paracrine/autocrine manner. In human skeletal myotubes and adult mouse skeletal muscle cultures, FGF21 promotes glucose uptake (100). In muscle-specific FGF21 knockout mice, the knockout mice were protected from starvation-induced muscle cachexia and mitophagy (101).

Murine cardiomyocytes produce FGF21, although at much lower levels than the liver and adipose tissues, and these levels are increased with cardiac damage under the regulation of the Sirt1-PPARα pathway. FGF21 protects against cardiac damage and hypertrophy in mice, as

FGF21 knockout mice have early-onset cardiac hypertrophy and dilatation, and FGF21 prevents isoproterenol-induced cardiac hypertrophy and pro-inflammatory pathways and enhances cardiac fatty acid oxidation (69). In clinical studies and models of many cardiovascular diseases, including atherosclerosis, diabetic cardiomyopathy, cardiac hypertrophy, and myocardial ischemia, FGF21 is increased, potentially as a compensatory mechanism (102). There is some proof that FGF21 therapeutics will be beneficial as a treatment for cardiovascular disease. Obese, insulin-resistant rats on a high-fat diet had a reversal of left ventricular dysfunction with long-term FGF21 therapy through a reduction of overall systemic and cardiac oxidative stress and a reduction of cardiac mitochondrial redox dyshomeostasis (103).

FGF21 is also produced in both the exocrine and endocrine pancreas, with around 20x higher expression in the acinar cells than in the islets (104). Pancreatic FGF21 acts as a secretagogue, promoting digestive enzyme secretion from the zymogen granules via the phospholipase C - inositol 1,4,5-trisphosphate – $Ca^{2+}$ pathway avoiding further endoplasmic reticulum stress (105). Pancreatic FGF21 is upregulated in obesity and downregulated by fasting, interestingly in contrast to hepatic FGF21, which is upregulated by starvation (104). In the endocrine pancreas, FGF21 regulates β-health and insulin production. C57Bl/6J global FGF21 KO mice have impaired glucose-stimulated insulin secretion and enlarged and distorted islets (106).

### *5 FGF21 Therapy: Comparisons of Humans, Non-Human Primates, and Rodents*

Given the myriad beneficial positive effects, FGF21 mimetics have been adapted for therapeutic use and have undergone preclinical trials in rodents and non-human primates and clinical trials (107). Native FGF21 has a very short elimination half-life of around 0.5 - 4.3

hours, dependent on the route of administration (70), and therapeutic variants have been developed with an increased half-life, resistance to proteolysis, and potential for commercial manufacturing in mind while retaining the efficacy of FGF21 (108).

One of the first FGF21 analogs was developed by Eli Lilly. LY2405319 is an engineered human recombinant FGF21 from a *Pichia pastoris* host expression system designed for increased thermal and conformational stability for a biopharmaceutical multiuse formulation, a once-daily administration profile, and a similar efficacy as native FGF21 (109). Although LY2405319 was engineered for reduced proteolytic cleavage, its small size (~22kD) still allowed for ready urinary excretion with minimal extension of biological half-life (109-111). In DIO C57Bl/6 and ob/ob mice, an engineered recombinant human FGF21, LY2405319, led to a dose-dependent decrease in body weight within two weeks, despite an increase in weight-normalized caloric consumption along with a reduction in non-fasted plasma glucose (109). In a dose escalation study treating diabetic rhesus monkeys with LY2405319, monkeys had a significant decrease in body weight, blood glucose, circulating triglycerides, an increase in plasma adiponectin, and an improvement in circulating cholesterol profile from baseline within two weeks at the starting 3 mg/kg/day dose. Additional parameters like decreases in plasma insulin and leptin showed eventual improvement at higher doses. These parameters returned to baseline during the withdrawal period. Unlike the study in mice, rhesus monkeys did have a reduction in food intake with LY2405319 treatment (112). In obese humans with type 2 diabetes mellitus (T2DM) and similar to the rhesus monkeys, dose-dependent improvements were seen in the circulating cholesterol profile, adiponectin, and insulin, along with a trend to decrease glucose. Weight loss was observed, but food intake was not measured (113).

Another FGF21 analog, PF-05231023 (original CVX-343), is made of two recombinant human FGF21 molecules covalently linked to a fragment antigen-binding region of a scaffold antibody (114). Mice treated with PF-05231023 had dose-dependent improvements in glucose excursion with an oral glucose tolerance test and weight loss (115). When tested in obese cynomolgus monkeys, similar to LY2405319, non-human primates had concurrent food intake and body weight decreases. One safety concern in a study of PF-05231023 in a study of humans with T2DM was an increase in the marker of bone resorption, carboxy-terminal collagen crosslinks, with concurrent decreases in markers of bone formation, osteocalcin, procollagen type I N-terminal propeptide and bone-specific alkaline phosphatase. The study acknowledged that these markers are confounded by accompanying weight loss, which will cause bone turnover. A significant limitation was that no bone mineral content was evaluated in the human subjects, although no changes in bone mineral content were observed in the monkeys using dual-energy X-ray absorptiometry (DEXA) (116). The inspiration for investigating bone markers in non-human primates was from reports of mice with decreased bone density from FGF21 therapy. Both transgenic FGF21-overexpression and pharmacologically administered FGF21 (for two weeks at a dose of 1 mg/kg/day intraperitoneal) had decreased trabecular bone and bone mineral density with osteoblastogenic inhibition to a shift of adipogenesis of bone marrow stem cells (117). Similar trabecular bone losses were seen in Wister rats on a high-fat diet administered 0.1 mg/kg/day FGF21 subcutaneously for four weeks (118). However, the role of FGF21 in bone and mineral homeostasis is controversial, as neither bone density nor bone marrow adiposity is changed in DIO mice given hundreds fold more human recombinant FGF21 over two weeks (up to 3 mg/kg/day intraperitoneal.) than reported in the FGF21 transgenic mice (119). In another study, mice treated with FGF21 adenoviral therapy had normal naso-anal and tibial length, no

difference in bone structure with micro-computed tomography, and no differences in bone mineral density or bone density mineral content (120).

Pegbelferin (or BMS-986036) is a PEGylated FGF21 analog causing similar circulating lipid profile changes as reported for other FGF21 analogs in humans and non-human primates. Interestingly, Pegbelferin did not lower HbA1c or weight in comparison to the placebo in humans despite weight loss in monkeys with concurrent reductions in lean mass, lean area, and fat area (121, 122). Notably, no bone mineral or density change was seen in adult male cynomolgus monkeys receiving weekly subcutaneous Pegbelferin for one year (122). In a phase 2a clinical trial in patients with non-alcoholic steatohepatitis, Pegbelferin significantly lowered the hepatic fat fraction and a biomarker of fibrosis, PRO-C3. In this study, at an 8-week prespecified interim analysis, it was shown that the hepatic lipid-reducing effects of Pegbelferin were strong enough (> 4.5% reduction from baseline) to discontinue additional patient enrolment (123). Common to PF-05231023, pegbelferin had nausea and gastrointestinal upset as overreported adverse events (116, 123, 124).

AKR-001 (Fc-FGF21-RGE, Efruxifermin) is an Fc-FGF21 fusion protein designed for longer, weekly or biweekly dosing intervals due to a prolonged circulating half-life and increased binding affinity to β-klotho. With weekly injections in DIO mice, there was a reduction in blood glucose, insulin, triglyceride, cholesterol and body weight characterized by a reduction of fat mass. Obese cynomolgus monkeys with impaired glucose tolerance similarly had a decrease in fasting blood glucose, insulin, amylin, glucagon, increases in HDL-cholesterol, and a reduction in body weight. Monkeys regained their body weight during the washout period (125). In a phase 1 clinical trial of obese type 2 diabetic humans, there was an improvement in glycemic control,

insulin sensitivity, and lipid homeostasis. However, there were no significant changes in body weight (126).

It seems that there are some species-dependent effects of FGF21 analogs. For instance, although most analogs reduce body weight, whether this is due to decreased caloric intake is inconsistent, as it appears to be in monkeys and not mice. The full translatability between preclinical models and humans of FGF21 analogs as a treatment is still being discovered. Other inconsistent effects of various FGF21 therapies include changes in bone density, changes in food intake, and even the degree of impact on metabolic parameters as observed with a lack of changes with H1Ac and Pegbelferin or body weight with Efruxifermin.

### *6 FGF21 in Domestic Animals*

FGF21 physiology is poorly studied within veterinary medicine. The translational capabilities of many FGF21 analogs to veterinary medicine is an open field, despite many potential applications. Many companion animals are overweight and obese with associated insulin resistance (127), and hepatic lipidosis is a common cause of morbidity and mortality among farm and companion animals (128, 129). As FGF21 has been shown to improve insulin resistance, decrease body weight, and decrease liver lipid, it behooves veterinary scientists to examine FGF21 as a potential therapy.

A few studies use canine diabetes models to study FGF21 physiology. One study evaluated streptozotocin (STZ)-treated Beagles treated with 0.5 mg/kg canine recombinant FGF21 once a day for 12 days. Despite the high toxicity of STZ to pancreatic β-cells, this study found partially restored circulating insulin and glucose and noted inhibition of the hepatic gluconeogenic enzymes glucose 6-phosphatase and phosphoenolpyruvate carboxykinase (130),

implicating FGF21 in islet function restoration post-STZ-induced damage and inhibition of hepatic gluconeogenesis. This group repeated their studies in STZ-induced diabetic dogs for an extended period (8 weeks) using PEGylated canine FGF21 (cFGF21) and compared their results to 2 U/kg porcine insulin treatment to investigate the practicality of using FGF21 treatment in the replacement of insulin in diabetic dogs (131). They found that a single dose of recombinant canine FGF21 maintained reduced blood glucose effects longer than insulin. However, dogs showed resistance to FGF21 glucose-lowering effects at around 30 days after the initiation of the study. Remnant insulin-immunoreactive islets were histologically visible within the FGF21 treated group, suggesting that FGF21 can either prevent further STZ-induced pancreatic β-cell death from progressing by downregulating inflammation and promoting regeneration of β-cells. Although STZ-induced models provide many benefits, such as decreased time and cost, it is not spontaneous and comes with drawbacks, such as direct STZ-induced renal and hepatic toxicity. Other canine models of type 1 diabetes mellitus (T1DM) use adjuvant therapies along with low-dose STZ to avoid the off-target toxic effects, such as in combination with partial pancreatectomy or other β-cell targeting drugs (132, 133), and it would be interesting to see how studies using a combination-induced T1DM model would differ from an STZ-treated only model. Follow-up studies in canines with spontaneously occurring insulin resistance, insulin-dependent diabetes mellitus, or non-insulin-dependent diabetes mellitus are needed to better evaluate the utility of FGF21 pathway targeting therapy in dogs.

Probably the most well-described domestic animal regarding FGF21 physiology is the dairy cow. Early lactating dairy cattle undergo massive lipid mobilization with concurrent FGF21, glucagon, and non-esterified fatty acid increases while producing high-fat, calorically dense milk in a negative energy balance (134). In a study evaluating this metabolically stressful

time of a cow, plasma FGF21 in cattle dramatically increased during early lactation from nearly 0 pg/ml to ~1600 pg/mL and had similar circulating levels in feed-restricted late-lactating dairy cows. As fluxes in circulating FGF21 correlated with hepatic FGF21 mRNA expression, FGF21 production in cows seemed to be driven by the liver with marginal contribution, if any, by the tail head (subcutaneous) white adipose tissue and no contribution by the skeletal muscle (135), similar to what is reported for other species (83). In the same study, this group also determined that B-klotho mRNA expression is highest in the adipose tissues (perirenal, omental, mammary, and subcutaneous – in decreasing order) in prepubertal 6-month-old heifers (135). In early lactating dairy cattle treated with 3 mg/kg LY2405319 boluses followed by nine consecutive days of an LY2405319 continuous rate infusion (CRI) of 6.3 mg/kg, there were no changes in the circulating metabolic parameters plasma glucose, insulin, adiponectin or other parameters like total milk production or food intake (111, 136). Despite the lack of adiponectin secretion or changes in circulating metabolic parameters, FGF21 activity on the white adipose tissue was confirmed by increased phosphorylation of the downstream target, ERK1/2, suggesting that the FGF21 signaling pathway is different in dairy cattle in comparison the more studied laboratory animal rodents, non-human primates, and humans (136). They followed this study by evaluating lipid parameters, including evaluating hepatic lipid accumulation through biopsies. The cows did have decreased circulating free fatty acids following the LY2405319 bolus, but this decrease was not sustained over the 9-day CRI period (134).

With the treatment of LY2405319, the cows did have decreased hepatic triglycerides despite being in the early lactating, negative energy balance phase when liver lipid storage is typically in excess (111, 128), demonstrating that there is an effect of FGF21 on lipid homeostasis in cattle. Human FGF21 (Uniprot identifier Q9NSA1[29-209]), of which

LY2405319 is a recombinant version, has 87.8% identity and 91.7% similarity and with bovine FGF21 (E1BDA6 [29-209]) (25), so utilization of this human protein in a cow is likely to have appropriate effects. It would be worthwhile to see if FGF21 can be therapeutic in cattle with hepatic lipidosis, as this disease most commonly occurs in early lactating cattle. Evaluation of the treatment with FGF21 in the late postnatal period and early lactational period to reduce the risk of ketosis or displaced abomasum would be interesting as this could provide a significant economic benefit. However, additional studies would also be needed to determine the effects on milk production.

The same group that studied FGF21 in cattle did a study that surveyed FGF21 signaling machinery and administered LY2405319 for 13 days to non-lactating Finn x Dorset ewes with adequate body condition (137). Out of the liver, subcutaneous adipose, omental adipose, retroperitoneal adipose, kidney, gracilis muscle, and lung, the group found FGF21 mRNA was most highly expressed in the sheep's liver at 17-fold higher than any other expressing tissue. Other tissues with lower expression were the subcutaneous and retroperitoneal adipose tissue and kidney. There was no expression in the omental fat and skeletal muscle. β-klotho mRNA was expressed in the subcutaneous, omental, and retroperitoneal adipose tissues and liver, and FGFR1c was expressed in the subcutaneous adipose tissue (other adipose stores were not examined), indicating that the adipose tissues and liver are FGF21 targets. FGF21 targeting of the adipose tissue was confirmed by increased pERK1/2 and EGR1 protein in the subcutaneous adipose tissue following a 5 mg/kg bolus. In contrast to the lack of insulin and glucose homeostasis changes in cattle with LY2405319 administration, sheep had decreased circulating glucose, a transient decrease in insulin, and increased adiponectin with a 15 mg/kg/day dose over

13 days. The conflicting actions of FGF21 in early lactating cattle and non-lactating sheep raise the question of whether early lactation is an FGF21-resistant state in ruminants.

## *7 Summary and Conclusions*

The endocrine Fibroblast Growth Factor family members, FGF15/19, FGF21, and FGF23, are vital to many homeostatic mechanisms in the body. The members of this family exert actions through a Fibroblast Growth Factor Receptor and a klotho family member. FGF21, via the co-receptors FGFR1c and β-klotho, is a potent regulator of lipid homeostasis and insulin sensitivity. FGF21 pathway-targeting therapies generally improve global metabolic health by decreasing body weight, insulin resistance, liver lipid concentration and fibrosis. However, despite similar metabolic diseases in domestic animals of obesity, insulin resistance, and increased liver lipid, FGF21 is poorly investigated in veterinary medicine. Given preliminary studies in domestic animals, FGF21 may prove helpful in some common diseases. Insulin-dependent diabetes mellitus in dogs in around 30% of cases is associated with pancreatitis, suggesting that these inflammatory processes destroy islets. As FGF21 therapy is associated with improvement of overall β-cell health in both rodent and canine studies, it seems that some rodent research can be translated to the dogs, and potentially FGF21 pathway-targeting therapy can be utilized to restore islet health in diabetic dogs. FGF21 therapy may also be beneficial as adjunct therapy in ruminants with hepatic lipidosis, as although it is not treating the underlying condition of being in a negative energy balance, it can alleviate some lipotoxicity within the hepatocyte and help restore hepatic function. This may translate to companion animals with fatty liver diseases as well, such as in cats. Hepatic lipidosis is a deadly, acute condition in the domestic cat. Use of FGF21 therapeutics to acutely allieviate the hepatic lipotoxicity and at least partially

restore liver function, allowing the veterinarian to deal with the underlying condition, could indeed be revolutionary for veterinary medicine.

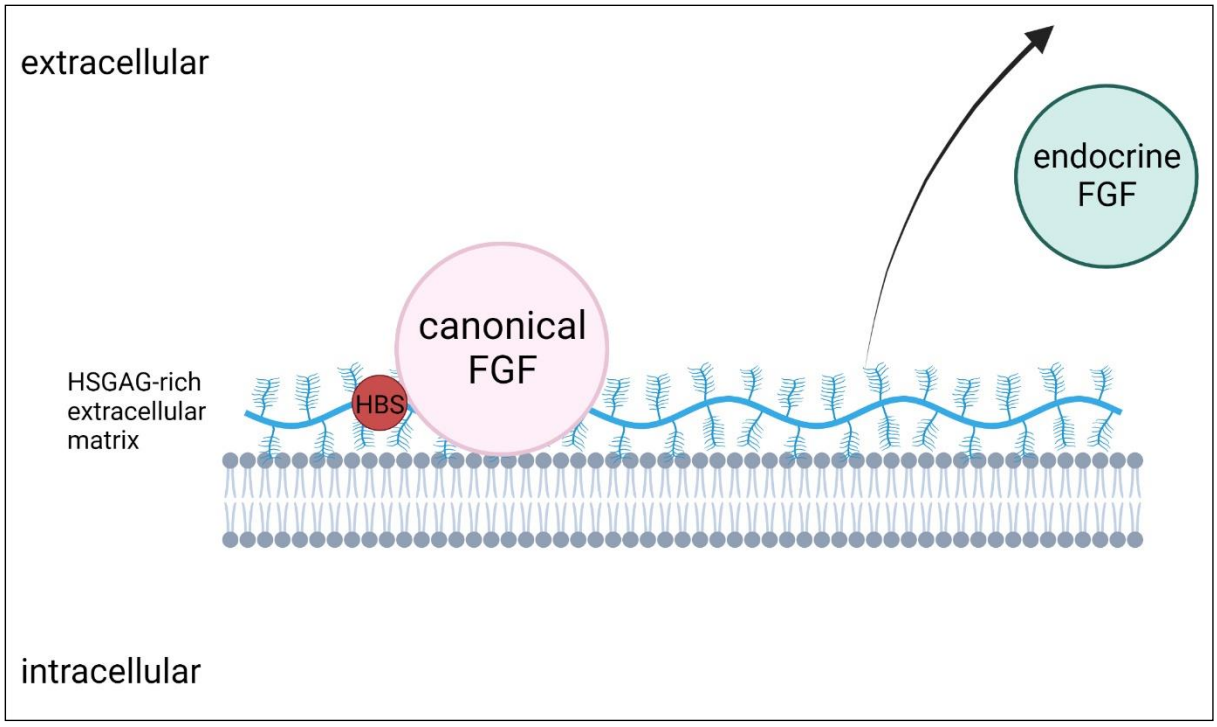


**Figure 1. The mechanism for escape into circulation by the endocrine FGF family.** The endocrine FGF family has a heparin sulfate glycosaminoglycan (HSGAG) binding site (HBS) with low affinity for HSGAGs within the cellular extracellular matrix. This low affinity lets the endocrine FGF family escape from the cell surface, allowing endocrine actions. This is compared to the canonical FGF family, with an HBS with a high affinity for HSGAGs, necessitating autocrine/paracrine actions.

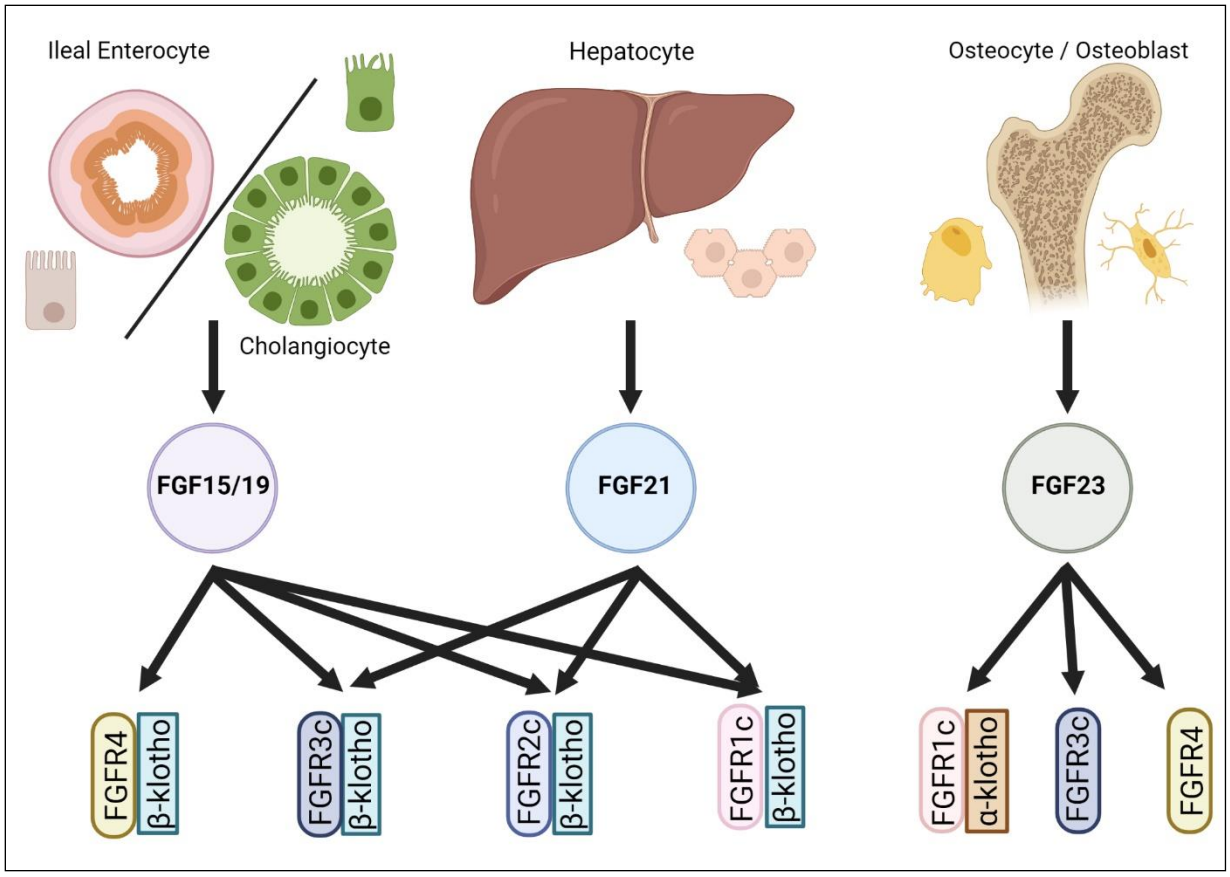


**Figure 2. The major sites of production and receptors for members of the endocrine FGF family.**

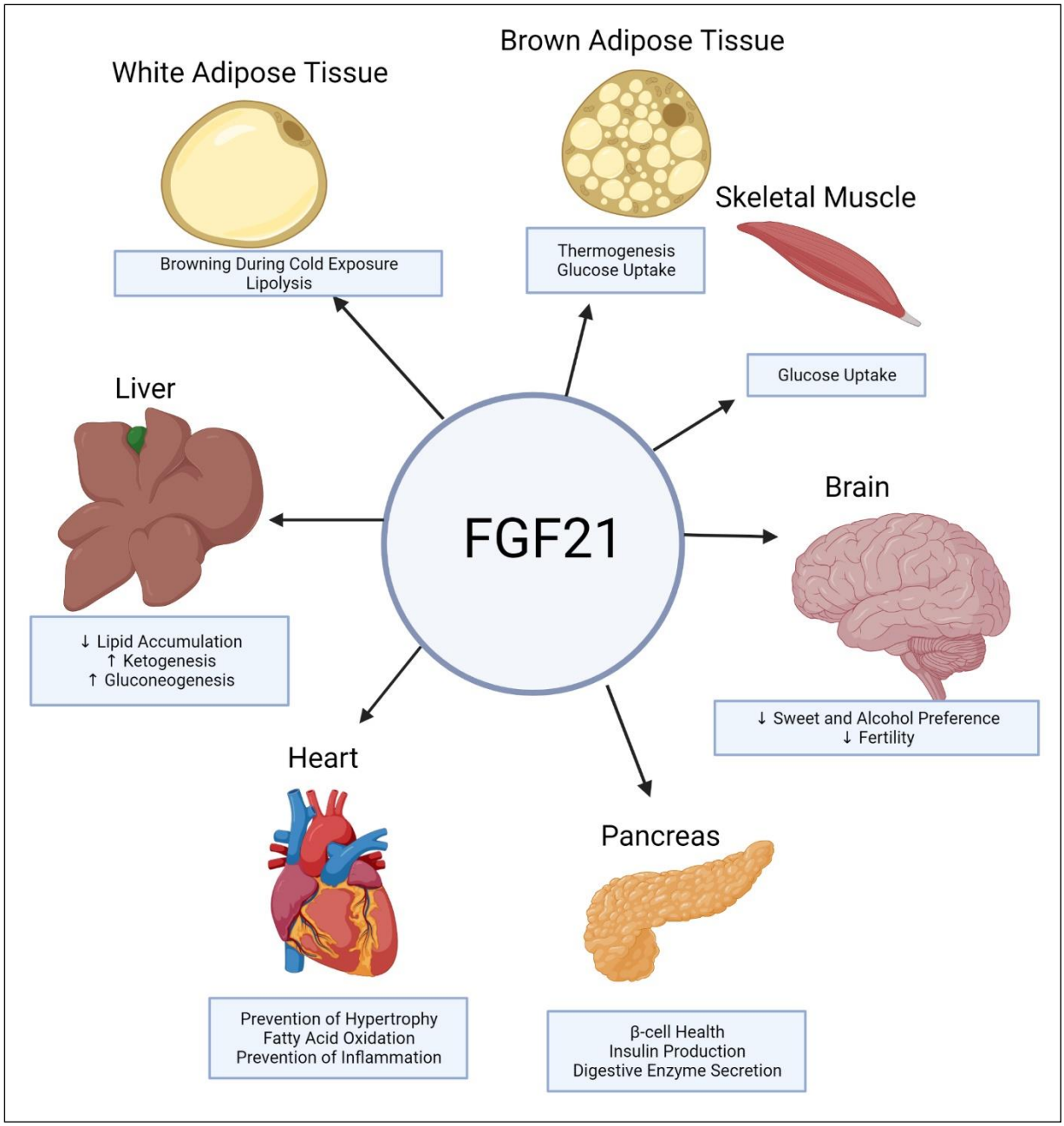


**Figure 3. FGF21 has many organ-specific functions.** Although most circulating FGF21 is produced in the liver, organ-specific autocrine and paracrine functions of FGF21 also drive metabolic processes.

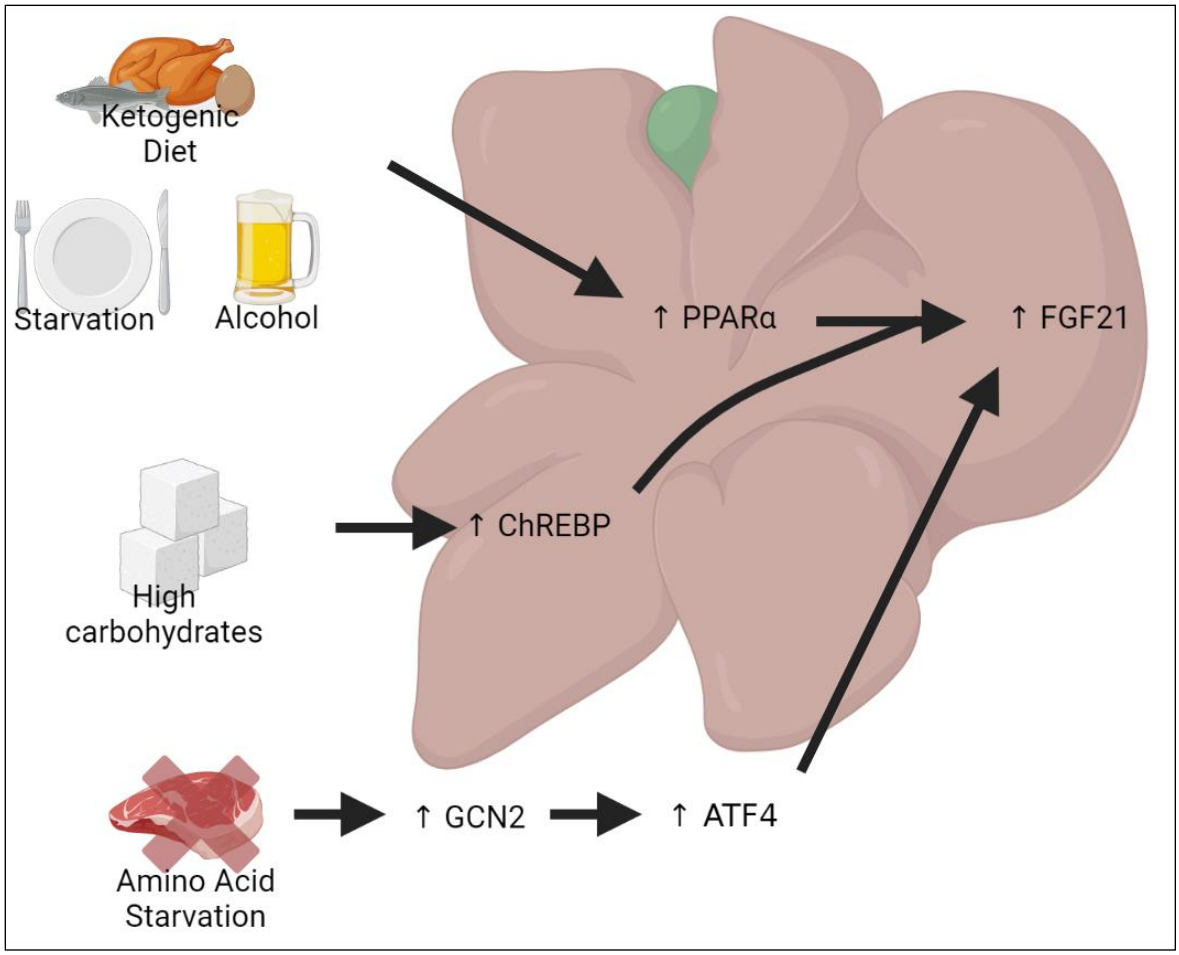


**Figure 4. The pathway of FGF21 production in the liver.** Ketogenic diets, starvation, and alcohol activate the nuclear hormone receptor PPARα, a transcription factor for FGF21 production. High carbohydrate (*e.g.*, fructose) diets promote hepatic ChERP production, a transcription factor that acts synergistically with PPARα to promote FGF21 transcription. Amino acid restricted diets indirectly increased ATF4, a FGF21 transcription factor.

# Chapter 2

## Direct activation of the Fibroblast Growth Factor-21 pathway in overweight and obese cats

Emily J. Brinker[1,2], Taylor J. Towns[1,2,] Rie Watanabe[1], Xiaolei Ma[1,3], Adil Bashir[4], Robert C. Cole[5], Xu Wang[1,2,6,7], Emily C. Graff[1,2]

[1]Department of Pathobiology, College of Veterinary Medicine, Auburn University, Auburn, Alabama, USA

[2]Scott Ritchey Research Center, College of Veterinary Medicine, Auburn University, Auburn, Alabama, USA

[3]School of Life Sciences and Technology, Tongji University, Shanghai, China

[4]Department of Electrical and Computer Engineering, Samuel Ginn College of Engineering, Auburn University, Auburn, Alabama, USA

[5]Department of Clinical Sciences, College of Veterinary Medicine, Auburn University, Auburn, Alabama, USA

[6]Center for Advanced Science, Innovation and Commerce, Alabama Agricultural Experiment Station, Auburn, Alabama, USA

[7]HudsonAlpha Institute for Biotechnology, Huntsville, Alabama, USA

## *1 Introduction*

Obesity is prevalent in domestic cats and is associated with many co-morbidities, including insulin resistance and type 2 diabetes mellitus (T2DM) (138, 139). A significant sequela associated with feline obesity is increased intrahepatic lipid accumulation, predisposing cats to hepatic lipidosis (140, 141). The health risks associated with increased baseline liver lipid content are compounded by the mobilization of fatty acids from adipose tissue, increased insulin resistance, and the release of inflammatory mediators.

Fibroblast growth factor 21 (FGF21) is a member of the endocrine subfamily of fibroblast growth factors primarily produced in the liver that regulates the metabolic adaptation to fasting by binding to primarily FGF receptor 1c (FGFR1c) and its cognate co-receptor β-klotho in metabolic tissues (142). Among its numerous downstream effects, FGF21 stimulates gluconeogenesis, ketogenesis, and fatty acid oxidation in the liver and stimulates glucose uptake, lipolysis, and β-oxidation in the white adipose tissue (143). FGF21 analogs have been used in humans and animal models to ameliorate metabolic dyscrasias secondary to obesity. Studies that evaluate exogenous administration of FGF21 in obese and insulin-resistant humans show significant benefits such as weight loss, reduced blood glucose, reduced cholesterols and low-density lipoproteins, and resolution of hepatic steatosis with minimal to no side effects (113, 121, 124). LY2405319 (Eli Lilly and Company, Indianapolis, IN) is a modified human recombinant FGF21 analog engineered for increased stability and retained metabolic benefits and has been successfully used to treat obesity and hyperglycemia in rodent and primate models (112, 144). A benefit of LY2405319 is that it is more easily produced in large scales and has increased thermal and conformational stability over unmodified human recombinant FGF21 (109), meaning it can be prepared for a potential commercial, multiuse formulation suitable for veterinary hospitals.

However, very little research has been done regarding FGF21 analog use in companion animals, and no research has been published on FGF21 in cats. Obese and overweight cats have an altered gut microbiota compared to lean cats (145), and common factors such as fasting have been shown to alter both circulating FGF21 and the gut microbiome (71, 146). While there is evidence that the microbiome regulates FGF21 (147), studies that evaluate the direct influence of exogenous FGF21 on the gut microbiome are limited (148).

Proton magnetic resonance spectroscopy (1H-MRS) is a non-invasive, highly sensitive and specific method of quantifying liver triglyceride content (149). 1H-MRS is commonly used for hepatic triglyceride quantification in studies of humans (150, 151) and many animal species (152, 153) and has been previously used to determine hepatic triglyceride content in lean and obese cats (140). Shear wave elastography methods are promising as a non-invasive tool for diagnosing and grading hepatic fibrosis and steatosis in humans (154, 155). Elastography has been safely used to evaluate the livers of healthy adult cats but has not been well explored in veterinary medicine as a point-of-care diagnostic and monitoring modality for hepatic lipidoses (156).

The overall objective was to explore if FGF21 could be used safely and efficaciously to treat common obesity-associated metabolic dyscrasias, utilizing a research colony of obese and overweight cats with similar insulin resistance and metabolic alterations. Specifically, we focused on body weight, serum metabolic parameters, serum liver enzymes, and intrahepatic lipid content. Our primary hypothesis was that FGF21 administration would lead to decreased body weight independent of food intake. Following that, our secondary hypotheses were that FGF21 administration would improve glucose and lipid homeostasis, decrease intrahepatic lipid content, and potentially alter gut microbiota, secondary to weight loss. We also hypothesized that

decreased liver lipid content would decrease hepatic elasticity and could potentially be used as a less invasive measure of hepatic lipid content in obese and overweight cats compared to a liver biopsy or 1H-MRS. In this preliminary study, we show that FGF21 significantly lowers body weight in cats. Additionally, FGF21-treated cats had a trend towards a decrease in hepatic triglyceride with a corresponding significant decrease in the enzymatic marker of hepatic triglyceride content, serum alkaline phosphatase (157). However, there were no detectable effects on lipid or glucose homeostasis or hepatic elasticity.

## *2 Materials and methods*

### *2.1 Animals*

Eight purpose-bred, specific pathogen-free, 6-year-old, neutered, Domestic Shorthair cat male cats were housed individually at the Scott Ritchey Research Center (Auburn University, AL). All studies were performed in line with the Auburn University Institutional Animal Care and Use Committee (IACUC) protocol (protocol number 2019-3482). Cats were provided environmental enrichment and allowed to group socialize under researchers' direct supervision once a day outside of their kennels. Animals were cared for according to the principles outlined by the United States Department of Agriculture (USDA) Animal and Plant Health Inspection Service's Animal Welfare Act and the American Associated for the Accreditation of Laboratory Animal Care (AAALAC) Guide for the Use of Laboratory Animals. No animals were euthanized for this study. All facilities are University IACUC approved, and USDA and AAALAC accredited.

Prior to the initiation of this study, cats were allowed to gain weight on a non-restricted chow diet formulated for cats (27.4% calories provided by fat, Feline Lab Diet, Purina, St. Louis,

MO). This ad libitum diet was continued throughout the remainder of the study. At the start of the study, all cats were overweight or obese (defined as a body condition score of > 5) and had evidence of insulin resistance but were not overtly diabetic or glucosuric. Based on comparisons from lean and obese body weight data and blood glucose levels, it was determined that a minimum of 3 cats for the treated and control groups was needed to get an effect size (β) of 0.8. At the start of the study, four cats were assigned to the treatment or control group (n = 4) to maintain no significant differences between blood glucose or body weight (unpaired t-test, p = 0.25 and p = 0.65, respectively) to conduct a cross-sectional study. After the initiation of saline injections, one of the control cats developed severe anorexia and was removed from the study on day 3 for medical reasons. Baseline blood glucoses and body weights remained non-significantly different after removal of the subject (p = 0.35 and p = 0.53, respectively).

*2.2 Treatment*

Cats were injected subcutaneously with a 10 mg/kg/day dose of sterile recombinant FGF21 (LY2405319) diluted with sterile saline to a final total daily injection volume of 5 mL or with 5 mL of sterile saline (control) for 14 days. Injection sites were rotated daily between the shoulder and hind limb and monitored for heat, redness, swelling, hair loss, or ulceration.

*2.3 Weight, food and water consumption measurements*

Food and water consumption and body weight were determined daily. Each cat was allowed 200 g of dry food and 500 mL of water per day, and at no point did any cat consume all food or water given within 24 hours.

*2.4 Blood, urine, and feces collections*

Before all blood, urine, and feces collections, cats were fasted for 10 hours. Blood was collected from cats under general anesthesia or sedation. The week before injections and on day

14 of treatment, a complete blood count (Advia 120 Hematology, Siemens), standard serum biochemistry panel with triglycerides (Cobas C 311 Analyzer, Roche), blood glucose (AlphaTrak2) (158), and a urinalysis (Multistix 10 SG, Siemens) was performed on each cat. Urine was collected either free catch with manual expression or with ultrasound-guided cystocentesis. Serum was separated from the remaining whole blood through centrifugation at 800 g for a minimum of 15 minutes (Heraeus Megafuge 16R, Thermo Scientific) and stored at -80˚ C until needed. Non-Esterified Fatty Acids (NEFAs) and insulin were quantified from serum using the commercially available HR Series NEFA-HR(2) (Wako Diagnostics) and Feline Insulin ELISA (Mercodia) kits (159), respectively. Feces were collected by placing a plastic fecal loop into the rectum and descending colon to obtain an adequate amount (> 200 mg) of feces. All fecal specimens were stored until analysis at -80 C. The homeostatic model assessment for insulin resistance (HOMA-IR) was calculated as the product of the basal glucose and insulin concentrations, divided by 22.5, as previously described and validated in the literature (160, 161). Adipose tissue insulin resistance (Adipo-IR) was calculated as the product of fasting serum insulin and NEFAs (162).

*2.5 Whole genome shotgun metagenomic sequencing of the fecal microbiome*

Two fecal samples were collected from each cat using a fecal loop with and without lubrication (N = 14 total; Table 1) (163). At least 200 mg feces were used for DNA extraction by Qiagen Allprep PowerFecal DNA/RNA kit (Qiagen), following the protocols provided by the manufacturer. During DNA extraction, fecal samples were homogenized by the Qiagen PowerLyzer24 instrument (Qiagen) to achieve homogeneous results. The extracted DNA concentrations were measured by the Qubit 3 Fluorometer (Invitrogen), and A260/A280 absorption ratios were assessed using the NanoDrop One C Microvolume Spectrophotometer

(Thermo Fisher Scientific). DNA fragmentation was performed by M220 Focused-ultrasonicator (Covaris) on 1.5~2 μg of DNA for each sample to achieve fragmented DNA of ~500bp. NEBNext Ultra II DNA Library Prep Kit for Illumina (New England Biolabs) was used to construct WGS metagenomic sequencing libraries using the fragmented DNA. Final library concentrations and size distributions were measured by LabChip GX Touch HT Nucleic Acid Analyzer (PerkinElmer) before being sequenced on an Illumina NovaSeq6000 sequencing machine on the 150-bp paired-end mode at the Genomics Service Laboratory at the HudsonAlpha Institute for Biotechnology (Huntsville, AL).

*2.6 Metagenomic data analysis*

Adapter sequences and low-quality sequences were eliminated with Trimmomatic (v0.36) (33). Filtered reads were then mapped to the cat reference genome (GCF_000181335.3), viral genome database, and rDNA sequences downloaded from National Center for Biotechnology Information (NCBI) using Burrows-Wheeler Aligner (BWA) (v0.7.17-r1188) (164) and SAMtools (v1.6) (165). The remaining microbial reads were extracted using BEDTools (v2.30.0) and aligned to the feline gut microbiome reference contigs (GCA_022675345.1) (145). The alpha- and beta-diversity of taxonomy profiles were performed using R package vegan v2.5.7 (166) at the species level using Shannon index and Bray-Curtis dissimilarity. Mann Whitney U Tests (167) and permutational multivariate analysis of variance (PERMANOVA) (168) were used to determine significant differences in α- and β-diversities between FGF21 and saline-treated cat groups. To assess the statistical significance of the differential abundance of species between treatments, Kruskal–Wallis tests (169) were performed in R. The adjusted P-values were calculated using R package qvalue (v2.22.0) (170). The criteria for detecting significantly alter microbial species are qvalue < 0.05 and log2 fold change > 1.5.

*2.7 Calculation of lipid fraction in liver*

Within one week prior to the start of FGF21 injections, cats were anesthetized and proton magnetic resonance spectroscopy (1H-MRS) using a Siemens Magnetom 7T Actively-Shielded Scanner was performed to determine the lipid fraction of the liver. 1H-MRS was repeated on day 14 of the FGF21 or saline injections.

Cats were positioned in ventral recumbency, and bellows were used for respiratory gating. The knee coil was used in signal acquisition. Three plane respiration-guided scout images were acquired for spectroscopy volume localization, and STEAM pulse sequence was used for MRS data acquisition. Data was acquired from 5 × 5 × 5 mm3 spectroscopic volume placed in the right hepatic lobe. Animals were allowed to breathe freely throughout the scan while ensuring data were collected from the specified voxel location in the liver via bellows-based respiratory gating. Data were acquired with TE = 8 ms, TR = 6 sec, TM = 20 ms, and 32 averages were collected. The spectral width was 3200 Hz, and the vector size was 2048 points.

Spectra were analyzed using the AMARES module of jMRUI (171, 172). Briefly, water (H2O at 4.7 ppm), methyl (CH3 at 1.3 ppm), and methylene (CH2 at 0.9 ppm) resonances were modeled with Lorenzian sinusoids to determine the area under the resonances. The fat fraction was defined as the ratio of the areas of the methyl and methylene resonances to that of the water plus methyl and methylene (140, 173). The average value of the fat fraction was determined from 2 unique liver voxels.

*2.8 Calculation of organ elasticity*

The use of 2D shear wave elastography with acoustic radiation impulse force (ARIF) technology is used to assess tissue elasticity (174). Elastography has been established in the livers of healthy cats (156) and is primarily used to evaluate feline chronic kidney disease (175).

Shear wave elastography was performed using a Toshiba Aplio 500 ultrasound machine with a 15L5 linear probe before and after the injection period under heavy sedation. Tissue elasticity value was recorded using shear wave speed quantified as Young's modulus and expressed in kPa. Between 6 and 8 intralobular sites within the right liver, central liver, and left liver were acquired with the tissue elasticity reported from the average across the three portions (right, central, left) of the liver. Areas within the liver devoid of large vascular or ductal structures were chosen. The shear wave sampling ROI and depth were kept uniform between patients.

### *2.9 Statistical analysis*

Metabolic parameters, liver lipid content, and elastography are all presented in box and whisker plots as individual animals change from baseline in both the FGF-treated and control groups. Whiskers on box and whisker plots represent minimum and maximum values. Unpaired student t-tests were performed to compare individual changes between FGF21 and control groups. Paired t-tests were performed for all comparisons within the FGF21 and saline groups.

Changes from baseline of weight, food, and water intake were calculated in a repeated measures fashion to account for individual variability. Water and food consumption were calculated as a ratio to body weight for each cat as mL/kg ("corrected water intake") or g/kg ("corrected food intake)" to control for differences in water and food intake that may be due to differences in body weight.

To determine the rate of weight loss and weight gain, the slope was obtained from simple linear regressions on the percentage weight change from baseline to the nadir weight (weight loss) and then from nadir weight to end of study weight (weight gain). All areas under the curve (AUC) represent net AUC with inclusion of peaks below baseline and no minimum peak height

and were calculated using the linear trapezoidal method. AUCs were compared by using unpaired t-tests.

For data with bar graphs of the metabolic, liver lipid content and elastography, absolute values at baseline and end point are plotted in bar graphs with individual animals denoted. Data represents mean ± SD. Paired t-tests were performed for all comparisons within the FGF21 and control groups, and unpaired t-tests were performed for all comparisons between the FGF21 and control groups.

All statistical methods except those used for microbiome analysis in the metagenomic data analysis section were performed using GraphPad Prism 9 (Dotmatics). An α level of 0.05 was used to determine statistical significance for all methods.

## *3 Results*

### *3.1 Morphometric Parameters*

FGF21-treated cats had a steady decrease in body weight percentage at a rate 2.54 times greater than the control cats (Figure 1A). The mean weight loss from baseline of the FGF21-treated cats reached a maximum of 0.375 kg on day 15 post initial FGF21 injection (Figure 2A, Table 2), corresponding to a 5.93% decrease in body weight. At the same point in the study (Day 15), the saline-treated group had only a mean weight loss of 0.017 kg in body weight or a 0.28% decrease in body weight. During the treatment period (Day 1 to Day 15), the rate of body weight loss for FGF21 treated cats was 0.34% (±0.062, 95% confidence interval [CI], $Y = -0.3395*X + 0.7709$, $R^2 = 0.68$) compared to 0.13% (±0.071, 95% CI, $Y = -0.1339*X + 1.407$, $R^2 = 0.25$) for control cats. During the two-week washout phase, or days 15 to 28, FGF21-treated cats began to regain weight. Each day without FGF21 treatment corresponded to a 0.265% (±0.11, 95% CI)

regain in weight compared to Day 15 ($Y = 0.2653*X - 9.452$, $R^2 = 0.30$). The net AUC for the weight change for days 1 to 28 for FGF-treated cats was -4.6 kg*day (±0.61, 95% CI), whereas the net AUC for this same period for the saline-treated cats was -0.13 kg*day (±0.44, 95% CI, $p < 0.0001$).

The FGF21-treated and control groups had similar food intake for the entire study period, or days 1 to 28 ($p = 0.26$, Figure 1B, Figure 2B). For the FGF21-treated group, the net AUC for corrected food intake from baseline between days 1 and 28 was -36.86 g*day/kg (±19.8, 95% CI). For the control group, the net AUC for corrected food intake for the same period was -20.58 g*day/kg (±17.4 g, 95% CI). When examined at different times during the study, the FGF21-treated and control groups also ate a similar amount of food during the treatment period (day 1 to 14) ($p = 0.11$) as well as during the washout period (day 15 to 28) ($p = 0.94$).

Both groups had similar water intake throughout the study period ($p = 0.27$, Figure 1C, Figure 2C).

*3.2 Metabolic parameters*

At the start of the study, baseline blood glucose was similar between treatment groups ($p = 0.35$, Figure 3). After 14 days of treatment, the changes in blood glucose between the FGF21-treated and control groups were also similar ($p = 0.52$, Figure 4A). In both groups, absolute blood glucose concentrations remained steady over the treatment period with no significant changes noted (FGF21; $p = 0.89$ and control; $p = 0.24$, Figure 3).

The serum insulin levels were similar at the beginning of the study between the FGF21-treated and control groups ($p = 0.74$, Figure 3B). There was no significant difference in the change in serum insulin concentrations between the FGF21 and control groups ($p = 0.79$, Figure 4B) following the 14-day treatment period. At the end of the treatment period (Day 14), the

groups had similar serum insulin levels with no significant difference detected ($p = 0.93$) (Figure 3B).

In cats, HOMA-IR is considered a predictor of insulin resistance (160) and correlates with body fat (161). FGF21 treatment did not significantly alter changes in insulin resistance, and the change in HOMA-IR between the groups was not significantly different following the treatment period ($p = 0.88$, Figure 4C), consistent with both insulin and glucose. However, the control group decreased insulin resistance between days 0 and 14 (Figure 4C). As with blood glucose and serum insulin, HOMA-IR between the FGF21-treated and control groups were similar at the beginning of the study ($p = 0.10$, Figure 3C).

FGF21 treatment did not significantly affect changes in serum NEFAs ($p = 0.61$, Figure 4D), triglycerides ($p = 0.47$, Figure 4E) or cholesterol ($p = 0.46$, Figure 4F) concentrations in cats. The NEFA, triglyceride, and cholesterol levels were similar at the beginning of the study for both the FGF21-treated and control groups ($p = 0.76$ and $p = 0.26$ and $p = 0.83$, respectively). Concentrations of the lipid parameters did not change within groups throughout the study (Figures 3D, 3E, and 3F).

Adipo-IR is used in humans and rodents as a non-invasive measure of insulin resistance in adipose tissues. FGF21 did not significantly alter changes in Adipo-IR between the FGF-21 and control groups ($p = 0.97$, Figure 3G). In both groups, Adipo-IR remained steady for the treatment period with no significant changes noted (FGF21; $p = 0.98$ and control; $p = 0.95$, Figure 3H).

### *3.3 Assessment of Hepatic Triglyceride Content and Elasticity*

Assessment of lipid fractions based on H1-MRS of regions from the right hepatic lobe indicates a trend toward decreased liver lipid content in cats treated with FGF21 compared to

control (Figure 5A, 5B); however, the change in liver triglyceride content between the two treatment groups did not reach statistical significance ($p = 0.055$, Figure 5A, 6A). As expected for obese and overweight cats and consistent with other studies (140), the baseline values for liver triglyceride content before treatment averaged 4.79% ± 3.36% SD, and there was no difference in liver lipid content between groups at the start of the study ($p = 0.10$). Despite significant and rapid weight loss, FGF21-treated cats had a 1.86% decrease in liver triglyceride content (Figure 6A). In contrast, saline-treated cats had a 2.89% increase in liver triglyceride content.

Liver tissue elasticity was evaluated using 2D shear wave elastography with acoustic radiation impulse force (ARIF) (Figure 5D). There was no difference in change in liver elasticity between treatment and controls ($p = 0.16$, Figure 5C, Figure 6B).

### *3.4 Serum hepatic analytes*

A significant difference was noted in the change in alkaline phosphatase (ALKP) activity between treatment groups ($p = 0.01$, Figure 7A, Figure 8A), a marker of feline hepatic lipidosis (157). There were no significant differences in the changes in serum alanine aminotransferase (ALT) ($p = 0.26$, Figure 7B, Figure 8B) or changes in total bilirubin ($p = 0.72$) (Figure 7C, Figure 8C) between control and FGF21 treatment. The individual changes in AST in FGF21 and control groups were similar ($p = 0.13$, Figure 7D, Figure 8D).

### *3.5 Gut microbiota*

A total of 168 Gb metagenomic sequences were obtained for the 14 fecal microbiomes, with an average of 79.9 million reads per metagenome (Table 1). The average host contamination is 10.6%. Taxonomic annotation and relative abundance quantification were performed according to a pipeline reported previously in (145). A total of 8582 bacterial species

were identified in the 14 cat metagenomes. Between the FGF21-treated and control saline-treated group, no significant difference in microbial alpha diversity was discovered ($p = 0.90$, Kruskal-Wallis rank sum test; Figure 9A). The Principal Coordinates Analysis (PCoA) plot of beta diversity did not reveal any significant separation of the two treatment groups either ($p = 0.13$, PERMANOVA, Figure 9B). At an FDR < 5% and minimum $\log_2$ fold change of 1.5, none of the microbial species have significant differences in abundance between FGF21 and saline-treated groups, suggesting a lack of changes in the gut microbiome.

*3.6 Safety*

There was no evidence of tissue necrosis or sloughing in the FGF21-treated and control cats at the injection sites. Some mild pain with palpation was noted at the injection site in both groups. All cats in the study remained healthy, apart from obesity, within a 6-month post-treatment observation period. All cats treated with FGF21 are alive and reportedly in good health at two years post-treatment follow-up.

## *4 Discussion*

This is the first study to describe the effects of activation of the novel FGF21 pathway in cats. This study provides strong evidence that FGF21 analogs can safely induce weight loss in obese and overweight cats without major influence on caloric (food) intake or water intake. Subcutaneous injections of 10 mg/kg/day of the FGF21 analog LY2405319 in obese and overweight cats safely, steadily, and significantly decreased their weight, despite ad libitum feeding and without changes in food intake, consistent with observations in many studies of FGF21 administration in rodents, non-human primates, and humans (112, 113, 115, 116, 176, 177). Once FGF21 was discontinued in the cats, we observed an immediate and steady return to

baseline body weight, similar to what was noted during the post-treatment period in non-human primates (112, 116, 178). The decrease in weight without a concurrent reduction in caloric intake points to increased energy expenditure via the basal metabolic rate modulation as reported in rodents (144, 179, 180). Mice treated with recombinant FGF21 have dose-dependent weight loss from increased resting energy expenditure and fat utilization without decreasing food intake (144, 179, 180). In non-human primates, many publications describe weight loss concurrent with reduced food intake, but whether or not the weight loss was solely due to decreased caloric intake is debated (112, 116, 176, 177). Other causes of weight loss without reduced caloric intake, rather than increased basal metabolic rate, such as decreased nutrient absorption, are unlikely as there were no supportive clinical signs such as diarrhea or steatorrhea. In addition, the absence of significant differences between control and FGF21-treated cats in the gut microbiome suggests GI malabsorption is unlikely. Future studies investigating FGF21 in cats should evaluate metabolic mechanisms for weight loss, including fat distribution and body composition, appetite, and resting metabolic rate determination. The significant decrease in body weight is somewhat surprising given the preliminary nature of this study and the low numbers of animals in each group. These findings indicate that the dose was sufficient to elicit an effect in obese and overweight cats.

Contrary to our expectations, we did not see changes in circulating glucose, insulin, or lipid parameters (NEFAs, cholesterol, triglycerides). HOMA-IR has been used as an indicator of insulin sensitivity in cats, and the overweight and obese cats used in this study had HOMA-IR calculations consistent with reported values for obese and overweight glucose intolerance (160). Additionally, overweight and obese cats with increased proportions of body fat have greater insulin resistance as calculated with HOMA-IR (161). We expected that FGF21 treatment would

improve insulin sensitivity as reported in other species, but the overall decreases in insulin sensitivity remained static between the control and FGF21-treated groups. Adipo-IR is a non-invasive predictor of specifically adipose tissue insulin resistance (162, 181). Our study did not show any alterations in Adipo-IR with FGF21 treatment, despite the weight loss. This suggests that FGF21 drives lipolysis of the adipose tissue stores without a change in adipose insulin resistance. The predictive measure Adipo-IR has not previously been used in cats, so further studies are needed to determine how well this value translates from humans and rodent models. One explanation for these findings is that none of the cats used in this study had marked metabolic dyscrasia or type 2 diabetes mellitus (T2DM), unlike the human and non-human primates in other studies treated with FGF21. Potentially, insulin resistance and dyslipidemia were not severe enough in our cats for FGF21 pathway activation to significantly affect the treatment group. A lack of FGF21 response in more metabolically healthy animals has been reported in Siberian hamsters in a study where the leaner animals had a reduced to absent effect of FGF21 on glucose homeostasis and weight loss (182). Another possibility is that the chow diet blunted the FGF21 response. Supporting this, non-obese chow-fed mice treated with FGF21 have blunted increase in energy expenditure than high-fat diet mice (183). These factors, in combination with the few subjects in each cohort, limited the power of the study to detect changes in these parameters. Further studies are warranted in cats with more severe metabolic disease to determine if FGF21 treatment indeed lacks influence on this species.

In rodent models, treatment with FGF21 has beneficial metabolic effects on adipose tissue, including adipose tissue browning and thermogenesis, increased insulin sensitivity of adipose tissue, a reduction of adipose tissue macrophages, promotion of adipose glucose disposal, and lipolysis of white adipose tissues. These mechanisms have a compounding effect

on increasing total energy expenditure, lowering blood glucose, and promoting weight loss (184-187). In our study, there was no significant change in Adipo-IR or blood glucose, but there was a decrease in body weight, suggesting that in cats FGF21 treatment did not significantly alter adipose insulin sensitivity or glucose disposal while still promoting lipolysis, suggesting that there are unique differences in the feline FGF21 pathway. Ideally, future studies should investigate adipose tissue stores from FGF21-treated and control cats and assess parameters including browning of adipocytes, FGF21 receptor distribution, inflammatory macrophage infiltration, and evaluation of markers of adipose tissue metabolism. Future non-invasive studies that evaluate FGF21 in vivo can investigate changes in circulating parameters such of obesity-associated inflammatory cytokines to indirectly assess adipose tissue inflammation (188), or determine if there are preferential sites of lipolysis in the adipose tissue (e.g. with computed tomography (CT)) (189). Determining if there is truly increased energy expenditure in cats, as suggested by the weight loss without increased caloric intake in our study, would require the use of metabolic cages adapted for cats (190).

While we observed substantial change in body weight, it is possible that the dose or treatment duration were not sufficient to produce a metabolic response. The dose, dose interval, and treatment duration were chosen based on published doses and time to parameter response without negative side effects for subcutaneous LY2405319 administrations in the published literature in obese humans with type 2 diabetes mellitus, type 2 diabetic rhesus macaques, and mice to determine the most likely effective dose and treatment period in cats. In obese T2DM humans, significant changes in metabolic parameters (serum glucose and triglycerides) were noted after 3 - 7 days at a dose of 3 mg per day. In rodents, subcutaneous administration of up to 1 mg/kg/day of LY2405319 resulted in decreased glucose by day 1 with a decreased plasma

insulin following 7 days (109). In diabetic rhesus monkeys in a dose escalation study, there was a significant decrease in plasma glucose, triglycerides, and cholesterol by day 21 and significant changes were noted when a dose of 9 mg/kg was achieved (112). The duration of treatment in this study was also influenced by a study of streptozotocin-induced diabetic dogs subcutaneously administered 0.5 mg/kg/day of recombinant canine FGF21, which brought the blood glucose to levels close to those of the control non-diabetic dogs by day 4 (130). We selected a route of administration that would be easy for veterinary personnel to utilize in a future potential clinical setting. Subcutaneous administration is an extremely common route of administration in veterinary medicine and is achievable by veterinary personnel of many different expertise levels or even trained owners.

It may be possible that the lack of metabolic changes in this study reflect some of the inconsistent outcomes reported in the literature regarding various FGF21 analogs in animal models of insulin resistance and obesity. While decreases in blood glucose, insulin, plasma triglycerides, and low-density cholesterols and increases in high-density cholesterols were observed in T2DM non-human primates and humans treated with LY2405319 (112, 113), another FGF21 analog, PF-05231023, in contrast, had minimal effect on glucose and insulin in humans and monkeys (116). Although FGF21 is able to stimulate beneficial effects on a wide variety of tissues, the overwhelming majority of the glucose and adipose regulating functions of FGF21 appear to be via signaling on the liver and adipose tissue (184). In murine livers, FGF21 induces free fatty acid oxidation and increases glucose tolerance and energy expenditure. In adipose tissue, FGF21 induces browning and lipolysis and increases energy expenditure (183, 184). It is possible that the hepatic downstream signaling of FGF21 is diminished or altered in

cats relative to the adipose tissue signaling, resulting in a decreased effect on insulin sensitivity compared to other animals.

One additional potential reason for the lack of metabolic changes is that LY2405319 is based on human FGF21 protein and not derived from the cat FGF21 protein. LY2405319 is a recombinant human FGF21 protein that had been engineered for increased Pichia pastoris host protein production and improved physical stability (109). The sequence chains of human FGF21 (UniProt identifier Q9NSA1[29-209]) and feline FGF21 (M3W7L7 [28-208]) have an 84.5% identity and an 89.5% similarity using the EMBOSS Needle Pairwise Sequence Alignment tool (25), a slightly higher degree of structural similarity compared to human and mouse FGF21 (Q9JJN1 [29-210]), which have 80.5% identify and 84.9% similarity. As LY2404319 has similar pharmacological effects as FGF21 in mice (109), it reasons that LY2405319 would have similar pharmacological effects as endogenous FGF21 in cats due to the high protein similarity with humans. However, LY2405319 and feline FGF21 are not identical, and it is possible that these differences are enough to have reduced receptor activation and, consequently, the observed lack of metabolic results. The co-receptors of FGF21, beta-klotho (KLB) and fibroblast growth factor receptor 1 (FGFR1), have similarly relatively good interspecies conservation between cats and humans. Although no work, to the authors' knowledge, has been done on the feline FGF21 pathway machinery, it can be inferred from this homology that the signaling pathway is conserved. Feline KLB (M3XDH3) and human KLB (Q86Z14) have 83.8% identity and 90.3% similarity, and feline FGFR1 (A0A2I2UK29) and human FGFR1 (P11362) have 95.1% identity and 95.4% similarity. Investigations in gene and protein expression of FGF21, its receptors, and its downstream mediators in tissues, particularly the liver and adipose tissue, are warranted to determine which FGF21 pathways drive energy expenditure and glucose and lipid homeostasis in

cats. In order to determine the cell-specific effects of the FGF21 pathway, additional studies are needed, particularly in primary feline hepatocyte and adipocyte cell cultures that investigate mechanisms such as adipokine and hepatokine secretion, lipolysis, and glucose disposal and consumption. Future potential studies such as these will allow us to investigate the physiologic responses in expected organ systems and help identify in vitro if species-specific differences in adipose or liver tissue signaling are contributing to the differences noted in cats (191, 192).

In our study, the change in liver triglyceride content based on 1H-MRS decreased in FGF21-treated cats and increased in the saline-treated cats, though these changes did not reach statistical significance. Concurrently, the change in ALKP was significantly decreased in FGF21-treated cats compared to the control cats. ALKP is a sensitive indicator of feline hepatic lipidosis (193) and based on our findings, we believe that a decrease in intrahepatic triglycerides may be driving these decreases in serum enzyme activity. These findings are particularly interesting as our obese cat colony does not have as marked an increase in hepatic triglyceride content compared to human and rodent studies. In our study, the baseline hepatic triglyceride content ranged from 2.71% to 12.19%. Studies investigating liver triglyceride content in obese non-human primates and humans report liver triglyceride contents consistently over 10% (194, 195), and in rodent studies, the hepatic triglyceride can reach near 90% (196). Changes in hepatic triglyceride content may be more pronounced in cats with hepatic pathology (e.g., lipidosis), and future studies are needed to determine if activation of the FGF21 pathway could be used to decrease hepatic triglyceride in more severely affected cats. There is some evidence that FGF21 can be used as an anti-inflammatory in pancreatitis (197, 198). As a large proportion of cats with pancreatitis also have hepatic lipidosis (199, 200), further investigation of the anti-inflammatory effects of FGF21 analogs in cats with pancreatitis and concurrent hepatic lipidosis is needed,

particularly since there are very few effective therapeutic options for these conditions, and access to medications that can reduce liver lipid content and reduce pancreatic inflammation could have an important impact on reducing the morbidity and mortality of hospitalized feline patients.

Compared to their baseline values, FGF21 treatment decreased serum AST activity on Day 14; however, there was no difference in the change in AST activity between saline-treated and FGF21-treated cats. A concurrent decrease in the hepatocellular leakage enzyme ALT was not observed and suggested that non-hepatic sources of AST activity, such as in the muscle (193, 201), could contribute to this finding. In mice, FGF21 acts as a myokine and is associated with decreased muscle mass and impaired mitochondrial function, but the biological significance of these findings is debatable due to low muscle receptor expression (101, 202). Investigations into FGF21 gene and receptor expression within skeletal muscle in cats may be needed to determine the effects of FGF21 on feline skeletal muscle.

There are limited studies that investigate the effects of FGF21 on the gut microbiome (148), and evidence suggests that the hepatic FGF21 adaptive metabolic response is mediated by the gut microbiome (147). We did not note any significant difference in microbial diversity between treated and control cats, and none of the eight thousand bacterial species showed significant change in abundance at a 5% FDR. If a less stringent statistical cut-off of 10% FDR was applied, 246 bacteria showed alterations in relative abundance. However, all but one had extremely low abundance (<0.01%), which is likely to reflect sampling variability rather than biological relevance. Concurrent with our results, a recent study in humans administered FGF21 also noted that treatment did not affect fecal microbiome taxonomy (148). Recently, the metagenomic sequence of the feline gut microbiome was described, and distinct differences in the diversity and abundance of certain species were noted between lean and obese cats (145).

While the cats in our study did lose significant weight, they did not lose enough weight to significantly reduce their body condition score or to reclassify them as having a healthy body weight. In this study, FGF21 was administered subcutaneously, meaning that effects, if any, would likely be associated with the ability of FGF21 to alter the host environment. It is also likely that the microbiome may alter the FGF21 adaptive stress response, but not the other way around.

Elastography measures the stiffness or viscosity of an organ and has been proposed as a point of care, non-invasive method to evaluate chronic liver diseases in humans, including the most common cause of liver disease in people, non-alcoholic fatty liver disease. In our study, there were no changes in hepatic elasticity before or after treatment, and there was no difference in the change of elasticity between treatment groups, consistent with other recent studies (203). For humans, shear wave elastography correlates well with fibrosis in liver biopsies, the current gold standard (204). Unlike feline chronic lymphocytic cholangiohepatitis (205) or congenital hepatic fibrosis (206), feline hepatic lipidosis is a more acute disease syndrome that does not involve substantial fibrosis or cirrhosis. As such, an additional goal of our study was to determine if liver elasticity would be affected by subtle changes in the liver lipid content associated with FGF21. Based on our findings, it is unlikely that elastography is sensitive enough to detect changes associated with lipid accumulation and thus has little potential to be used as a less invasive point-of-care monitoring tool for feline hepatic triglyceride content, but further studies, including the use of other modalities of elastography, are needed to evaluate the clinical use of elastography in chronic veterinary hepatic diseases, particularly those with prominent fibrosis. Additional diagnostic tools to better quantify liver lipid content rapidly and effectively could provide greater insight into hepatic health. It would also be interesting to investigate

changes in liver elasticity in animals with more severe hepatic lipid accumulation, such as hepatic lipidosis.

One major limitation of our study was the number of cats in each group, which was limited by the number of obese and overweight cats within the feline obesity research colony. This likely led to an underpowering of many of the metabolic and liver parameters. Despite this underpowering, the FGF21 treated group had a significantly increased rate of weight loss compared to the control group indicating a significant drug effect. As we know that FGF21 treatment is safe, it would be worthwhile to, in a clinical trial study, expand FGF21 treatment to a larger cohort of cats, potentially overweight or obese client-owned cats with hepatic lipidosis or at risk for hepatic lipidosis, and evaluate if there are decreases in or further prevention of liver lipid accumulation in the target population. It is possible that repeating the study with a longer treatment period may yield more dramatic changes. Additional studies are needed to supplement these pilot data in order to fully explore the pharmacokinetics of this FGF21 mimetic in cats, particularly if there are potential therapeutic benefits to cats.

In summary, activation of the FGF21 pathway can safely induce weight loss with trends to improve liver lipid content in obese and overweight cats. Under these study conditions, FGF21 does not appear to alter glucose homeostasis or serum lipids in cats with mild metabolic dyscrasias. Independent of lipid and glucose-modulating effects, manipulation of the FGF21 pathway may potentially be therapeutic for feline obesity and, more importantly, hepatic lipidosis. This is the first study investigating an FGF21 analog in cats and demonstrates a potential unique metabolic response. Further work is needed to better understand the feline FGF21 signaling pathway.

**Table 1.** Whole genome shotgun metagenomic sequencing yield, control statistics, and accession IDs.

| cat ID | Treatment | Sample Number | Accession ID | # of reads | Sequences (GB) | host contamination % |
|---|---|---|---|---|---|---|
| D001 | FGF21 | 1 | SRR18550130 | 86,166,510 | 12.9 | 1.08% |
| | | 2 | SRR18550144 | 96,593,290 | 14.5 | 0.96% |
| F001 | FGF21 | 1 | SRR18550129 | 101,557,634 | 15.2 | 31.78% |
| | | 2 | SRR18550143 | 123,360,100 | 18.5 | 22.24% |
| H001 | FGF21 | 1 | SRR18550141 | 112,269,038 | 16.8 | 16.29% |
| | | 2 | SRR18550135 | 43,897,220 | 6.6 | 6.34% |
| K001 | FGF21 | 1 | SRR18550138 | 91,228,332 | 13.7 | 6.59% |
| | | 2 | SRR18550132 | 23,219,858 | 3.5 | 25.47% |
| I001 | saline | 1 | SRR18550140 | 84,738,496 | 12.7 | 8.73% |
| | | 2 | SRR18550134 | 42,586,664 | 6.4 | 17.24% |
| G001 | saline | 1 | SRR18550142 | 86,937,904 | 13.0 | 1.16% |
| | | 2 | SRR18550136 | 72,136,664 | 10.8 | 2.73% |
| J001 | saline | 1 | SRR18550139 | 72,200,540 | 10.8 | 3.12% |
| | | 2 | SRR18550133 | 81,111,494 | 12.2 | 4.04% |

**Table 2**. Weights of each cat assigned to either the FGF21-treated or control group taken during baseline (Day 0), post-treatment period (Day 15), and post-washout period (Day 28). Each row represents an individual cat.

| | **Baseline weight (kg)** | **Post-treatment weight (kg)** | **Post-washout period weight (kg)** |
|---|---|---|---|
| FGF21-treated cats | 6.95 | 6.60 | 6.90 |
| | 5.50 | 5.10 | 5.30 |
| | 6.55 | 6.10 | 6.45 |
| | 6.30 | 6.00 | 6.25 |
| Control cats | 5.30 | 5.25 | 5.30 |
| | 6.95 | 6.95 | 6.85 |
| | 5.60 | 5.60 | 5.60 |

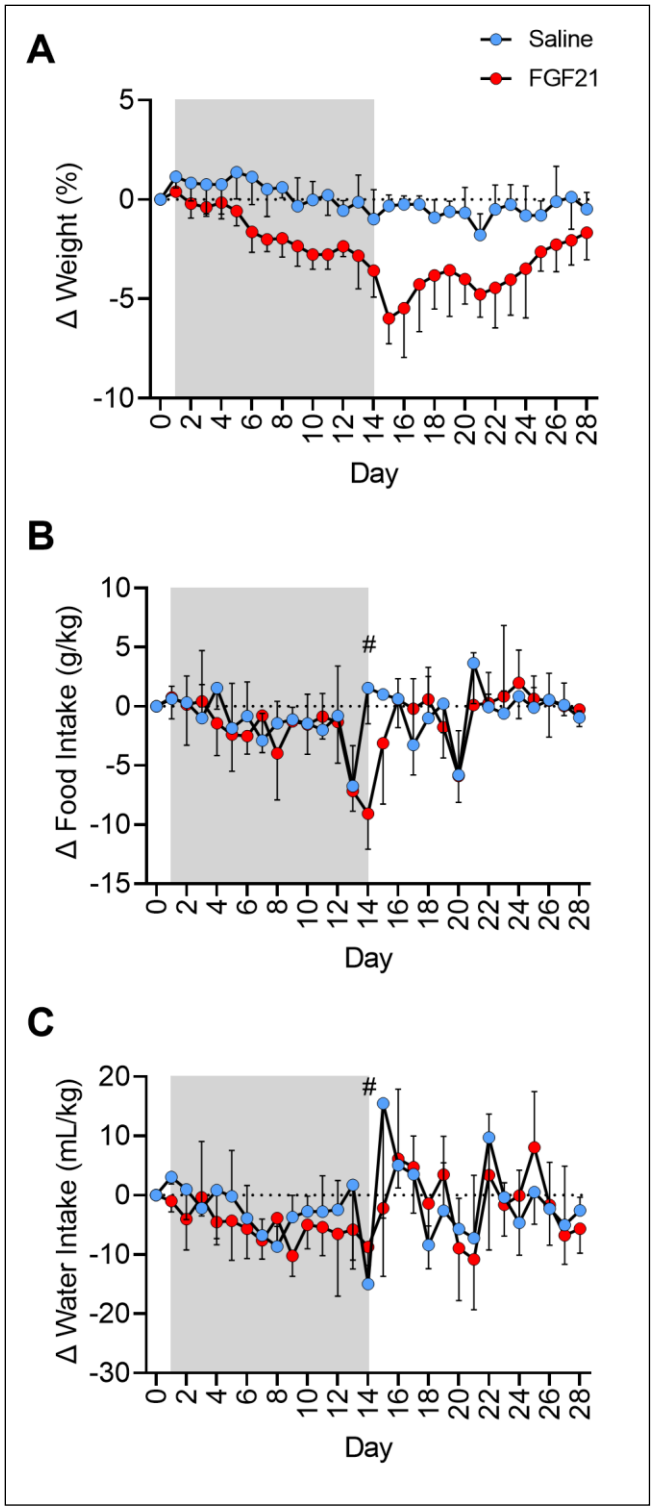


**Figure 1. FGF21 reduces body weight independent of changes in food or water intake. (A)** Treatment with FGF21 resulted in a significant decrease in body weight at a rate 2.54 times faster than in saline-treated cats. On day 15, FGF21-treated cats had a 5.93% decrease in body

weight, with only a 0.28% decrease in body weight in saline-treated cats. Discontinuation of FGF21 resulted in a rapid regain of weight. **(B)** For the FGF21-treated group, the net AUC of corrected food intake from baseline for the treatment period was −26.75 g*day/kg (±13.1, 95% CI). The net AUC of corrected food intake for this same treatment period for the saline-treated group was similar at −17.08 g*day/kg (±12.6, 95% CI). Additionally, the FGF21-treated and saline-treated groups ate a similar amount of food during the washout period ($p = 0.94$). For the FGF21-treated group, the net AUC of corrected food intake from baseline for the washout period was −4.02 g*day/kg (±13.6, 95% CI). The net AUC of corrected food intake for this same washout period for the saline-treated group was similar at −4.78 g*day/kg (±11.6, 95% CI). **(C)** The net AUC for corrected water intake from baseline for Days 1 to 28 of the study for the FGF21 treatment was −82.93 mL*day/kg (±42.7, 95% CI), and the net AUC for corrected water intake for the same period for the saline-treated group was −46.27 mL*day/kg (±47.5, 95% CI). The FGF21-treated cats drank a similar amount of water during the treatment period (Days 1 to 14) as the saline cats ($p = 0.10$). During the treatment period for the FGF21-treated cats, the net AUC for corrected water intake was −68.12 mL*day/kg (±26.8, 95% CI). For the same period, the net AUC for corrected water intake for the saline-treated cats was −35.68 mL*day/kg (±23.3, 95% CI). Both groups had similar levels of water intake during the washout period, or from day 15 to 28 ($p = 0.95$). For the washout period, the net AUC of corrected water intake for the FGF21 treated cats was −9.358 mL*day/kg (±30.8, 95% CI), and the net AUC of correct water intake for the control cats was −10.84 mL*day/kg (±40.2, 95% CI). Each data point of food and water intake represents 24 hours of intake. On day 14 (#), cats were held without food overnight in preparation for general anesthesia and 1H-MRS data. Shaded areas between days 1 and 14 represent the period where either FGF21 or saline vehicle were given.

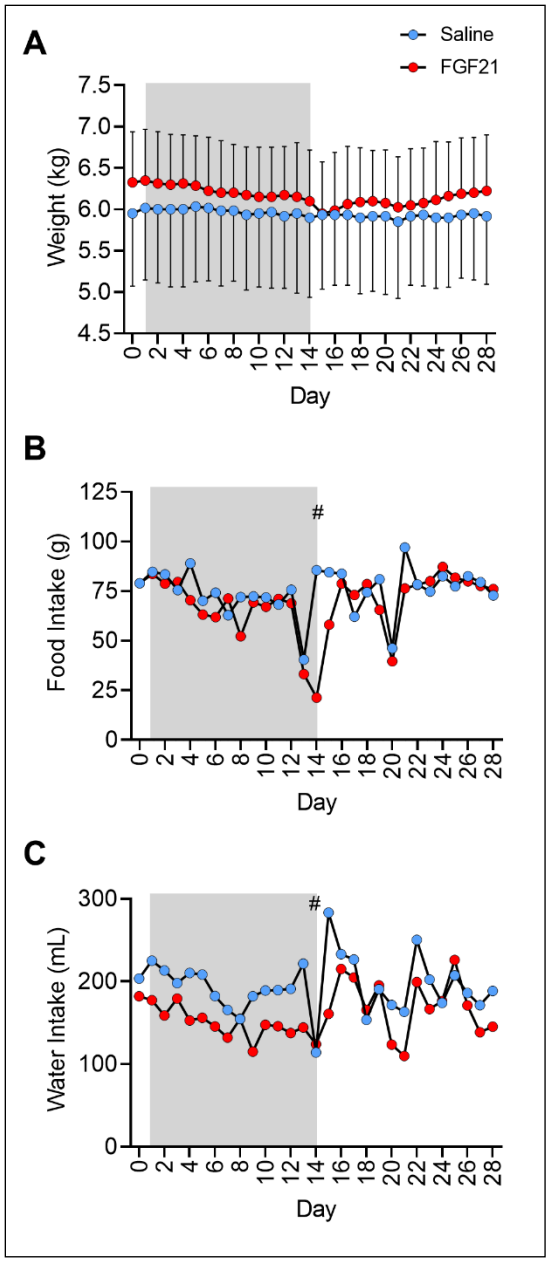


**Figure 2. Total weight, water intake and food intake of cats over the study period.** On day 14 (#), cats were held without food overnight in preparation for general anesthesia and 1H-MRS data. Shaded areas between days 1 and 14 represent the period where either FGF21 or saline vehicle were given.

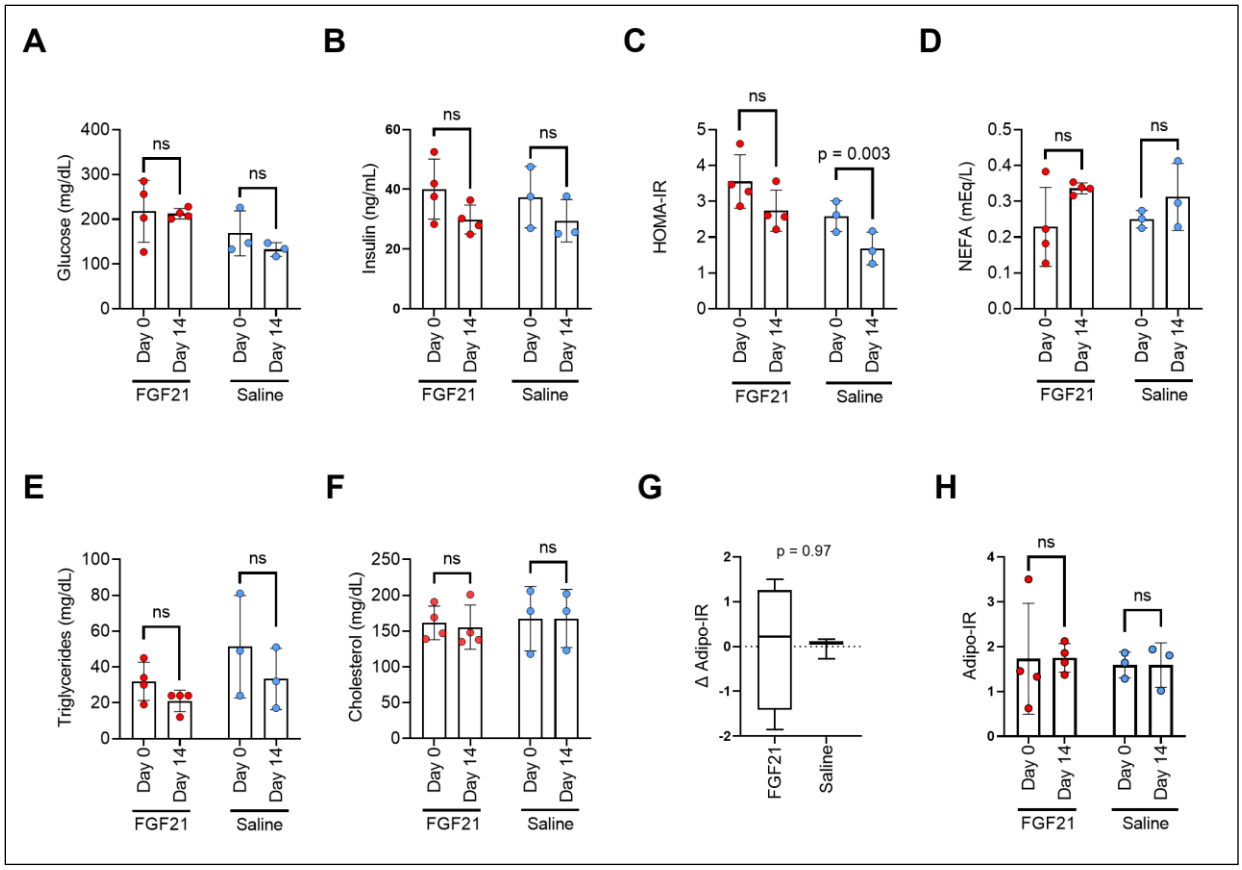


**Figure 3. Circulating metabolic parameters. (A)** Baseline blood glucose was similar between treatment groups, although the blood glucose concentration in the FGF21-treated cats was 29.1% higher (49.1 mg/mL) than the saline blood glucose concentration. **(B)** In the FGF21-treated group, serum insulin decreased 25.5% from 40.08 ng/mL to 29.86 ng/mL. **(C)** In the FGF21-treated group, HOMA-IR decreased 22.9% from 3.55 to 2.74. In the control group, HOMA-IR decreased 35.0% from 2.59 to 1.68. **(D)** In the FGF21-treated group, NEFAs increased 46.8% from a mean of 0.23 mEq/L to 0.34 mEq/L. In the control group, NEFAs increased 24.9% from 0.25 mEq/L to 0.31 mEq/Le. **(E)** Serum triglycerides in the control group decreased 35.1% from 51.33 mg/dL to 33.33 mg/dL, and decreased 34.4% in the FGF21 treated group from 32.0 mg/dL to 21.0 mg/dL. **(F)** Serum cholesterol in the control group rose 0.20% from 167.3 mg/dL to

167.7 mg/dL, and serum cholesterol in the FGF21-treated group decreased 3.72% from 161.5 mg/dL to 155.5 mg/dL. **(G)** Treatment with FGF21 did not alter Adipo-IR. **(H)** In the FGF21-treated group, Adipo-IR increased 1.27% from 1.728 to 1.75. Adipo-IR in the control group remained at a mean of 1.60.

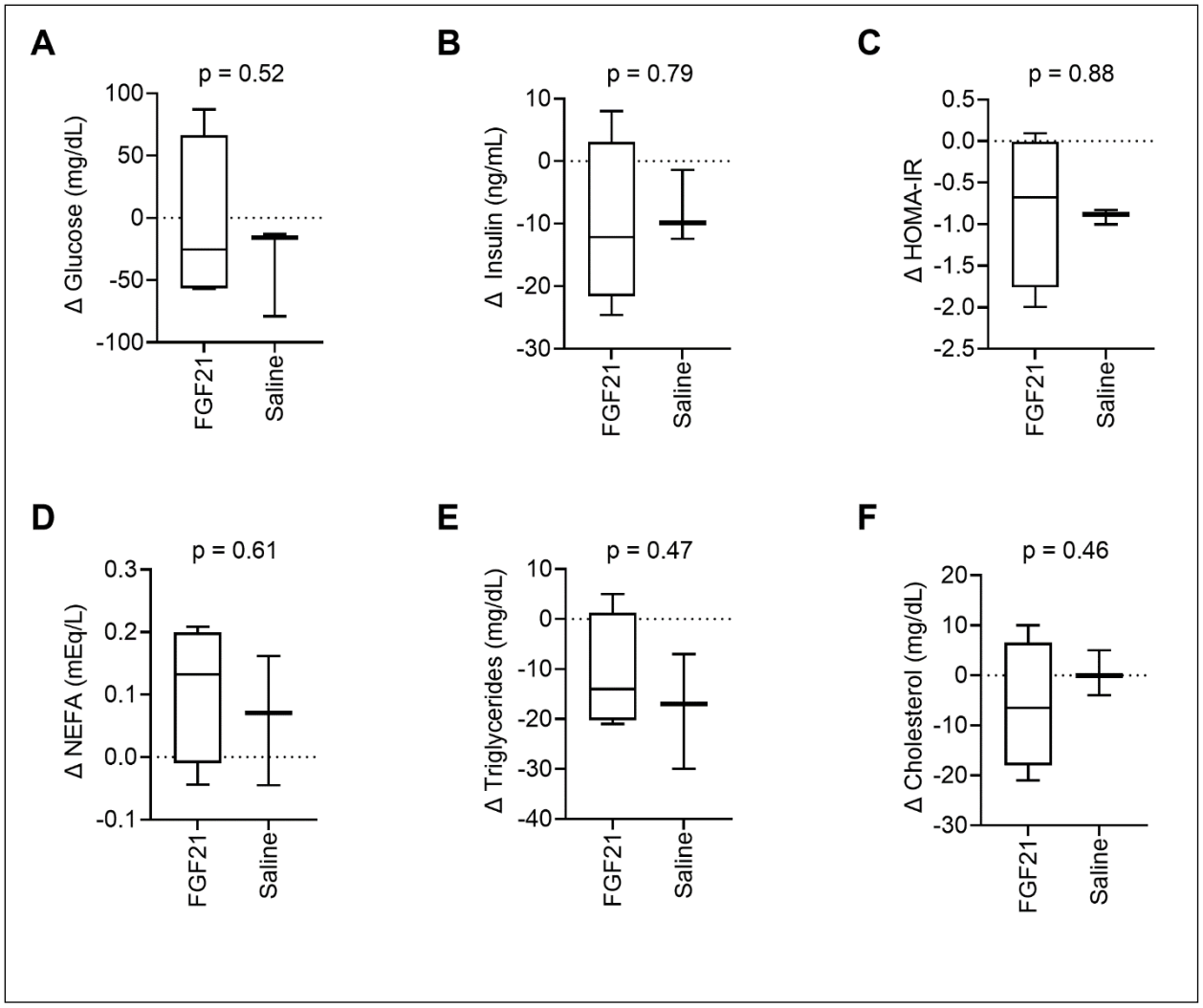


**Figure 4. Circulating metabolic parameters. (A)** Treatment with FGF21 did not alter blood glucose differently than saline (unpaired t-test). Similar findings were noted with **(B)** insulin, **(C)** insulin resistance, **(D)** non-esterified fatty acids, **(E)** triglycerides, and **(F)** cholesterol.

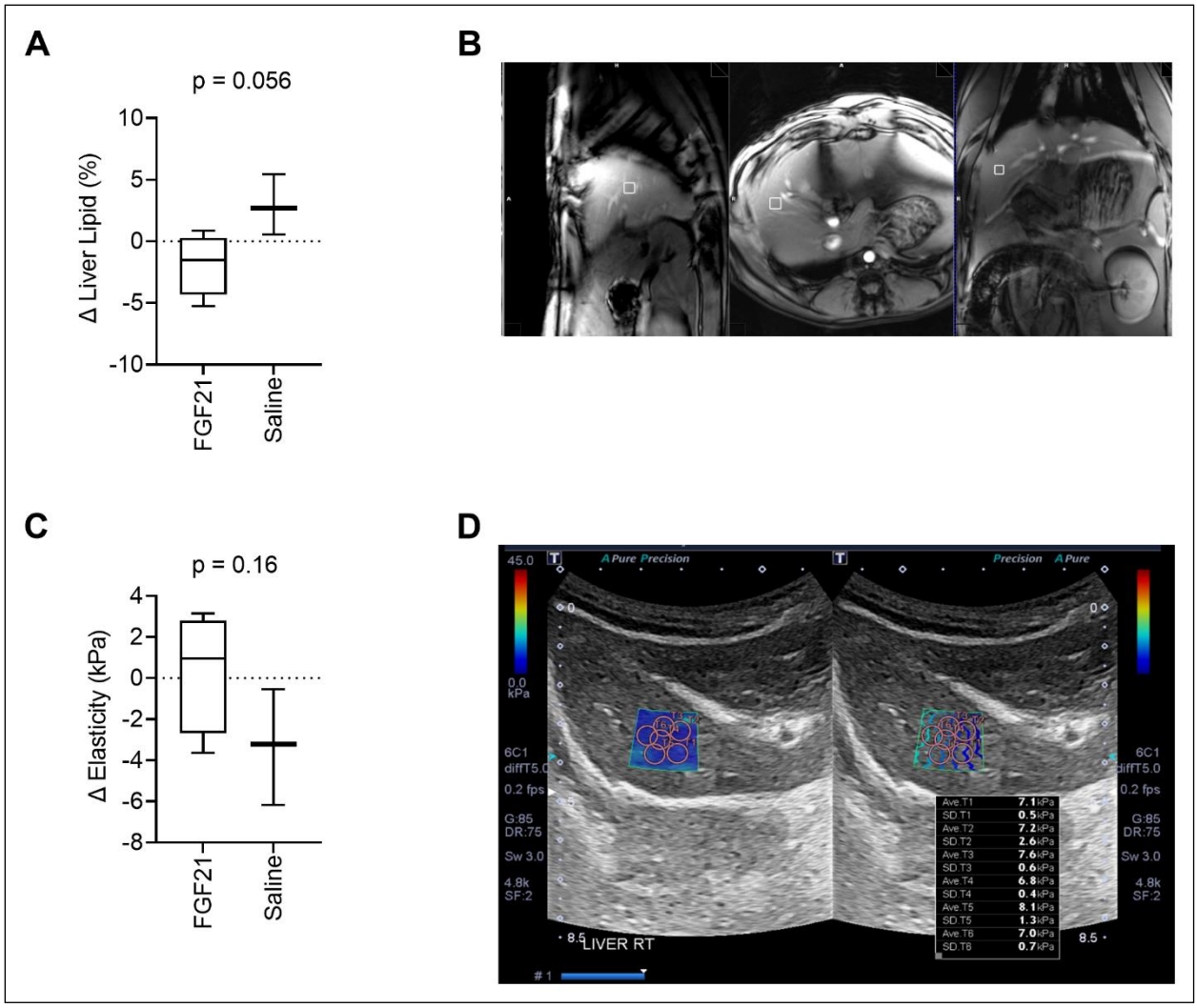


**Figure 5. FGF21 tends to protect from liver lipid accumulation but does not alter liver tissue stiffness. (A)** The fraction liver lipid measured by 1H-MRS is not significantly altered by FGF21 but tends to decrease compared to lipid alterations from saline treatment (unpaired t-test). **(B)** Example of voxel selection for 1H-MRS from a control cat. The white box delineates the voxel region. **(C)** Liver tissue stiffness is not altered by FGF21 treatment (unpaired t-test). **(D)** Example of measurements of stiffness using elastography of a single hepatic lobe from a saline-treated cat

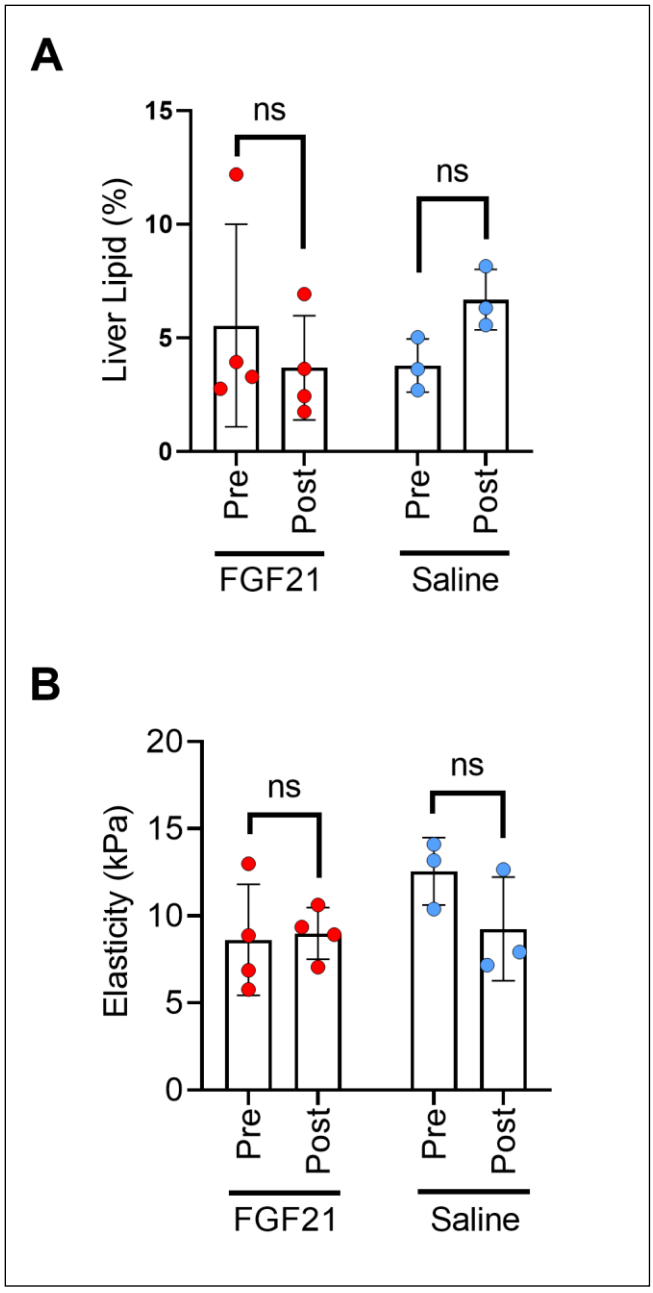


**Figure 6. FGF21 tends to lower liver lipid stores but does not alter liver tissue stiffness. (A)** The fraction liver lipid measured by 1H-MRS is not significantly altered by FGF21 (paired t-test). **(B)** In the control group, liver elasticity decreased 26.4%, from 12.6 kPa to 9.25 kPa, while liver elasticity in the FGF21 group increased 4.25%, from 8.63 kPa to 9.0 kPa with treatment.

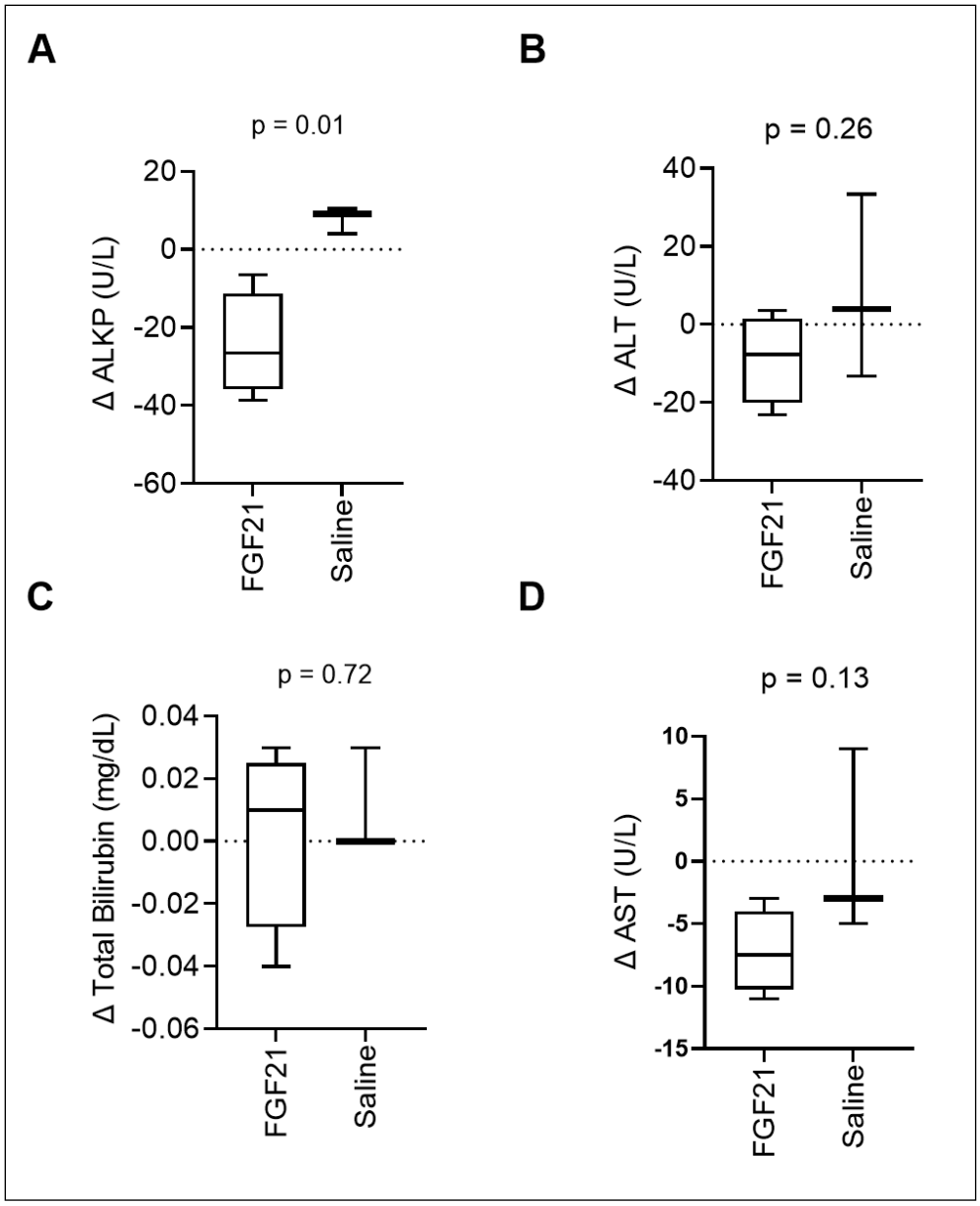


**Figure 7. Hepatic serum biomarker changes are consistent with decreased liver lipid content. (A)** ALKP activity, an inducible liver enzyme and a sensitive indicator of hepatic lipidosis in cats, overall significantly decreases with FGF21 treatment (unpaired t-test). **(B)** ALT, **(C)** Total Bilirubin, and **(D)** AST are not altered by FGF21 treatment when compared to alterations by saline.

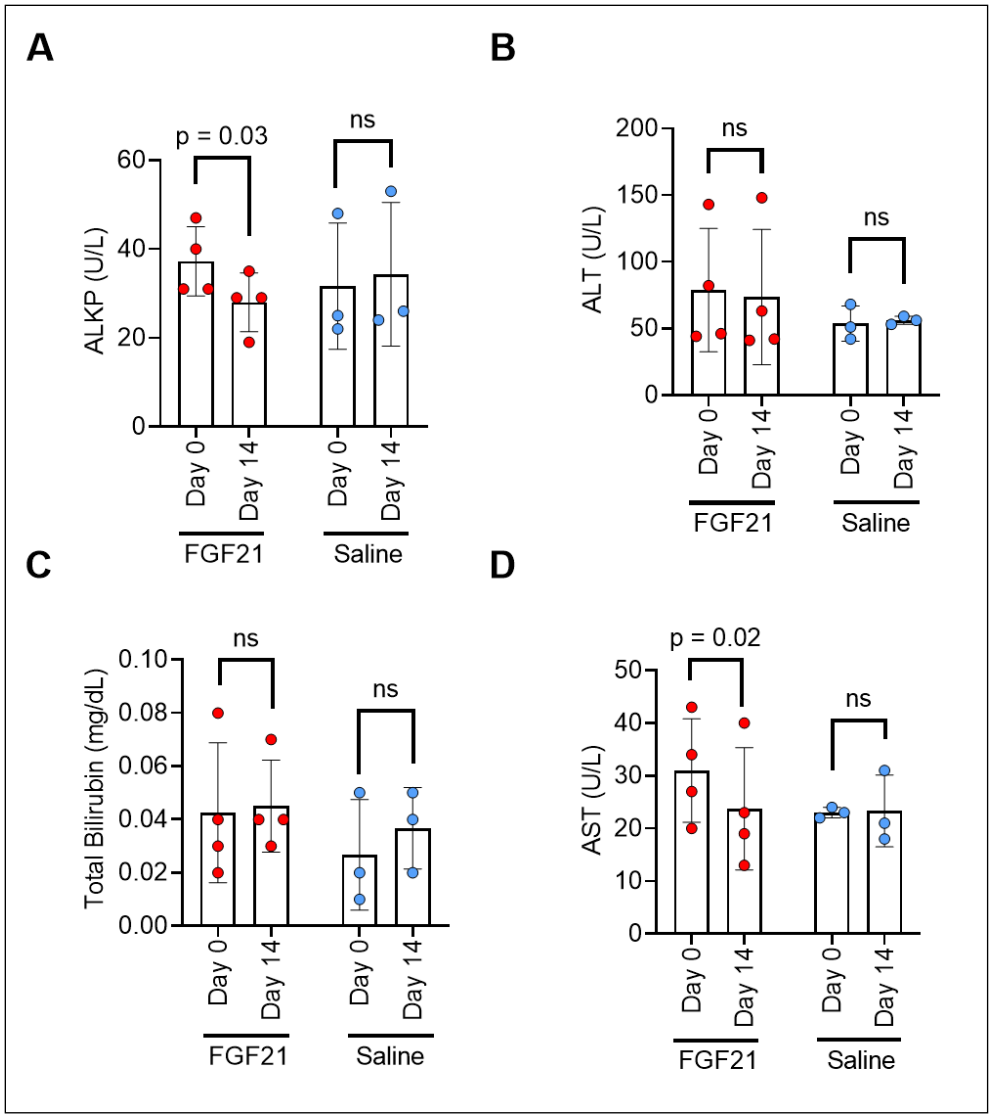


**Figure 8. Liver serum biomarker changes are consistent with decreased liver lipid content.** **(A)** In the control group, ALKP increased 8.4% during the treatment period, while ALKP activity in the FGF21-treated group decreased 24.8% from a mean of 37.25 U/L to 28.00 U/L. **(B)** ALT and **(C)** Total Bilirubin are not altered by FGF21 treatment. **(D)** There was a 23.4% decrease in the enzyme aspartate aminotransferase (AST) in the FGF21-treated cats, from 31 U/L to 23.75 UL. The control cats had a 1.43% increase in AST, from 23 U/L to 23.3 U/L.

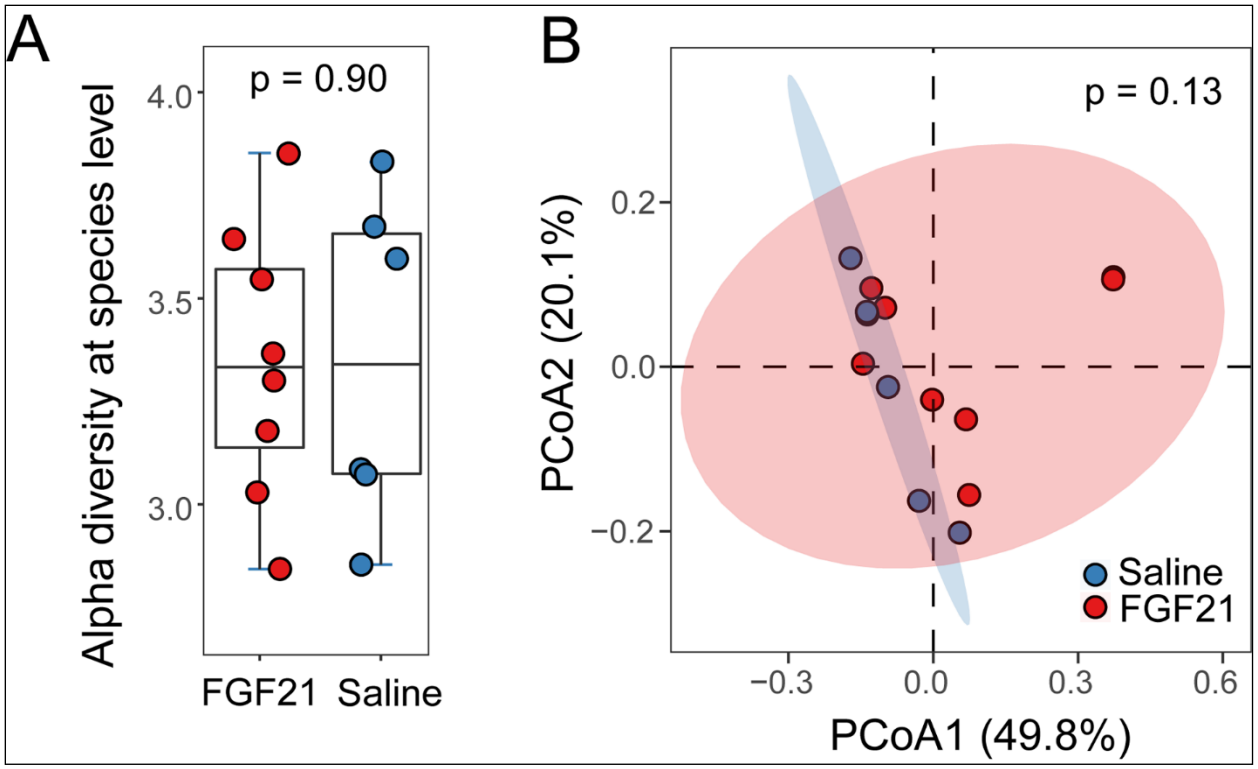


**Figure 9. FGF21 treatment did not alter the feline gut microbiome. (A)** Boxplots of alpha diversity in cat gut microbiome of FGF21-treated (red) and saline-treated (blue) groups at the species level measured by the Shannon index. **(B)** The Principal Coordinates Analysis (PCoA) plots of beta diversity between FGF21-treated (red) and saline-treated (blue) groups using Bray-Curtis distance. Statistical significance was assessed using permutational multivariate analysis of variance (PERMANOVA).

# Chapter 3

## The Feline Fibroblast Growth Factor-21 Pathway in Health and in Feline Pancreatitis

Emily J. Brinker[1,2], Heather P. Hamilton[1], Rie Watanabe[1], Emily C. Graff[1,3]

[1]Department of Pathobiology, College of Veterinary Medicine, Auburn University, Auburn, Alabama, USA

[2]Scott Ritchey Research Center, College of Veterinary Medicine, Auburn University, Auburn, Alabama, USA

## *1 Introduction*

Fibroblast Growth Factor-21 (FGF21), a member of the endocrine Fibroblast Growth Factor family, is primarily a starvation-stress response hormone. Circulating FGF21 is secreted by the liver. However, FGF21 produced in other organs, like the adipose tissues, skeletal muscles, pancreas, and heart, has autocrine and paracrine functions. Systemic effects of circulating FGF21 include increased thermogenesis, lipid metabolism regulation, adiponectin production, protection against insulin resistance, reduced inflammation, and maintenance of pancreatic islet survival (184, 207). The beneficial metabolic and anti-inflammatory effects of FGF21 are implicated by the binding of the tyrosine kinase receptor Fibroblast Growth Factor Receptor 1c (FGFR1c) and its coreceptor β-klotho (KLB) (184).

FGF21 analogs have been developed for pharmaceutical use for their numerous beneficial regulatory effects on lipid metabolism and insulin sensitivity. LY2405319, an FGF21 analog developed for increased stability and multiuse formulation (109), improves circulating lipid homeostasis and decreases body weight and fasting insulin in obese humans and rhesus monkeys with type 2 diabetes mellitus (T2DM) (112, 113). A preliminary study on the effects of subcutaneous administration of LY2405319 in obese and overweight cats showed that despite rapid weight loss, cats did not significantly improve in circulating lipids or insulin homeostasis as seen in other species (208). Rapid weight loss is implicated in the development of hepatic lipidosis in domestic cats; however, the significant weight loss induced by LY2405319 administration was not associated with lipid accumulation, and treated cats had significantly reduced alkaline phosphatase compared to control controls. These findings suggest unique aspects of the FGF21 pathway in the domestic cat that leads to lipolysis and weight loss without

significant liver lipid accumulation and an absence of metabolic alterations, specifically a lack of improved insulin resistance and lipid homeostasis.

In mice, organ-specific knockout studies have determined that circulating FGF21 is produced almost entirely by the liver (83). Hepatic FGF21 has been proven or hypothesized to signal to the brain, heart, skeletal muscle, brown and white adipose tissues, and pancreas (209). Both white and brown adipocytes produce FGF21 but do not produce meaningful levels within the circulation, suggesting that adipose tissue-derived FGF21 has an autocrine/paracrine signaling pathway primarily driven by induced expression of PGC-1α (83, 210). FGF21 promotes thermogenesis and uncoupling in the brown adipose tissue to increase energy expenditure (93). In the white adipose tissue, liver-produced FGF21 upregulates hormone-sensitive lipase to induce lipolysis and subsequent weight loss (80, 89, 211, 212). Additionally, many of the glucose and insulin homeostatic and anti-lipotoxic effects of FGF21 in mice are thought to be through the autocrine-mediated downstream release of adiponectin by the adipose tissues (97, 98). In human and mouse skeletal myotubule cultures, FGF21 promotes glucose uptake and mitophagy in a paracrine/autocrine manner (100). FGF21 is also produced in the heart and protects against myocardial oxidative stress (103).

Autocrine and paracrine signaling of FGF21 also plays a vital role in pancreatic health and disease. In mice, FGF21 is produced in the exocrine pancreatic acinar cells and acts in an autocrine/paracrine manner to stimulate the secretion of digestive enzymes, reduce endoplasmic reticulum stress, and maintain exocrine acinar cell proteostasis (105). In acute and chronic pancreatitis cases, acinar cells lose FGF21 expression by activating the integrated stress response (ISR) pathway (197). In mouse models, the addition of FGF21 resolves pancreatitis through the alleviation of the ISR pathway (197, 198).

Pancreatitis is a common condition in the domestic cat, and comorbidity with hepatic lipidosis, inflammatory bowel disease, cholangitis, and diabetes mellitus is common (213). One prospective study identified pancreatitis in 67% of cats submitted for necropsy, with 60% of affected cats having chronic pancreatitis and 15.7% of cats having acute pancreatitis (214). Currently, there is no targeted therapy for treating pancreatitis in cats, and current guidelines suggest supportive and symptomatic care with the removal of the inciting cause, which in most cases is unknown (215). Alterations in the FGF21 pathway have not been investigated in feline pancreatitis, and future FGF21 pathway-targeting therapy deserves to be studied as a potential treatment for cats with pancreatitis.

In this study, our overall objective was to better understand the FGF21 signaling pathway in domestic cats by characterizing the relative mRNA and protein expression profiles of FGF21 and its receptors, FGFR1c and KLB, in different tissues based on RT-PCR and immunohistochemistry in health. In addition, we wanted to explore changes in FGF21 protein expression in the pancreas in cats with pancreatitis. We hypothesized that the pathway for FGF21 signaling would be similar between rodents, humans and cats, with FGF21 highly expressed in the liver and the receptors KLB and FGFR1c highly expressed in the target adipose tissue. Additionally, we hypothesized that FGF21 would have a lower but still present expression in the pancreas compared to the liver, which would be altered in states of pancreatitis. This study shows that, consistent with all other species studies thus far, FGF21 in domestic cats is produced primarily in the liver and less so in the exocrine pancreas, but unlike humans and rodents, FGF21 is not expressed the adipose tissue. Additionally, we show that FGF21 protein exists in a subset of macrophages in cases of spontaneous feline pancreatitis.

## *2 Methods*

### *2.1 RT-PCR*

Falciform fat, subcutaneous fat, liver, pancreas, lung, cerebral cortex (brain), mesenteric lymph node, heart, kidney, a hind limb flexor skeletal muscle, jejunum, colon skeletal muscle, and spleen from four clinically healthy cats were selected from -80° C storage banks at the Scott-Ritchey Research Center in Auburn, AL, USA. Characteristics of cats used in this study, including sex, age, and breed, are in Table 3. All animals used for RT-PCR were maintained according to Auburn University's IACUC protocols until euthanasia and tissue banking. Feline health status was based on normal CBC, biochemistry profile and urinalysis performed just prior to euthanasia. Tissue RNA extraction from the falciform and subcutaneous fats and brain was performed with the RNasy Lipid Tissue Mini Kit (Qiagen). Extraction from the jejunum, colon, heart, and skeletal muscle was done with the RNeasy Fibrous Tissue Mini Kit (Qiagen), and extraction from the mesenteric lymph node, lung, pancreas, kidney, liver and spleen was done with the RNeasy Mini Kit (Qiagen) all according to the manufacturer's instructions. Tissue-specific cDNA was created using the qScript cDNA Synthesis Kit (Quantabio). PCR primers were designed using the primer design tool Primer3-BLAST (216) with organism specificity set to 'Felis catus' using the mRNA sequences for feline FGF21, KLB, FGFR1, and β-actin (ACTB) (Table 1). RT-PCR was performed in duplicate for each tissue cDNA using the QuantStudio™ 3 Real-Time PCR System (Applied Biosystems) using standard protocols. $C_t$ values of < 34 were considered amplified. Gene expression ratios were calculated using a modified $\Delta\Delta C_t$ method compared to the housekeeping gene β-actin (217). Transcript expressions of FGF21, FGFR1, and KLB were calculated relative to the lowest consistently expressing tissue, as calculated by the gene expression ratios, in all samples.

*2.2 Immunohistochemical study*

The visceral (falciform) fat, liver, lymph node, pancreas, spleen, subcutaneous (inguinal) fat, and coronal sections of the frontoparietal region of the brain from the four clinically normal cats used for RT-PCR, one cat with severe chronic pancreatitis, and one cat with severe hepatic lipidosis (Table 3) were retrieved from storage in 10% neutral buffered formalin or formalin-fixed paraffin-embedded (FFPE) blocks from the Scott-Ritchey Research Center. High lipid content tissues – the subcutaneous fat, the falciform fat, and the brain – were processed with a 22-hour cycle to ensure adequate tissue penetration by solvents. All other tissues were processed with a routine 12-hour cycle.

Antibodies for immunohistochemistry (IHC) were selected based on high percent identity with target proteins (≥ 82%) with no to low percent identity with off-target proteins within the species *Felis catus* (< 49%) using NCBI protein-protein BLAST (218) (Table 2). The Iba1 antibody was selected as it has been successfully used in IHC to identify feline macrophage lineage cells in FFPE sections (219, 220).

FFPE sections were cut at 4 µm, mounted on positively charged glass slides, and dried overnight at a minimum, upright at 37 °C. Slides were deparaffinized in d-Limonene (Hemo-De) and rehydrated in a graded ethanol series to deionized (DI) water. Heat-induced epitope retrieval was done as indicated in Table 2 using a Decloaking Chamber™ NxGen (Biocare Medical). All IHC was performed on an Intellipath FLX Automated Slide Stainer at room temperature.

The FGF21, FGFR1, and KLB IHC were performed with the Starr Trek Universal HRP Detection System (Biocare Medical) per the manufacturer's protocol. Briefly, these sections were first rinsed with buffer (TBS Automation Wash Buffer, Biocare Medical), and endogenous peroxidase was blocked with Peroxidazed 1 (Biocare Medical) for 5 minutes and followed by

two rinses with buffer. Endogenous avidin and biotin sites were blocked with 20-minute avidin and biotin blocking steps (Avidin-Biotin Kit, Biocare Medical), with a single intermediate and two following rinses in buffer. Slides were blocked with Background Sniper (Biocare Medical) for 15 minutes, rinsed twice with buffer, incubated with the appropriate primary antibody in the dilution (in PBS) and time outlined in Table 2, and then rinsed three times with buffer. Following primary antibody incubation, slides were incubated with Trekkie Universal Link (Biocare Medical) for 20 minutes, rinsed three times with buffer, and then incubated with TrekAvidin-HRP (Biocare Medical for 10 minutes and rinsed three times again with buffer. DAB Chromogen (Betazoid DAB, Biocare Medical) was applied for 10 minutes, followed by two rinses with buffer and one rinse with DI water.

For the Iba1 IHC, following an endogenous peroxidase block similar to the other IHC stains and a rinse with buffer, slides were incubated with Background Punisher (Biocare Medical) for 5 minutes, then rinsed with buffer and incubated with Iba1 antibody diluted in Da Vinci Green diluent (Biocare Medical) (Table 2). After applying the primary antibody and a rinse with buffer, slides were incubated for 1 hour with MACH 2 Rabbit HRP-Polymer (Biocare Medical) and then rinsed with buffer three times. Finally, Betazoid DAB was applied for 5 minutes and then rinsed with DI water twice.

All IHC slides were counterstained with CAT Hematoxylin (Biocare Medical) for 1-5 minutes, followed by two rinses with buffer and one rinse with DI water. After counterstaining, slides were then thoroughly dried at 60 C and coverslipped. For negative control tissues, the primary antibody was replaced with an equivalent dilution of normal goat serum (Cell Signaling Technology). A wild-type (WT) C57Bl/6 mouse liver FFPE section was used as positive control tissue for FGF21, FGFR1, and KLB immunohistochemistry. A board-certified anatomic

pathologist (EB) interpreted and described relative immunoreactivity across tissues. Due to inconsistent durations of tissues stored in 10% neutral buffered formalin (between weeks to years), staining intensity was not examined.

### *2.3 Pancreatitis case selections*

Electronic records of cats submitted for postmortem examination between January 2013 and January 2023 to Auburn University's Department of Pathobiology were searched for a histological diagnosis of pancreatitis. FFPE blocks and hemotoxylin and eosin (H&E)-stained slides of the selected cases were retrieved from the archives (Table 3). Cases were confirmed to be pancreatitis by a board-certified veterinary anatomic pathologist (EB) and classified as acute or chronic based on previously published criteria (214). Cases were excluded if there was inadequate histological tissue quality, such as severe autolysis or decalcification artifact, or if the H&E-stained slide or FFPE blocks were not present in the archives, or the following confounding diseases were identified: feline infectious peritonitis, feline immunodeficiency virus, or hepatobiliary and/or gastrointestinal neoplasia. Cases of pancreatitis were scored in severity and classified as acute, chronic, or mixed acute and chronic using a previously published grading and classification scheme (214). The maximal severity score possible for chronic pancreatitis was 9, and the maximal severity score possible for chronic pancreatitis was 6. Due to an unknown fixation time of the archived cases, staining intensity was not measured. FGF21 IHC grading was based on a percentage of pancreatic lobules containing FGF21-immunoreactive macrophages. A score of 1 was 1-15% of pancreatic lobules, a score of 2 was 15-50% of lobules, a score of 3 was 30-50% of lobules, and a score of 4 was > 50% of lobules.

### *2.4 Statistical Analysis*

All statistical analyses were performed with GraphPad Prism version 9.5.1 (Dotmatics). For statistical analyses, the α level is set at 0.05. For the relative expression data, 2-way ANOVAs were performed and compared with Tukey's multiple comparison test. For analysis of qPCR for genes with non-detects (FGF21), the $C_t$ was set to the maximum limit of detection ($C_t$ = 34). Error bars on graphs represent the standard error of the mean. Linear regression was performed between pancreatitis severity scoring and FGF21 staining scores. Letters in bar graphs represent significance groups.

## *3 Results*

### *3.1 Transcript expression of FGF21 and its co-receptors, FGFR1 and KLB*

From the clinically normal cats, FGF21 mRNA was consistently amplified in the liver, pancreas, and cerebral cortex and was inconsistently amplified from the heart (2/4), lymph node (2/4), and lung (1/4). FGF21 mRNA could not be amplified from the spleen, kidney, falciform fat, inguinal fat, colon, skeletal muscle, or jejunum from any cat. The lowest FGF21 gene expression ratio from tissues that could be consistently amplified was in the cerebral cortex. The liver had 320X the cerebral cortical FGF21 mRNA expression ($p = 0.02$, 2-way ANOVA, $p = 0.02$, Tukey's multiple comparisons test) (Figure 1). The pancreas, heart, lung, and lymph node were similar in FGF21 mRNA expression to the brain ($p > 0.99$).

KLB mRNA was consistently detected in all examined tissues. The lowest KLB gene expression ratio from tissues that could be consistently amplified was in the colon. The falciform fat had the highest average increased fold KLB mRNA expression at 2860X the colonic mRNA expression (2-way ANOVA, $p < 0.01$; Tukey's multiple comparisons test, $p < 0.05$) (Figure 2). The subcutaneous fat, liver, pancreas, cerebral cortex, lymph node, heart, kidney, colon, lung,

skeletal muscle, and spleen average KLB mRNA expression levels were similar to the colonic expression level ($p > 0.05$).

FGFR1 mRNA was consistently detected in all examined tissues. The lowest FGFR1 gene expression ratio from tissues that could be consistently amplified was in the colon. The subcutaneous fat had the highest average increased fold expression at 21X the colonic FGFR1 mRNA expression (2-way ANOVA, $p = 0.0001$; Tukey's multiple comparisons test, $p < 0.01$) (Figure 3), followed by the pancreas and falciform fat with average FGFR1 mRNA expression at 19X and 17X fold the average colonic expression ($p < 0.05$). The FGFR1 mRNA expression of the lymph node was similar to that of the kidney, heart, liver, lung, skeletal muscle, cerebral cortex, spleen, colon, and jejunum ($p > 0.05$).

*3.2 Immunohistochemical Expression of FGF21 and its co-receptors, FGFR1 and KLB*

In the positive control WT C57Bl/6 mouse liver tissue section, centrilobular hepatocytes had strong cytoplasmic FGF21 immunoreactivity that formed a lobular pattern (Figure 4A). The negative control tissues for FGF21 IHC of the feline liver, pancreas, subcutaneous fat, mesenteric lymph node, spleen, falciform fat, and cerebral cortical white matter (Figures 4B-H) had minimal background chromogen staining.

In the mouse liver positive control for KLB IHC, hepatocytes and biliary epithelial cells had strong diffuse cytoplasmic KLB immunoreactivity with more intense immunoreactivity of the sinusoids (Figure 5A). Lipofuscin, a golden-brown pigment commonly found in cats in the centrilobular hepatocytes (221), was prominent in the negative liver control (Figure 5B). Additionally, rare stippled golden brown DAB staining was noted in the negative control sections of feline adipose tissue (Figures 5D, 5F). The pancreas, lymph node, spleen, and

cerebral cortex had minimal background staining (Figures 5C, 5E, 5G, 5H). Some acid hematin pigmentation was noted, particularly in the spleen.

In the mouse liver positive control for FGFR1 IHC, the tissue had diffuse and strong cytoplasmic immunoreactivity in the hepatocytes and biliary epithelial cells with moderate to strong cytoplasmic immunoreactivity to the arteriolar smooth muscle cells (Figure 6A). The negative control tissues for FGFR1 IHC of the feline liver, pancreas, subcutaneous fat, mesenteric lymph node, spleen, falciform fat, and cerebral cortical white matter (Figures 6B-H, respectively) had minimal background chromogen staining.

### *3.2.1 Liver*

The clinically normal cats (Figures 7A-D) and the cat with hepatic lipidosis (Figure 7F) had diffuse hepatocytic cytoplasmic immunoreactivity for FGF21, although, in two cats, the cytoplasmic immunoreactivity was more robust in the midzonal (Figure 7B) or the periportal (Figure 7D) hepatocytes. The cat with pancreatitis had FGF21 immunoreactivity more localized to the cytoplasm of the periportal hepatocytes with progressively diminishing reactivity towards the centrilobular zones (Figure 7E). All cat livers had diffuse cytoplasmic immunoreactivity for KLB (Figure 8) and FGFR1 (Figure 9) within the hepatocytes and biliary epithelial cells.

### *3.2.2 Pancreas*

Generally, the clinically normal cats had multifocal FGF21 immunoreactivity, predominately within the exocrine acinar cells within the center of the pancreatic lobules (Figures 10A-D). The islets lacked FGF21 immunoreactivity. In the cat with severe pancreatitis (Figure 10E) and the cat with severe hepatic lipidosis (Figure 10F), multifocal exocrine acinar cells did have moderate FGF21 immunoreactivity, and the most robust FGF21 immunoreactivity was within the cytoplasm of macrophages, particularly those embedded within bands of

perilobular fibrosis. Diffuse strong cytoplasmic KLB (Figure 11) and FGFR1 (Figure 12) immunoreactivity was within the pancreatic acinar cells, islet cells, ducts, and ductules of all cats, regardless of health. KLB immunoreactivity was not within the fibroblasts of the fibrous connective tissue of the cat with pancreatitis (Figure 11E). The pancreatic arterioles additionally had cytoplasmic immunoreactivity to FGFR1.

### *3.2.3 Subcutaneous Fat*

Cats had inconsistent adipocytic cytoplasmic immunoreactivity to FGF21, with the cytoplasm compressed and marginalized to the periphery of the cell by a single large lipid vacuole. Of the clinically normal cats, 3 of 4 had patchy, multifocal to diffuse immunoreactivity to FGF21 (Figure 13A-D). The subcutaneous adipose of the cat with pancreatitis had similar patchy FGF21 immunoreactivity (Figure 13E), while the subcutaneous adipose of the cat with hepatic lipidosis lacked immunoreactivity (Figure 13F). The subcutaneous fat of all cats had adipocytic cytoplasmic immunoreactivity to KLB (Figure 14) and FGFR1 (Figure 15).

### *3.2.4 Falciform (Visceral) Fat*

Of the clinically normal cats, the falciform fat of 2 of 4 cats lacked FGF21 immunoreactivity (Figures 16C, 16D). Of the cats with FGF21 immunoreactivity, one cat had diffuse adipocytic cytoplasmic FGF21 immunoreactivity of the falciform fat (Figure 16B), and the other had mild and multifocal adipocytic cytoplasmic FGF21 immunoreactivity of the falciform fat (Figure 16A). The falciform fat of the cat with pancreatitis and the cat with hepatic lipidosis lacked FGF21 immunoreactivity (Figures 16E, 16F). The falciform fat of all cats had multifocal immunoreactivity to KLB (Figure 17). Most cats had absent to sporadic falciform adipocytic immunoreactivity to FGFR1 (Figure 18), and one of the clinically normal cats had more widespread adipocytic immunoreactivity to FGFR1 (Figure 18C).

### *3.2.5 Cerebral Cortex*

In most cats (5 of 6), a subset of oligodendrocytes within the cerebral cortical white matter had strong cytoplasmic immunoreactivity to FGF21 (Figure 19A-E). The exception of FGF21 immunoreactivity was in the cat with hepatic lipidosis, where the cytoplasm of the oligodendrocytes has been artifactually lost, evidenced by the perinuclear halo or "fried egg" appearance typical of delayed formalin fixation (222) (Figure 19F). Notably, the cat with hepatic lipidosis was found dead and not euthanized immediately prior to necropsy like the other cats, and the death to necropsy interval is unknown. Despite the FGF21 immunoreactivity of the oligodendrocytes, the cerebral cortical white matter lacked immunoreactivity to KLB (Figure 20) and FGFR1 (Figure 21) in all cats.

### *3.2.6 Mesenteric Lymph Node*

FGF21 in the lymph nodes of cats was generally sporadic. Half of the clinically normal cats and the cat with hepatic lipidosis lacked FGF21 immunoreactivity in the lymph node (Figures 22B, 22C, 22F). The other clinically normal cats had mild and multifocal cytoplasmic immunoreactivity within the macrophages (Figures 22A, 22D). The cat with severe pancreatitis had moderate to strong cytoplasmic FGF21 immunoreactivity within the macrophages of the lymph node, as evidenced within the nodal subcapsular sinuses (Figure 22E). In all cats, the mesenteric lymph node had weak to moderate cytoplasmic KLB immunoreactivity localized to the macrophages (Figure 23). For FGFR1, there was variable immunoreactivity for the macrophages and lymphocytes. Two clinically normal cats (Figures 24B, 24C) had diffuse strong cytoplasmic leukocytic immunoreactivity of FGFR1 within both the lymphocytes and macrophages. In the other two normal cats, the cat with pancreatitis, and the cat with hepatic

lipidosis, the FGFR1 immunoreactivity was weak to moderate and variably within leukocytes (Figures 24A, 24D-F).

### *3.2.7 Spleen*

The clinically normal cats lacked significant FGF21 immunoreactivity within the spleen (Figures 25A-D). The two diseased cats had moderate to strong cytoplasmic immunoreactivity to FGF21 within their macrophages (Figures 25E, 25F). Three clinically normal cats had mild to moderate cytoplasmic lymphocytic immunoreactivity to KLB (Figures 26A, 26B, 26D). The cats with pancreatitis and hepatic lipidosis lacked KLB immunoreactivity (Figures 26E, 26F). Three clinically normal cats and the cat with hepatic lipidosis had strong cytoplasmic immunoreactivity in the lymphocytes and macrophages for FGFR1 (Figures 27A, 27B, 27D, 27F). The other clinically normal cat and the cat with pancreatitis had more variable leukocytic immunostaining (Figure 27C).

## *3.3 FGF21 in Feline Pancreatitis*

From January 2013 – January 2023, there were a total of 480 feline necropsies performed at Auburn University's College of Veterinary Medicine Department of Pathobiology. Of these 480 cases, 45 (9.38%) had a histological diagnosis of pancreatitis. Of these 45 cases, 18 cases met the inclusion criteria for further examination with FGF21 IHC (Table 3). Of the 18 examined cases, 10 (55.6%) were classified as chronic pancreatitis, 3 (16.6%) were classified as acute pancreatitis, and 5 (27.8%) were classified as mixed acute and chronic pancreatitis.

Cases of chronic pancreatitis had some degree of interstitial fibrosis (Figure 28A) with varying numbers of lymphocytic, plasmacytic, and histiocytic infiltrates. The presence of cystic degeneration was variable. In all cases, both the chronic, acute, and mixed chronic and acute cases of pancreatitis had a portion of macrophages with strong cytoplasmic immunoreactivity

FGF21 and Iba1 (a commonly used histiocytic marker). The FGF21 immunoreactivity contrasts with clinically normal cats, which lack FGF21-immunoreactive macrophages (Figures 10A-D). The chronic pancreatitis severity score was positively correlated with the FGF21 staining score ($Y = 0.3088*X + 0.6676$, $R^2 = 0.30$. $p = 0.03$) (Figure 29). Cases of acute pancreatitis contained varying numbers of neutrophilic infiltrates, fat necrosis, and edema. The acute pancreatitis severity score was not correlated with the FGF21 staining ($Y = -0.1635*X + 2.843$, $R^2 = 0.05$, $p = 0.57$) (Figure 30). In the cases of spontaneous acute and chronic pancreatitis, variable groups of acinar cells had mild to moderate, patchy cytoplasmic immunoreactivity for FGF21 (Figure 28E, 28F), similar to the clinically normal cats (Figures 10A-D).

## *4 Discussion*

This study is the first to characterize the FGF21 signaling pathway in domestic cats. Like many studies in other species (83, 135, 223, 224), including humans, non-human primates, mice, and cattle, a major organ of FGF21 production is the liver, as evidenced by elevated relative FGF21 mRNA expression and consistent protein detection in the hepatocytes of all cats in our study. Within the liver, FGF21 is suspected of having autocrine and paracrine effects on hepatic metabolism by regulating gluconeogenesis, ketogenesis, and lipid homeostasis (225). We demonstrated that the co-receptors for FGF21, KLB and FGFR1 are expressed by feline hepatocytes, indicating that the hepatic autocrine/paracrine function of FGF21 is present in the feline liver. The protein and receptor machinery for a hepatic autocrine/paracrine pathway is consistent with our previous preliminary study evaluating the FGF21 analog, LY2405319, in cats. In our earlier study, compared to the controls, the cats treated with FGF21 tended to have decreased liver lipid as determined by proton magnetic resonance spectroscopy and significant

decreases in the inducable hepatic enzyme, alkaline phosphatase, a sensitive marker of hepatic lipid accumulation (208). Our findings suggest that FGF21 is a hepatokine with paracrine/autocrine actions on the liver by decreasing hepatocellular triglyceride content in cats.

Contrary to the rodent literature (184, 207), FGF21 was not expressed in the adipose tissue of cats, as no cats had amplification of FGF21 mRNA from the subcutaneous or falciform fat. Additionally, there is inconsistent protein expression for FGF21 by IHC in the falciform and subcutaneous fats, likely due to inconsistent protein localization of FGF21 in the fat from endocrine circulation instead of local production. The lack of FGF21 mRNA expression in the adipose stores suggests that the adipokine role of FGF21 is not conserved in the cat, and there is a loss of the autocrine and paracrine FGF21 signaling system. Interstingly, the adipose tissues of domestic cats express the mRNA and protein of the KLB and FGFR1 receptors for FGF21. Due to the conserved receptors within the adipose tissue and the relative lack of local FGF21 hormone, it seems that the endocrine signaling of FGF21 to the adipose tissues is maintained, despite that the paracrine/autocrine signaling of FGF21 is not.

Exogenous administration of FGF21 leads to decreased plasma glucose and triglycerides in *ob/ob* and *db/db* mice (70), reduced fasting glucose, fasting insulin, and improved circulating lipid profile in T2DM rhesus monkeys (112), and reduced fasting insulin and improved lipid profile in T2DM obese humans (113). From mouse studies, it is known that the upregulation of adiponectin by autocrine signaling of FGF21 drives the effects of FGF21 on lipid homeostasis, insulin sensitivity, and glucose homeostasis (97). In monkey and human studies, favorable dose-dependent increases in adiponectin, particularly high-molecular-weight adiponectin in humans, were also seen with FGF21 administration (112, 113, 226). Cats treated with exogenous FGF21 do not have significant alterations in serum triglycerides and cholesterol, changes in basal

circulating insulin and glucose, or changes in indirect measures of circulating or adipose-specific insulin resistance (208). Adiponectin may not be a downstream mediator of FGF21 signaling, sequentially, an absence of many FGF21-driven metabolic effects in the cat as seen in rodents, non-human primates, and humans. Further studies are needed to determine the role of FGF21 on feline adipocytes, particularly with the adipocytic autocrine and paracrine FGF21 pathways and the involvement of adiponectin.

There was consistently measurable FGF21 mRNA within the cerebral cortex, although at levels much lower than in the liver. With IHC, FGF21 protein was localized to the cytoplasm of multifocal oligodendrocytes within the white matter in 5 of 6 cats. Notably, the only cat that did not have FGF21 immunoreactivity in the white matter (the cat with hepatic lipidosis) was the only cat with an unknown death to necropsy interval. Consequently, in this cat, autolytic changes are associated with the oligodendrocytes on FFPE sections, including loss of cytoplasm (222), which likely affected FGF21 immunoreactivity. The role of FGF21 in the cat oligodendrocyte is unknown. In a mouse model of demyelination, pancreas-derived FGF21 stimulates the proliferation of oligodendrocyte precursor cells to drive remyelination (227). The FGF21-immunoreactive cells we observed may be early lineage oligodendrocytes that are uptaking FGF21 rather than producing it locally. However, in mice, the effects of FGF21 were blocked with inhibition of β-klotho expression, suggesting that the receptor β-klotho is necessary for FGF21 location in oligodendrocyte precursor cells (227). In our study, no oligodendrocytes in the white matter expressed either β-klotho or FGFR1, suggesting that FGF21 was produced in the cell *de novo* and not localized to the cell from endocrine trafficking. Much has yet to be discovered about the role of FGF21 in the feline oligodendrocyte, and further studies on the role of FGF21 in the brain regarding the glial cells of all species are needed.

In C57Bl/6J mice, the acinar tissue expresses 20-fold more FGF21 than the islets (104). FGF21 and its receptors are expressed and localized to the acinar cells in the feline pancreas. Interestingly, in our study, only the receptors KLB and FGFR1 were localized in the pancreatic islet cells through IHC and not FGF21. Our findings indicate in the domestic cat that FGF21 in the pancreatic islet may be under endocrine regulation rather than autocrine/paracrine signaling, as the FGF21 receptors are present within the islets but not the FGF21 protein. In rodent studies, FGF21 promotes insulin expression in islets and protects islet cells from glucolipotoxicity and apoptosis (228, 229). As cats with T2DM develop hydropic degeneration from islet cell damage and a reduction in β-cells, further exploration in the islet-specific FGF21 pathway may prove beneficial (230). One pitfall of this study is the possibility that our FGF21 IHC was not sensitive enough to pick up low amounts of protein in the islets. Additional studies on feline islet culture or other imaging modalities, such as RNAscope, may be needed to determine the expression profile and impact of FGF21 in islet cells.

FGF21 does have functions in the exocrine acinar cell. FGF21 acts as a secretagogue in rodents by reducing endoplasmic reticulum (ER) stress and thus facilitating the secretion of digestive enzymes through the phospholipase C-inositol triphosphate receptor signaling cascade (105). In cerulein-induced mouse models of pancreatitis, FGF21 mRNA and protein are downregulated by the acinar cell's integrated stress response (197). However, with FGF21 treatment in different studies, FGF21 can downregulate the stress response and mitigate cerulein-induced pancreatitis (197, 198). Comparison of cerulein-induced rodent models of pancreatitis with spontaneous disease pathology is problematic, as cerulein toxicity best replicates a very acute, edematous phase of human pancreatitis, and adjuvant toxic compounds often need to be added to reflect spontaneous acute pancreatitis (39). The edema in cerulein-induced pancreatitis

models may have caused an artificial, dilutional decrease in expression in the other studies, making the FGF21 downregulation in pancreatitis inaccurate. In our study of cases of spontaneous pancreatitis, many of the exocrine acinar cells retained FGF21 immunostaining. It is possible that the integrated stress response pathway in cats does not suppress FGF21 levels uniformly in the pancreas.

In the cases of feline pancreatitis, a subset of macrophages had strong cytoplasmic immunoreactivity for FGF21, with much stronger immunoreactivity than the adjacent exocrine pancreatic cells. Confirming that these are macrophages, FGF21 IHC was compared to areas of Iba1 IHC, a general histiocytic lineage marker known to work in cats (231), and it was noted that a portion of the Iba1-expressing cells also express FGF21. To the authors' knowledge, no published studies evaluate the FGF21 expression of macrophages within pancreatitis in any species. FGF21 has been shown to promote an anti-inflammatory or 'M2' phenotypic polarization in macrophages by enhancing AMPKα phosphorylation, activating Nrf2, and inhibiting the NF-κB pathway (232, 233). The presence of immunoreactivity for FGF21 in the subset of macrophages in feline pancreatitis may indicate an attempt at alleviating the associated inflammation (Figure 31). In support of this theory, in our retrospective study, FGF21 immunoreactivity within macrophages was positively correlated with the severity of chronic pancreatitis in our retrospective study, a disease state associated with an increase in M2 macrophage polarity (234, 235). Conversely, no correlation of FGF21 immunoreactivity within macrophages was found with acute pancreatitis, a disease state associated with an increase in M1 macrophage polarity (234, 236). Potential future directions include correlating these FGF21-expressing macrophages with CD163, CD68, pSTAT1, and other IHC markers of M2 macrophage polarization (237).

Supporting the role of FGF21 in leukocytes, FGF21, KLB, and FGFR1 receptor mRNA and protein expression was variably seen within the spleen and lymph node. As not all cases had strong macrophage immunoreactivity, the variable IHC expression of FGF21 may reflect the current state of polarization of trafficking macrophages in the lymph node and spleen.

One major pitfall of this paper is the inconsistent fixation times of cat tissues. Clinically normal cats were fixed up to years within formalin, which may have hindered IHC capabilities, although expression was seen in at least one tissue of each cat. The clinical cases of pancreatitis were obtained from archived samples, with no records on the fixation duration. Because of this large variability in fixation, we opted not to make quantitative staining intensity comparisons.

This paper is the first to characterize the transcript and protein profile of FGF21 and its primary signaling pathway in cats. In this study, we have shown that cats have many species-specific differences in the FGF21 pathway, including low mRNA and protein production of FGF21 in adipose tissue, which may be partially why domestic cats have a blunted metabolic response when administered FGF21. Additionally, we demonstrated that FGF21-expressing macrophages have a role in pancreatitis in domestic cats. FGF21 has a role in polarizing macrophages to an M2 phenotype, and future FGF21 pathway therapies in cats may serve a role in mitigating the pancreatic inflammatory response in cats.

**Table 1. Primers for RT-PCR of FGF21 and co-receptors with the corresponding reference sequence.**

| Target | NCBI Reference Sequence | Primer (5′ → 3′) |
|---|---|---|
| FGF21-F | XM_003997528.3 | GACAGCGGTTCCTCTACACG |
| FGF21-R | | TCAAAGCGGAGCGATCCAT |
| | | |
| KLB-F | XM_003985434.5 | AGTAACGACACCTACCGGGCAG |
| KLB-R | | CAATCCGACTGCAGAGACAGCG |
| | | |
| FGFR1-F | XM_045055547.1 | GCACATCGAGGTGAATGGGA |
| FGFR1-R | | TAGAGTTACCCGCCAAGCAC |
| | | |
| ACTB-F | XM_006941899.3 | GGCCGAGGACCUUGACUGUACA |
| ACTB-R | | CUCAGGGAGAAAUGGGGUGGCU |
| | | |

**Table 2. Antibodies and protocols used for immunohistochemistry.**

| Antigen | Dilution | Clone | Identity of Immunogen to Feline Protein (%) | Distributor (catalog #) | Incubation Time (hrs) | Antigen Retrieval |
|---|---|---|---|---|---|---|
| FGF21 | 1:500 | JA10-97 (rabbit) | 82.00 | Invitrogen (MA5-32652) | 2 | None |
| KLB | 1:1000 | Rabbit polyclonal | 91.67% | Invitrogen (PA5-121806) | 1 | Borg Decloaker (Biocare Medical) |
| FGFR1 | 1:1000 | M2F12 (mouse) | 100.00% | Abcam (ab829) | 1 | Reveal Decloaker (Biocare Medical) |
| IBA1 | 1:750 | Rabbit polyclonal | N/A | Biocare (290) | 1 | Diva Decloaker (Biocare Medical) |

**Table 3. Characteristics of cats used for RT-PCR and IHC analysis**. Y – years, M – months, MI – male intact, MC – male castrated, FI – female intact, FS – female spayed.

| Case | Age | Sex | Breed | Chronic Pancreatitis Score | Acute Pancreatitis Score | FGF21 Score |
|---|---|---|---|---|---|---|
| 1 | 13Y | FS | Domestic Shorthair | 6 | - | 1 |
| 2 | 7Y | FS | Domestic Shorthair | 5 | - | 2 |
| 3 | 10Y | MC | Domestic Shorthair | 4 | 2 | 3 |
| 4 | 8Y | MC | Domestic Longhair | - | 6 | 1 |
| 5 | 3M | MI | Siamese | 2 | - | 1 |
| 6 | 13Y | FS | Domestic Shorthair | 2 | 4 | 3 |
| 7 | 3Y | FS | Manx | 2 | - | 2 |
| 8 | 11Y | A | Domestic Shorthair | 3 | - | 1 |
| 9 | 13Y | MC | Domestic Shorthair | 3 | - | 1 |
| 10 | 4Y | FI | Domestic Mediumhair | 3 | - | 1 |
| 11 | 16Y | FS | Domestic Shorthair | 2 | 2 | 1 |
| 12 | 3Y | FS | Domestic Shorthair | - | 4 | 1 |
| 13 | 16Y | MC | Domestic Shorthair | 7 | 2 | 4 |
| 14 | 14Y | FS | Domestic Shorthair | - | 6 | 3 |
| 15 | 11Y | FS | Domestic Longhair | 3 | - | 1 |
| 16 | 17Y | FS | Domestic Shorthair | 7 | - | 3 |
| 17 | 13Y | MC | Domestic Shorthair | 4 | 3 | 2 |
| 18 | 10Y | MC | Domestic Shorthair | 2 | - | 1 |
| Normal 1 | 5Y | FI | Domestic Shorthair | | | |

| | | | |
|---|---|---|---|
| Normal 2 | 7Y | FI | Domestic Shorthair |
| Normal 3 | 5Y | MI | Domestic Shorthair |
| Normal 4 | 7Y | FI | Domestic Shorthair |
| HL Cat | 3Y | MC | Domestic Shorthair |
| Pancreatitis Cat | 7Y | MC | Domestic Shorthair |

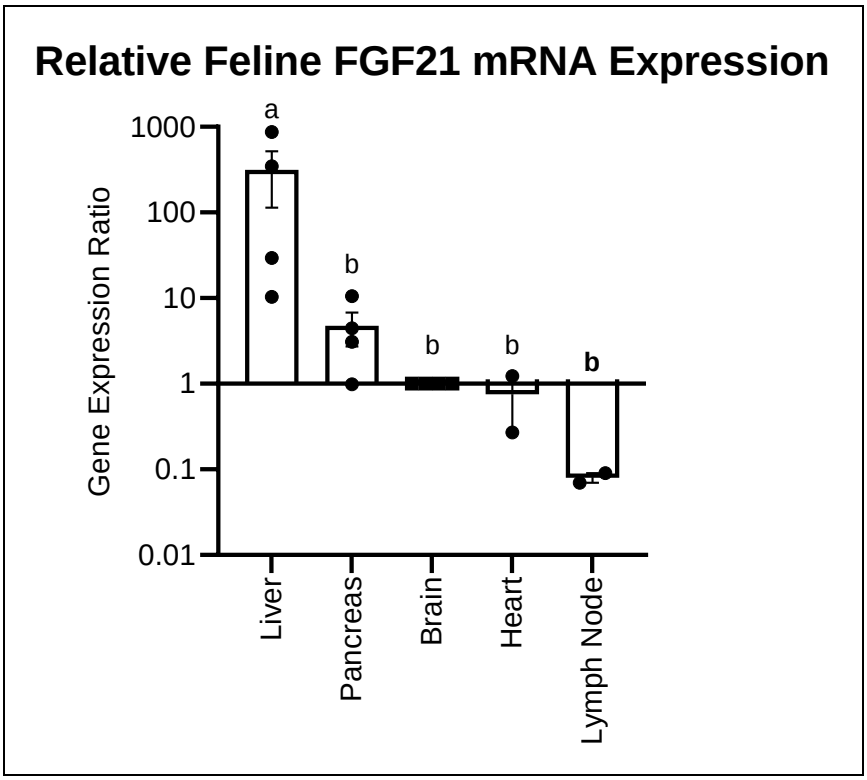


**Figure 1. FGF21 mRNA expression relative to the brain, normalized to the endogenous standard β-actin.** The liver, pancreas, and brain were consistently amplified (Ct < 34, n = 4). The heart and lymph node were inconsistently amplified (n = 2). The highest expressing tissue was the liver at 320X the expression of the brain, followed by the pancreas at 4.8X the expression of the brain; however, this was not a significant increase (2-way ANOVA, p = 0.02). Error bars represent ± SEM.

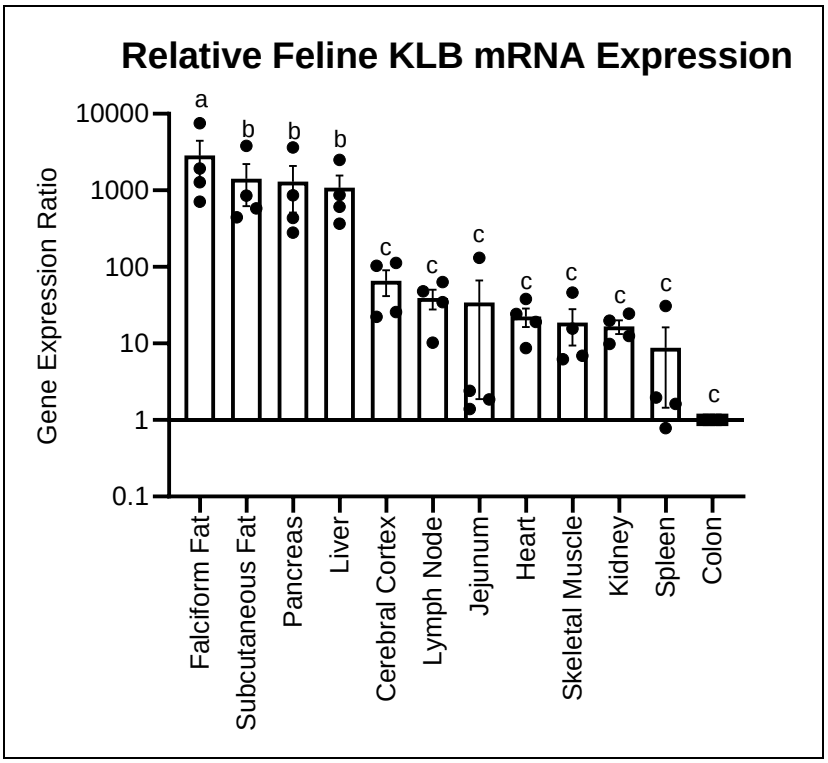


**Figure 2. KLB mRNA expression relative to the colon, normalized to the endogenous standard β-actin.** All examined tissues were amplified (Ct < 34, n = 4). The highest expressing tissue was the falciform fat at 2863X the expression of the colon (2-way ANOVA, $p < 0.01$; Tukey's multiple comparisons test, $p < 0.05$). Error bars represent ± SEM. Lower case letters over bars represent significance groups.

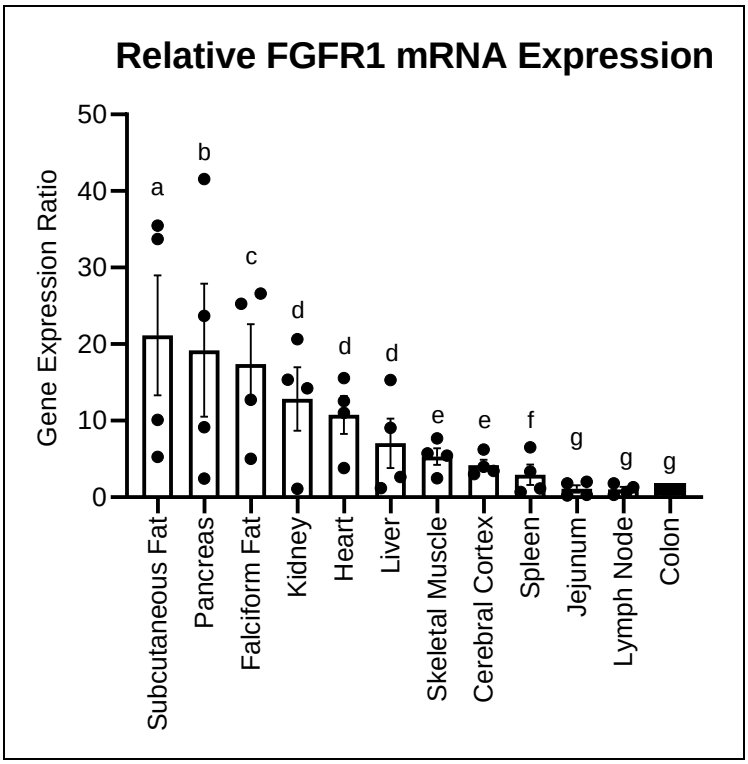


**Figure 3. FGFR1 mRNA expression relative to the colon, normalized to the endogenous standard β-actin.** All examined tissues were amplified (Ct < 34, n = 4). The highest expressing tissues were the subcutaneous fat, pancreas, and falciform fat at 21X, 19X, and 17X the colonic expression of FGFR1 (2-way ANOVA, $p < 0.0001$; Tukey's multiple comparisons test, $p < 0.05$). Error bars represent ± SEM. Lower case letters over bars represent significance groups.

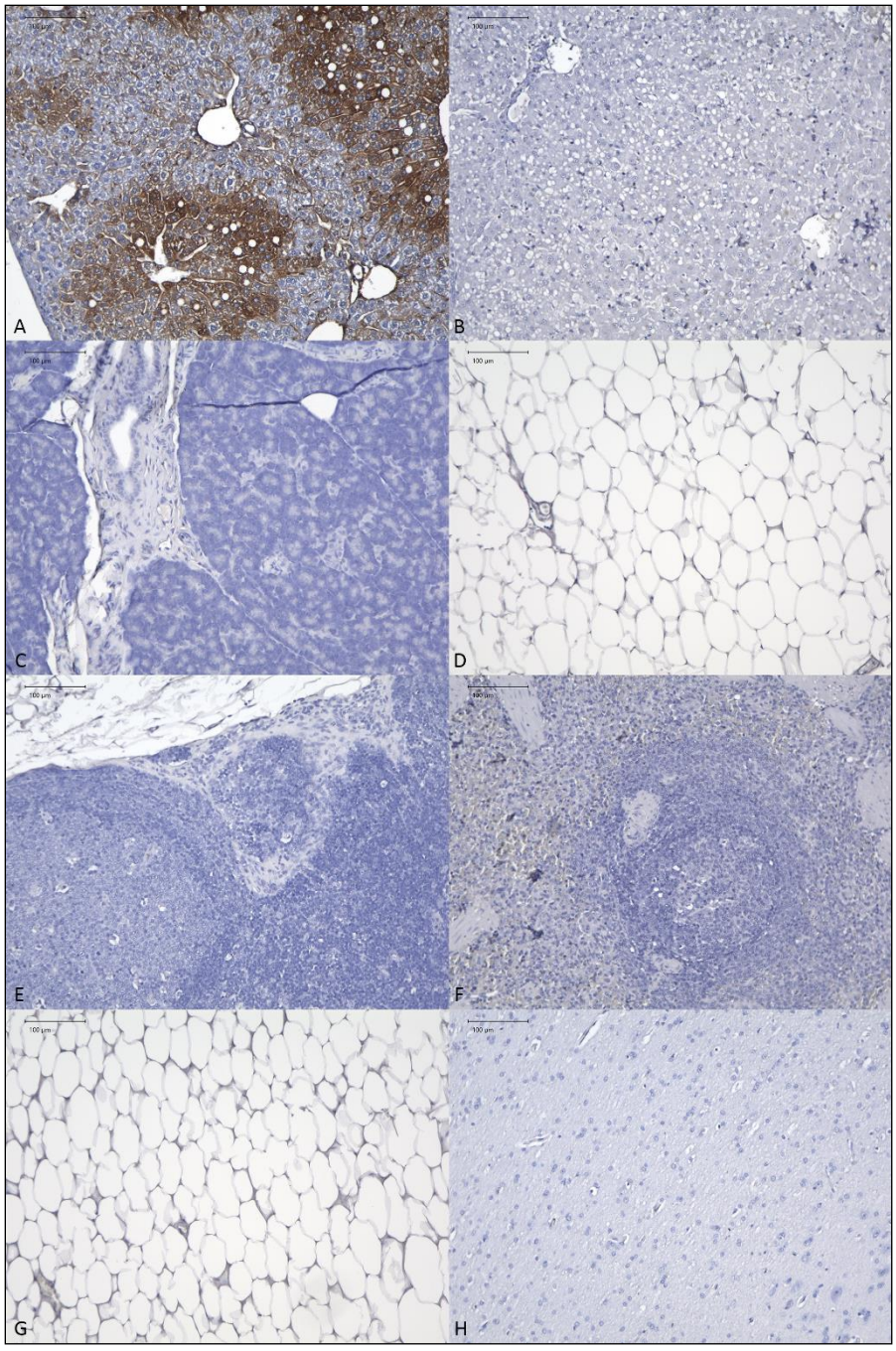


**Figure 4. Positive and negative controls for FGF21 IHC.** (A) WT mouse liver positive control. Negative controls of (B) liver, (C) pancreas, (D) subcutaneous fat, (E) mesenteric lymph node, (F) spleen, (G) falciform fat, and (H) cerebral cortical white matter. Negative controls were done with 1:200 goat serum diluted in PBS, replacing the anti-FGF21 antibody.

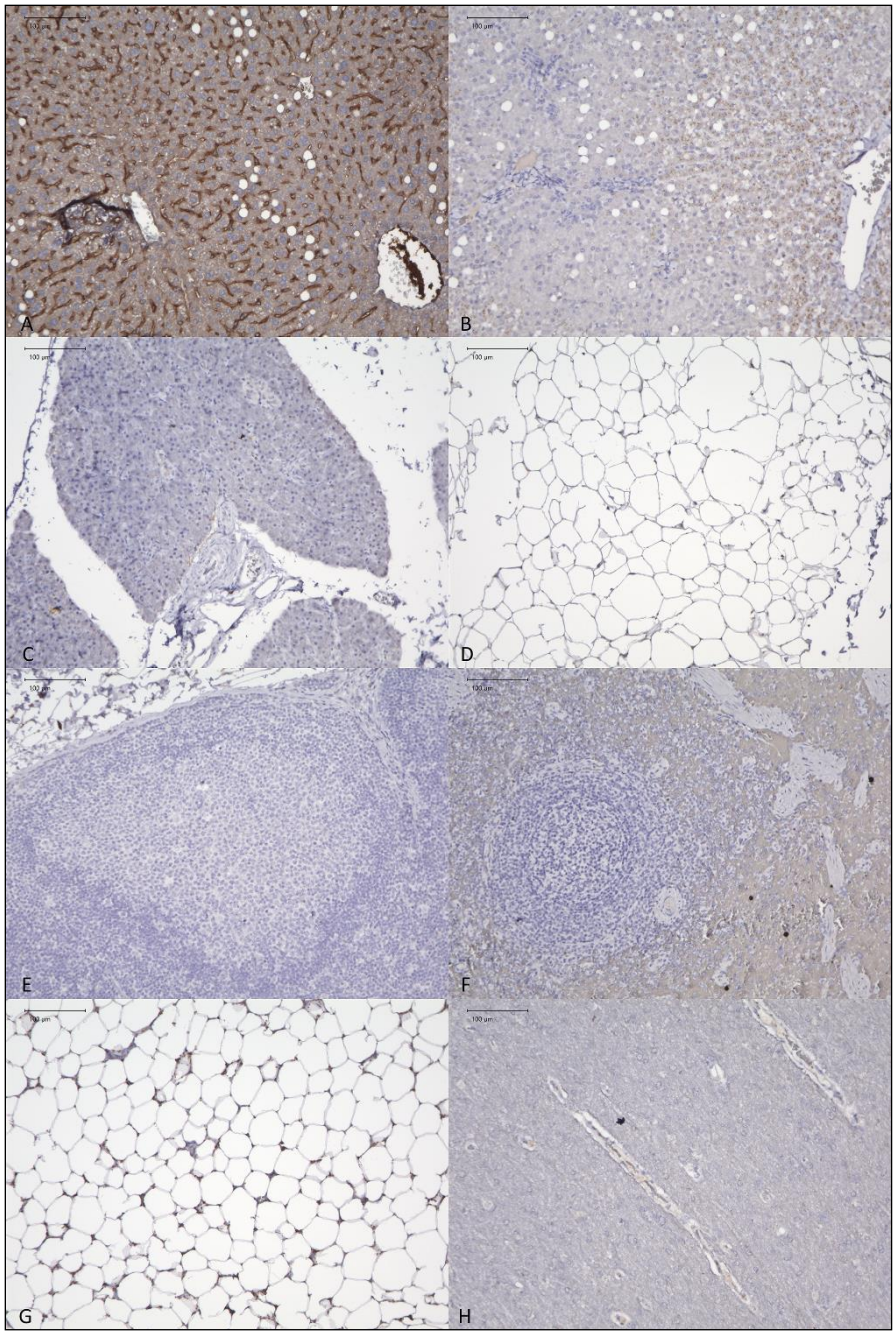


**Figure 5. Positive and negative controls for KLB IHC.** (A) WT mouse liver positive control. Negative controls of (B) liver, (C) pancreas, (D) subcutaneous fat, (E) mesenteric lymph node, (F) spleen, (G) falciform fat, and (H) cerebral cortical white matter. Negative controls were done with 1:1000 goat serum diluted in PBS, replacing the anti-KLB antibody.

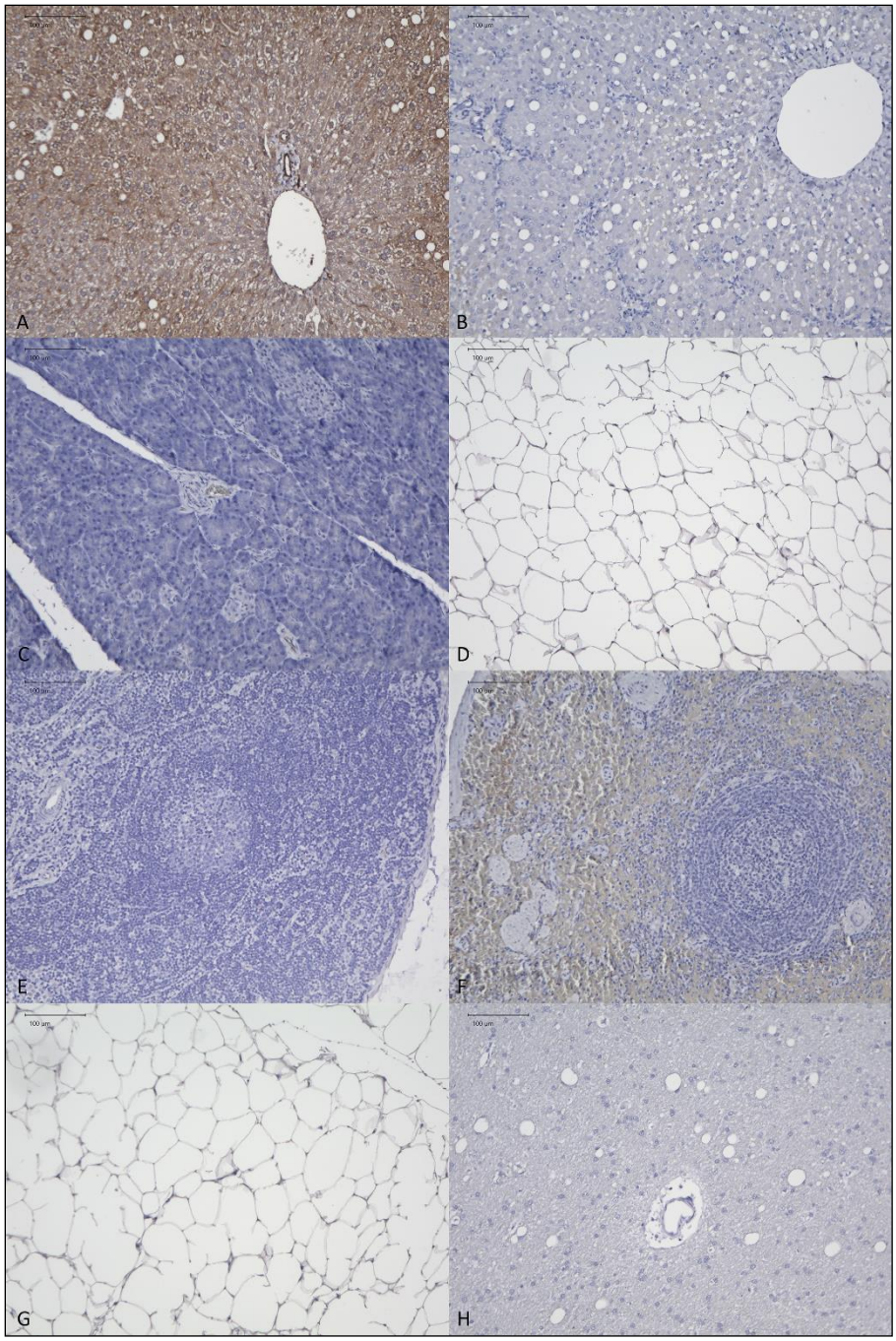


**Figure 6. Positive and negative controls for FGFR1 IHC.** (A) WT mouse liver positive control. Negative controls of (B) liver, (C) pancreas, (D), subcutaneous fat, (E) mesenteric lymph node, (F) spleen, (G) falciform fat, and (H) cerebral cortical white matter. Negative controls were done with 1:200 goat serum diluted in PBS, replacing the anti-FGFR1 antibody.

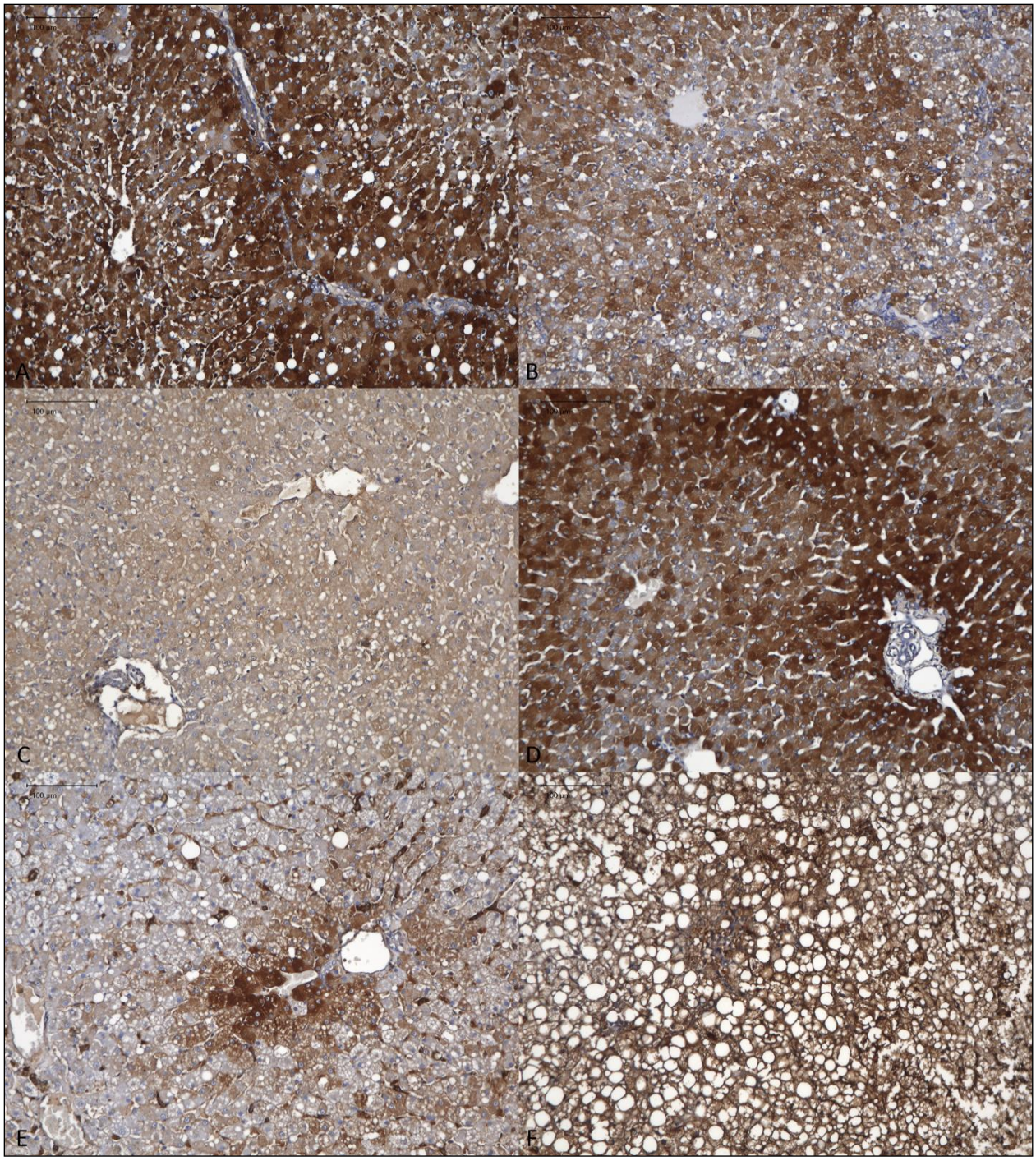


**Figure 7. Hepatic FGF21 IHC**. (A-D) clinically healthy cats, (E) cat with pancreatitis, (F) cat with hepatic lipidosis.

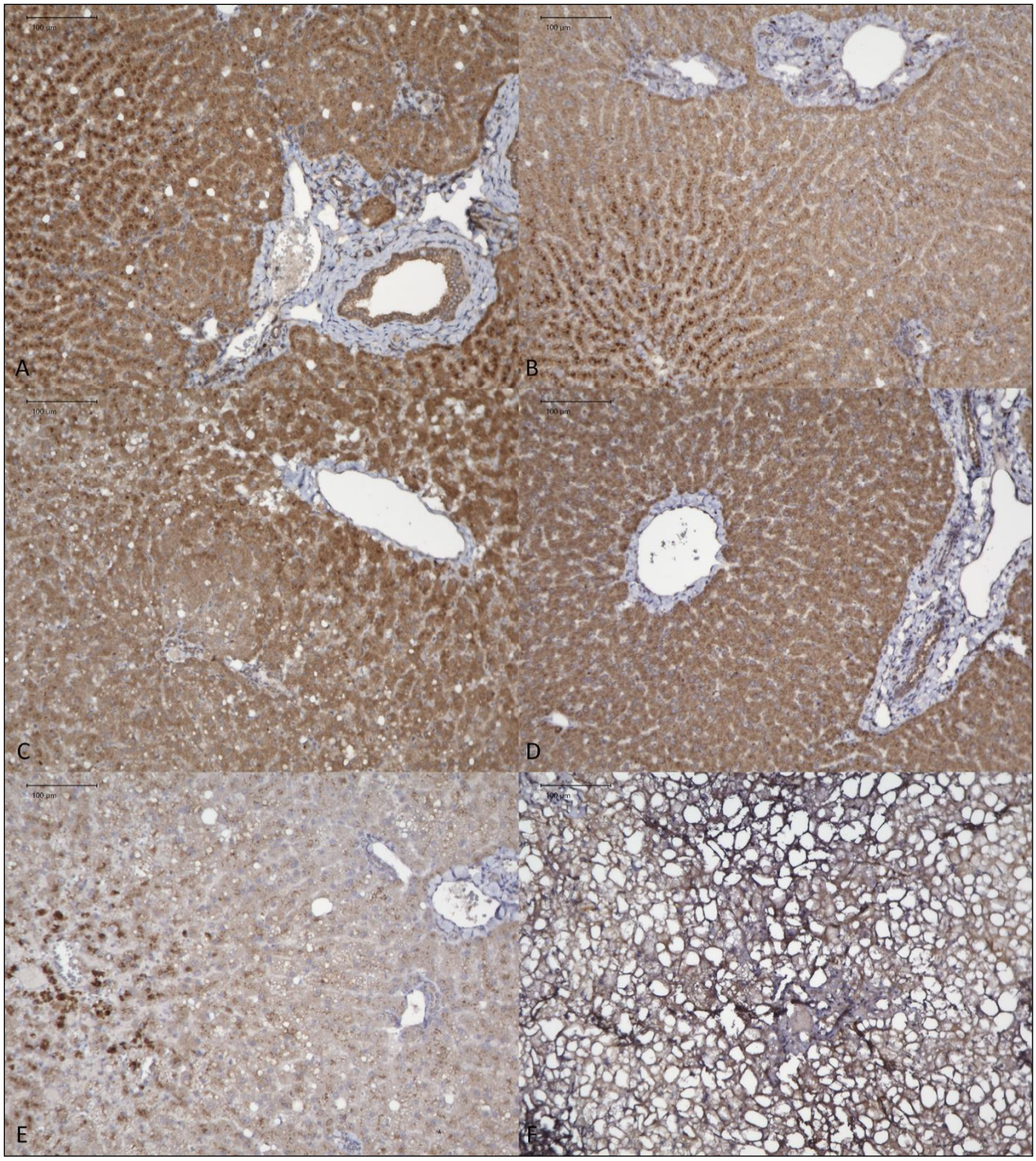


**Figure 8. Hepatic KLB IHC**. (A-D) clinically healthy cats, (E) cat with pancreatitis, (F) cat with hepatic lipidosis.

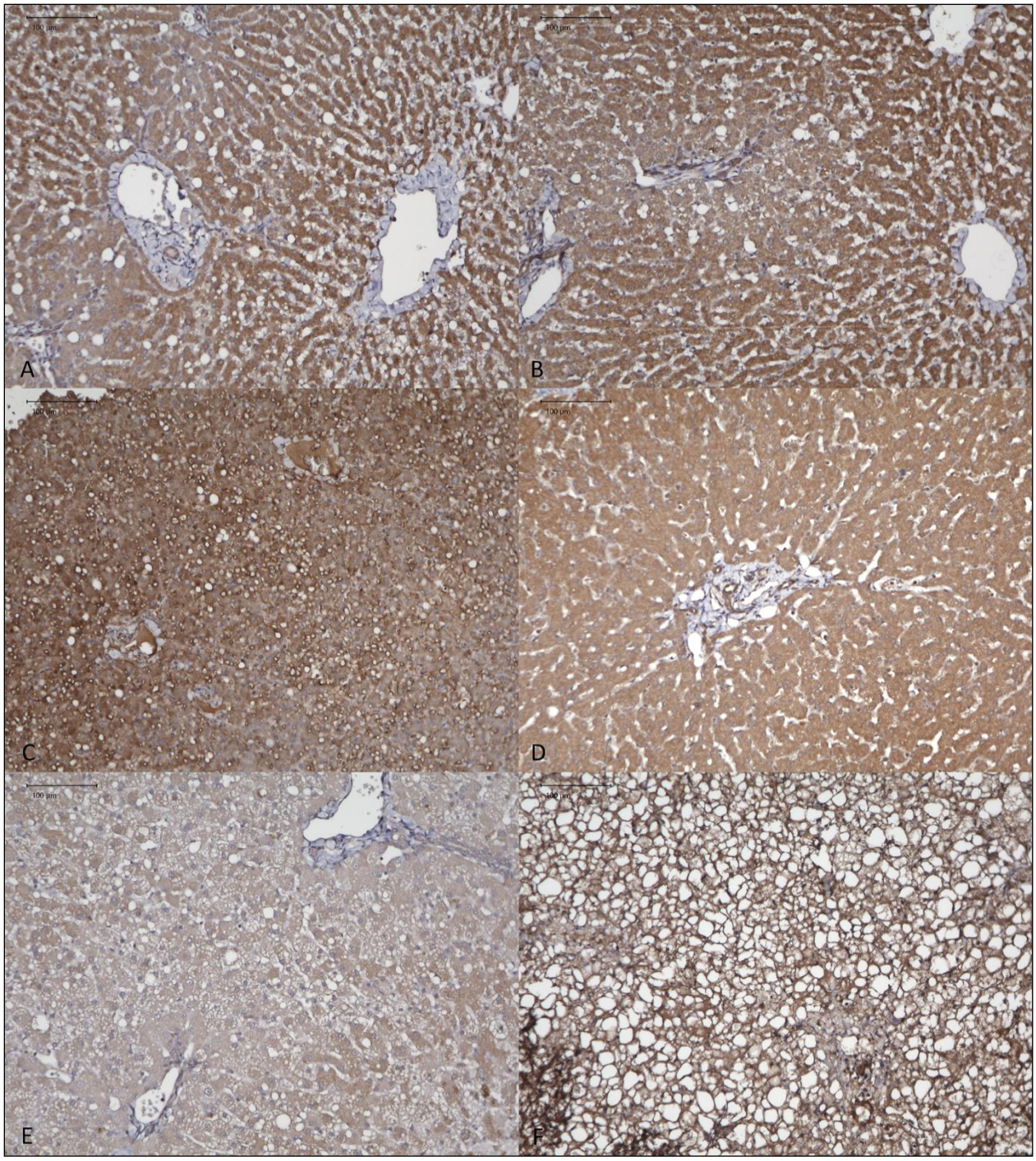


**Figure 9. Hepatic FGFR1 IHC**. (A-D) clinically healthy cats, (E) cat with pancreatitis, (F) cat with hepatic lipidosis.

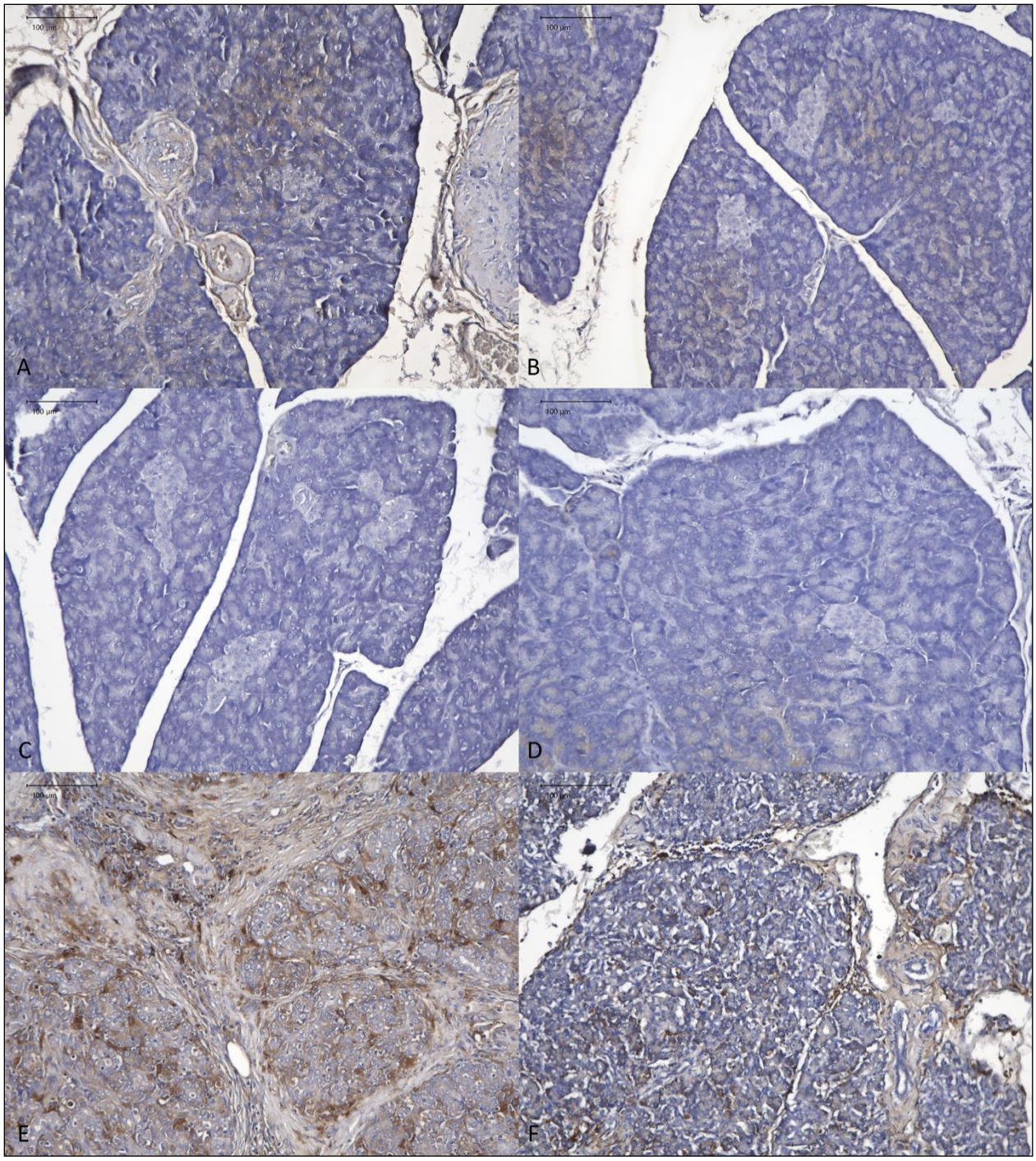


**Figure 10. Pancreatic FGF21 IHC**. (A-D) clinically healthy cats, (E) cat with pancreatitis, (F) cat with hepatic lipidosis.

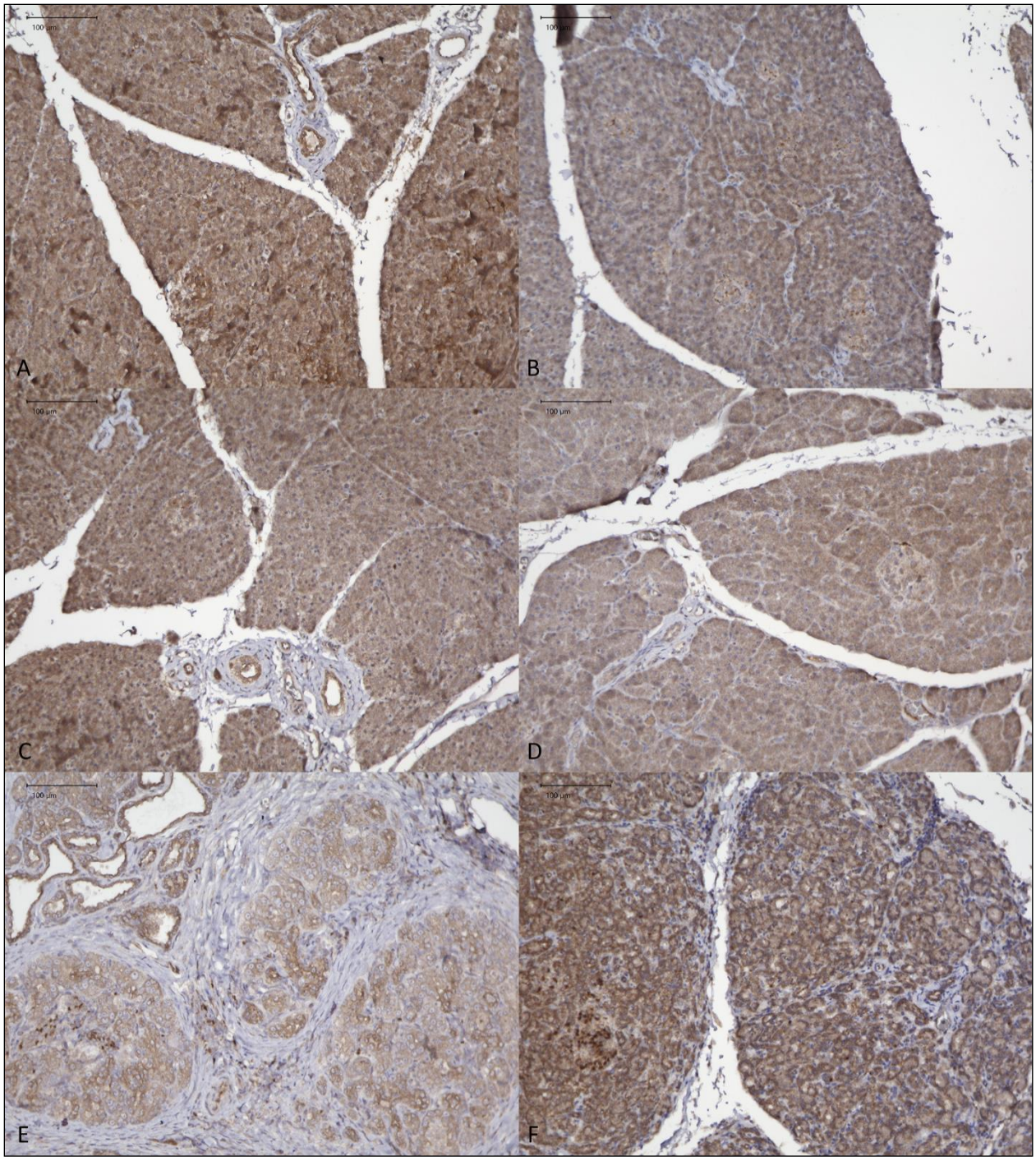


**Figure 11. Pancreatic KLB IHC**. (A-D) clinically healthy cats, (E) cat with pancreatitis, (F) cat with hepatic lipidosis.

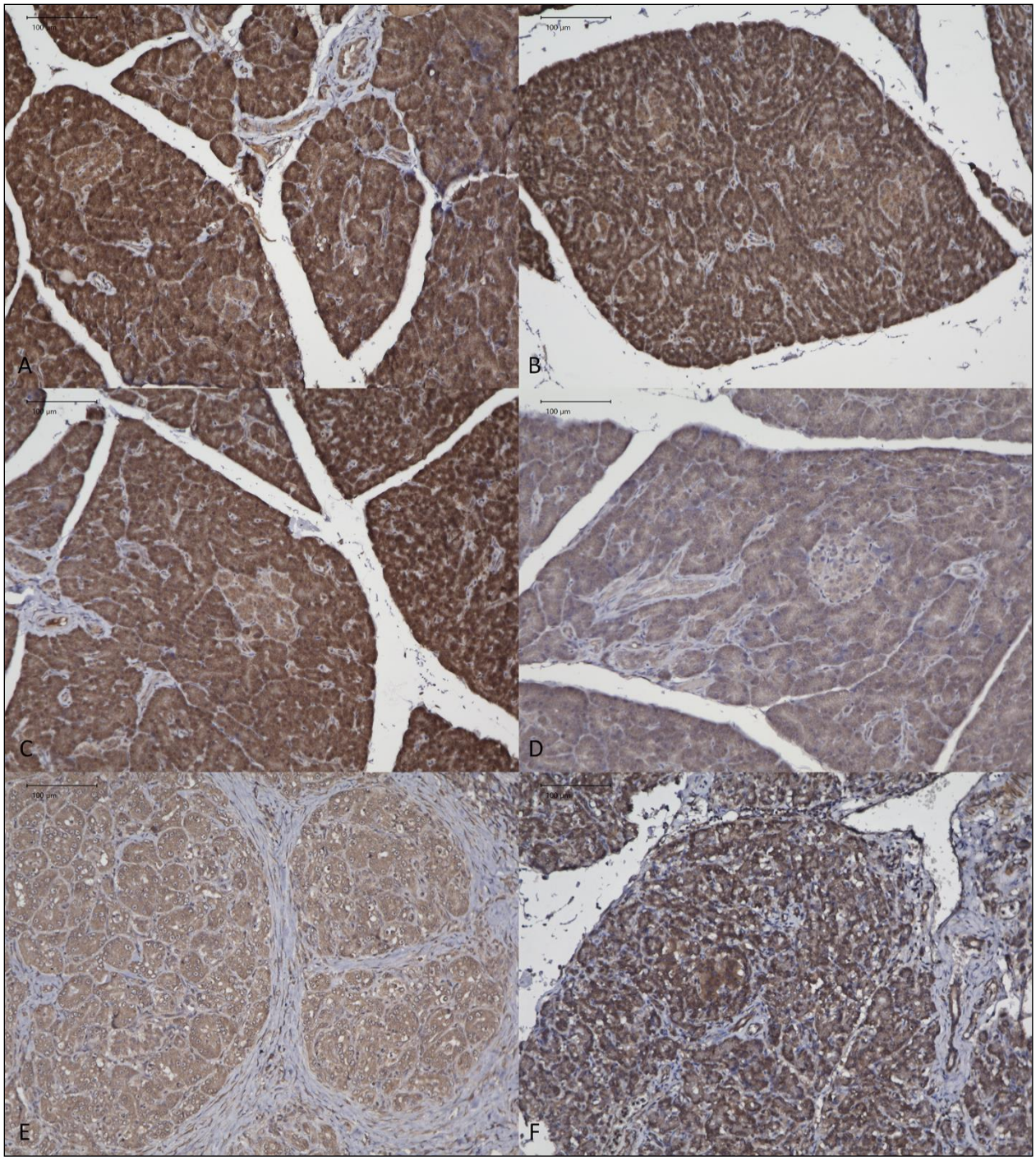


**Figure 12. Pancreatic FGFR1 IHC**. (A-D) clinically healthy cats, (E) cat with pancreatitis, (F) cat with hepatic lipidosis.

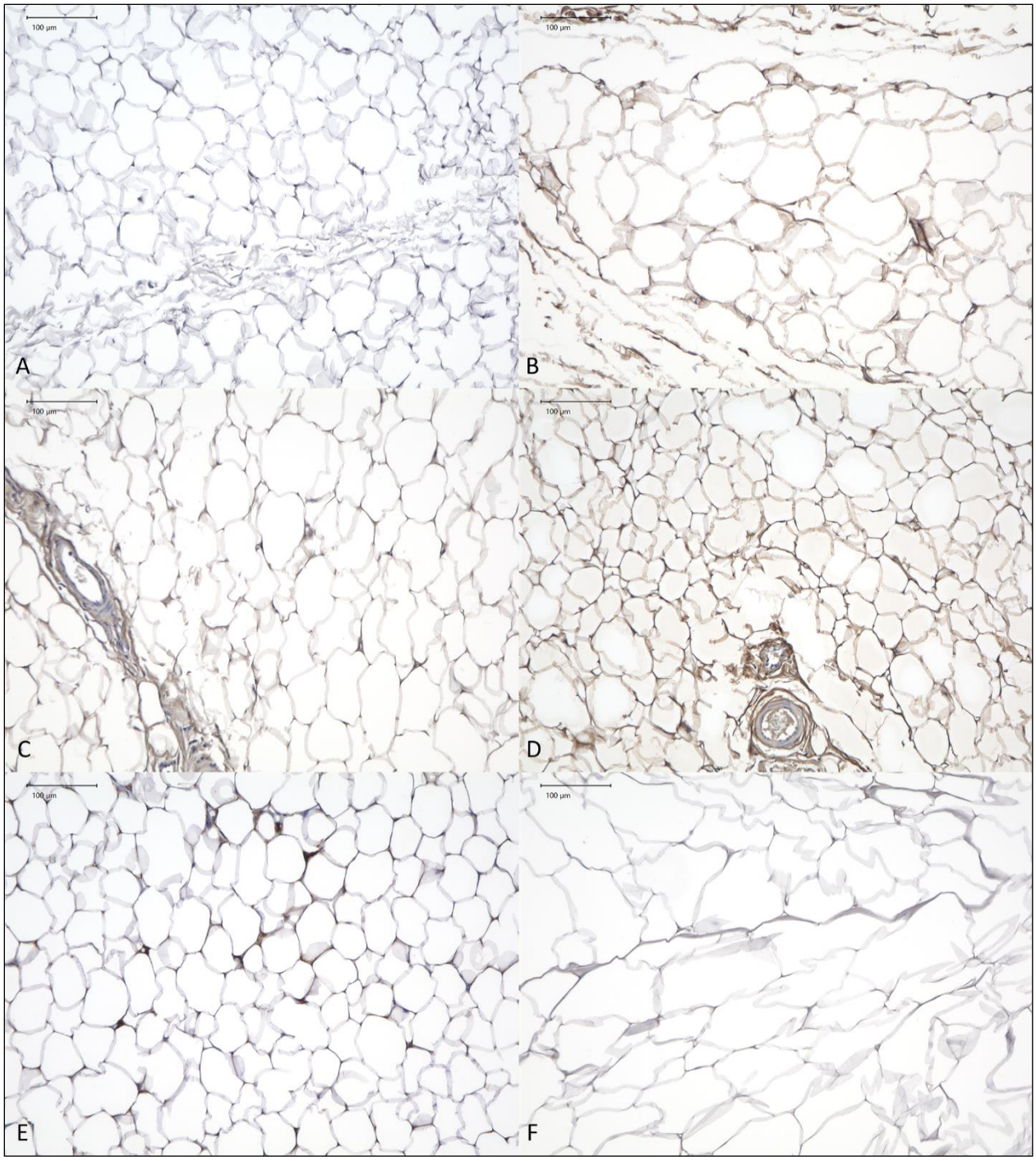


**Figure 13. Subcutaneous fat FGF21 IHC**. (A-D) clinically healthy cats, (E) cat with pancreatitis, (F) cat with hepatic lipidosis.

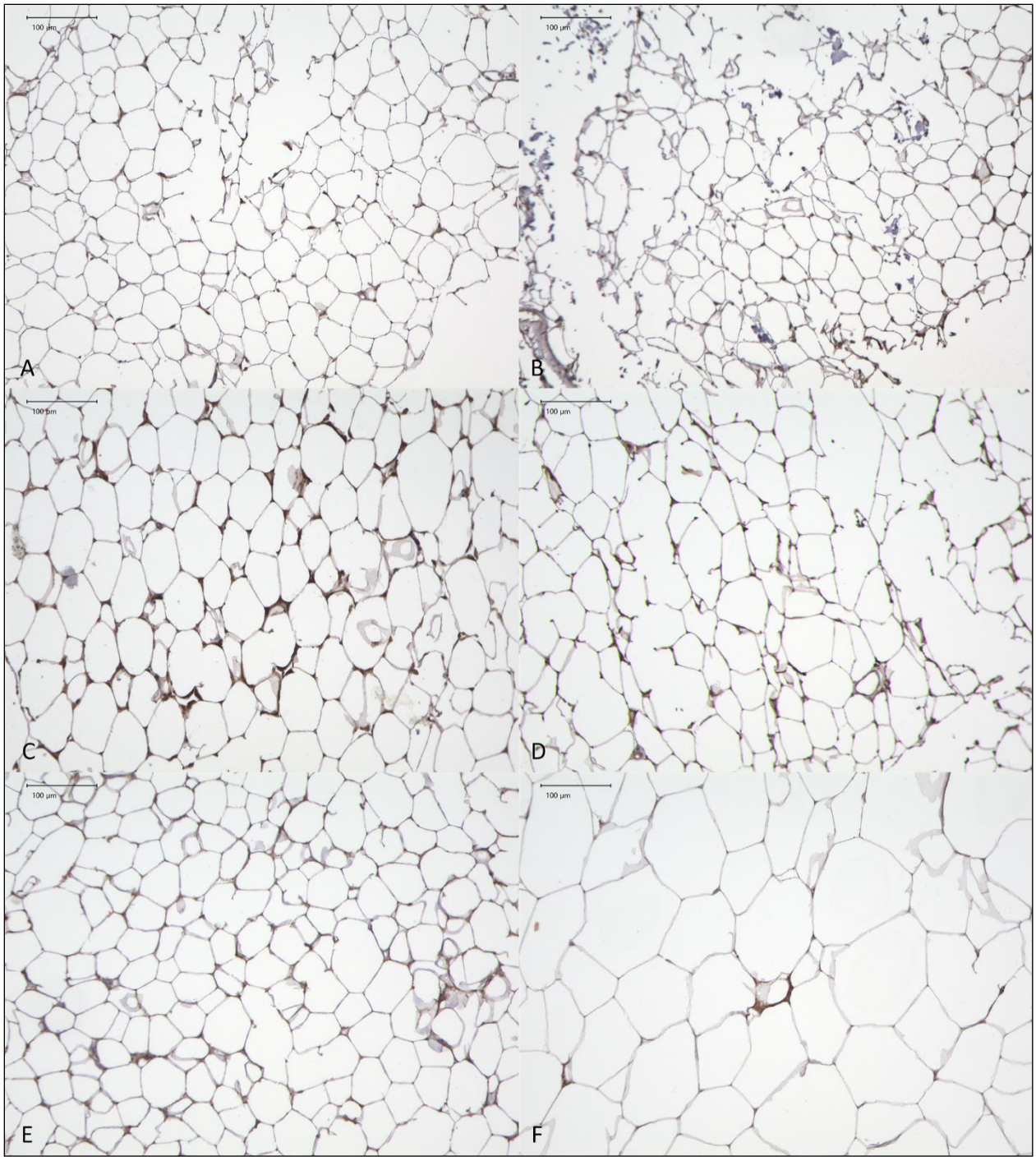


**Figure 14. Subcutaneous fat KLB IHC**. (A-D) clinically healthy cats, (E) cat with pancreatitis, (F) cat with hepatic lipidosis.

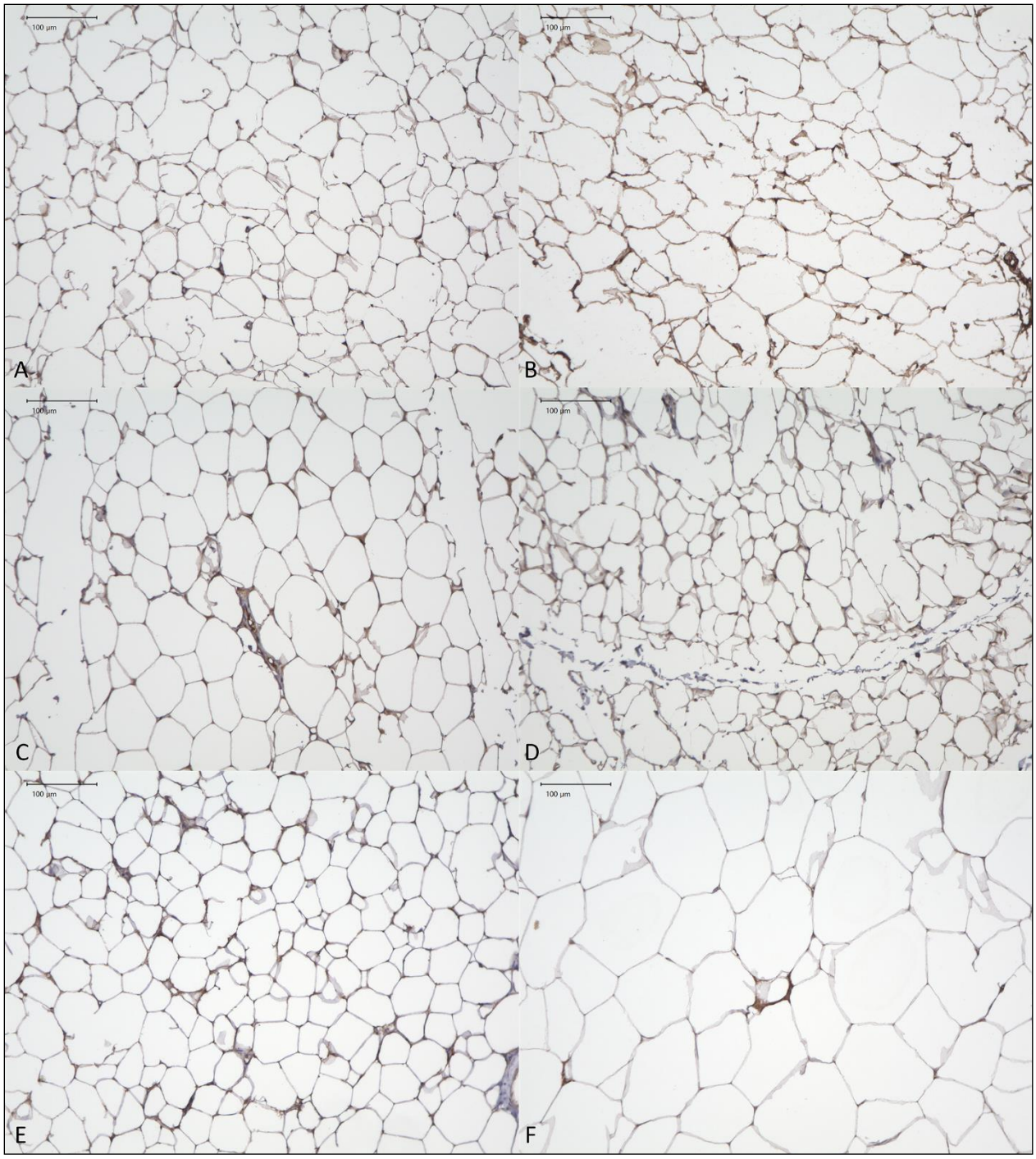


**Figure 15. Subcutaneous fat FGFR1 IHC**. (A-D) clinically healthy cats, (E) cat with pancreatitis, (F) cat with hepatic lipidosis.

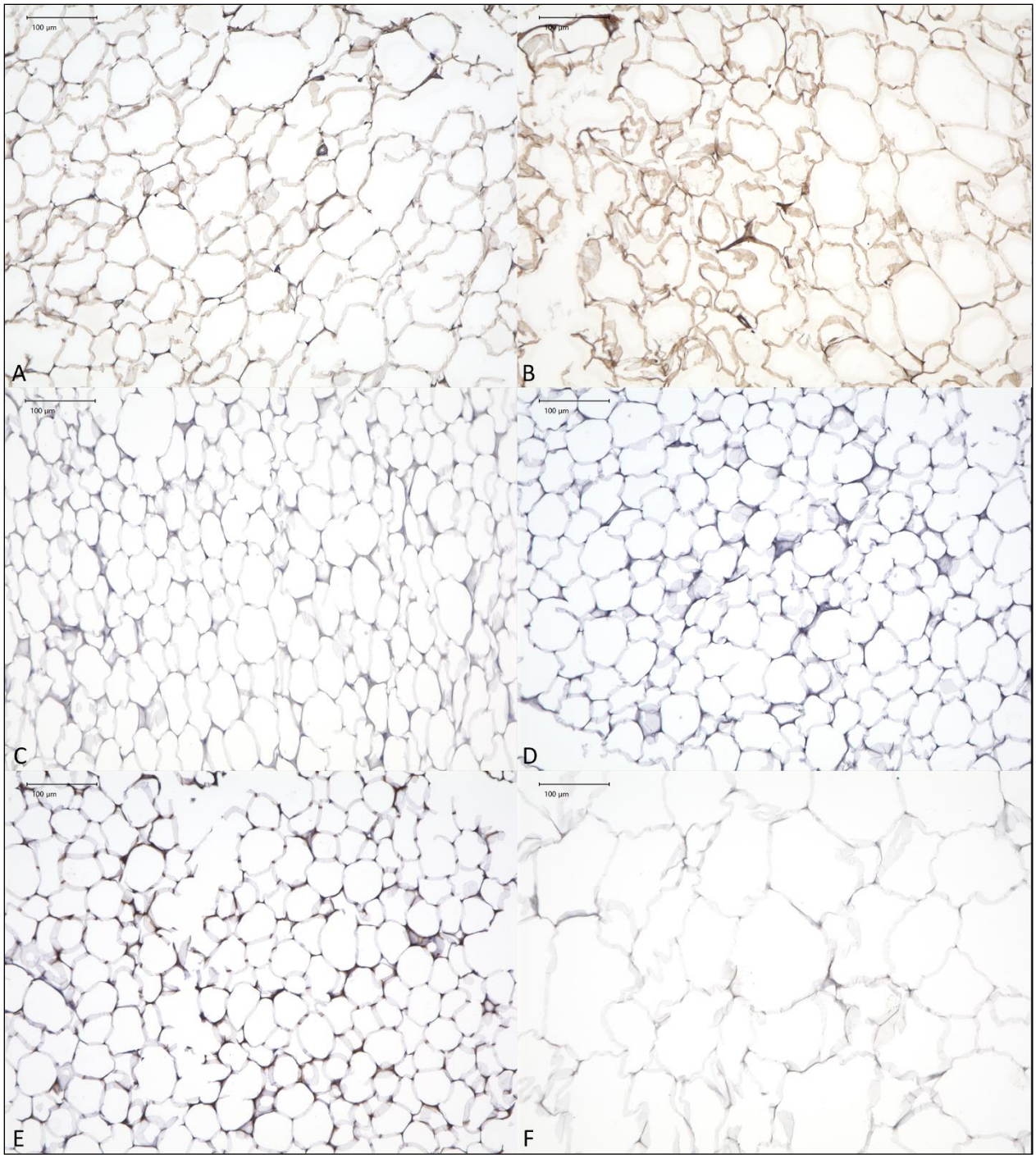


**Figure 16. Falciform fat FGF21 IHC**. (A-D) clinically healthy cats, (E) cat with pancreatitis, (F) cat with hepatic lipidosis.


**Figure 17. Falciform fat KLB IHC**. (A-D) clinically healthy cats, (E) cat with pancreatitis, (F) cat with hepatic lipidosis.


**Figure 18. Falciform fat FGFR1 IHC**. (A-D) clinically healthy cats, (E) cat with pancreatitis, (F) cat with hepatic lipidosis.

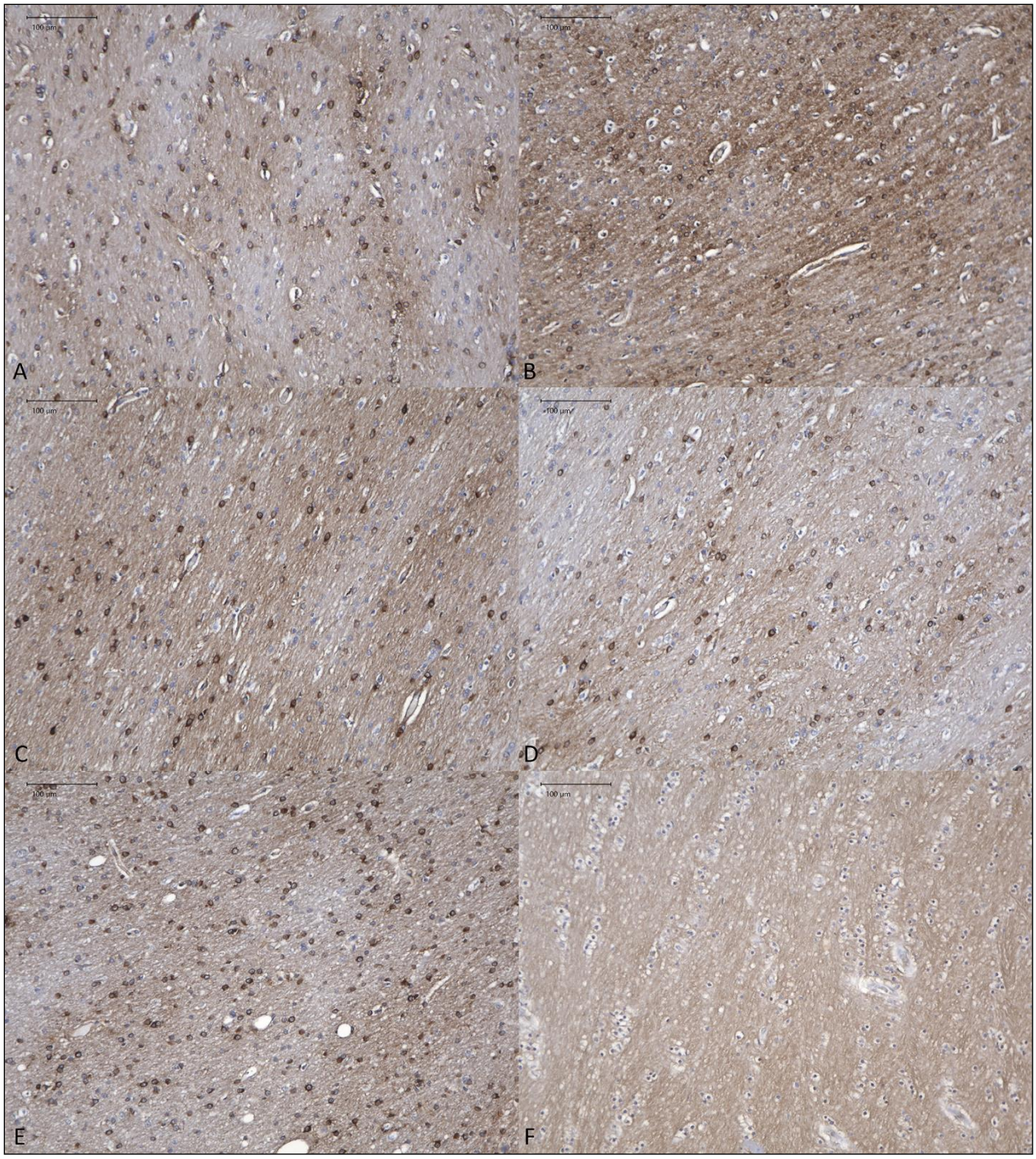


**Figure 19. Cerebral cortical white matter FGF21 IHC**. (A-D) clinically healthy cats, (E) cat with pancreatitis, (F) cat with hepatic lipidosis.

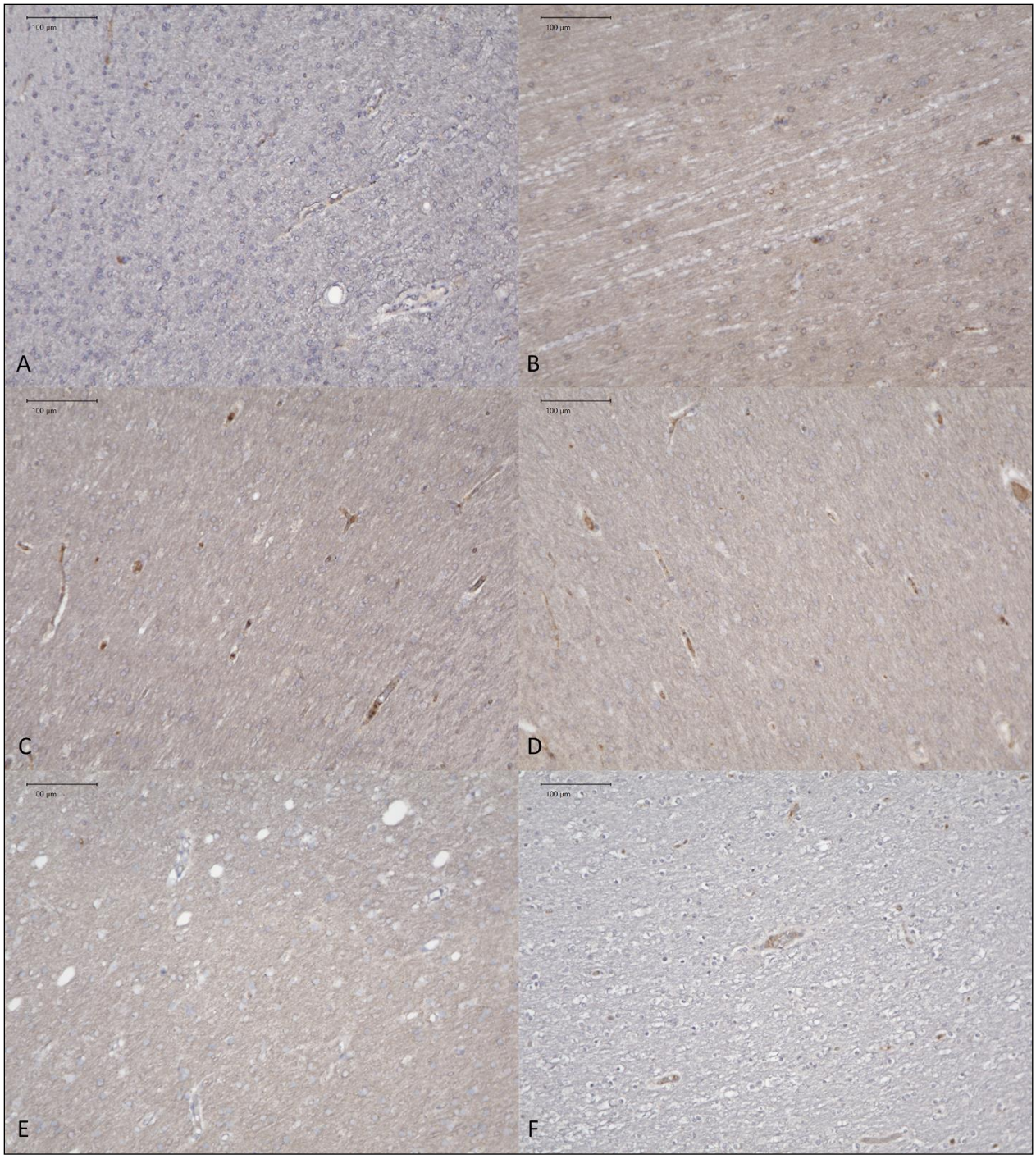


**Figure 20. Cerebral cortical white matter KLB IHC.** (A-D) clinically healthy cats, (E) cat with pancreatitis, (F) cat with hepatic lipidosis.

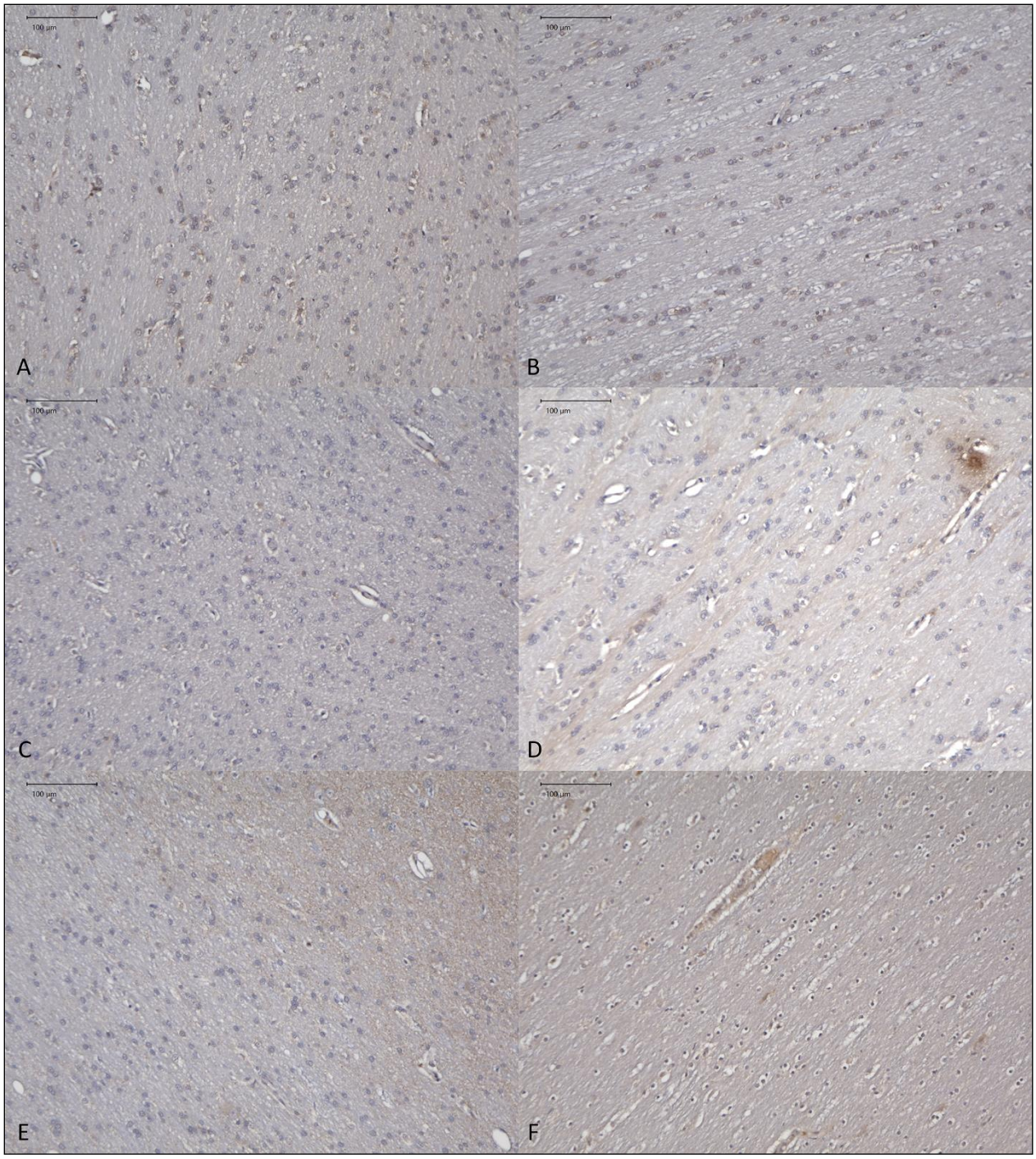


**Figure 21. Cerebral cortical white matter FGFR1 IHC**. (A-D) clinically healthy cats, (E) cat with pancreatitis, (F) cat with hepatic lipidosis.

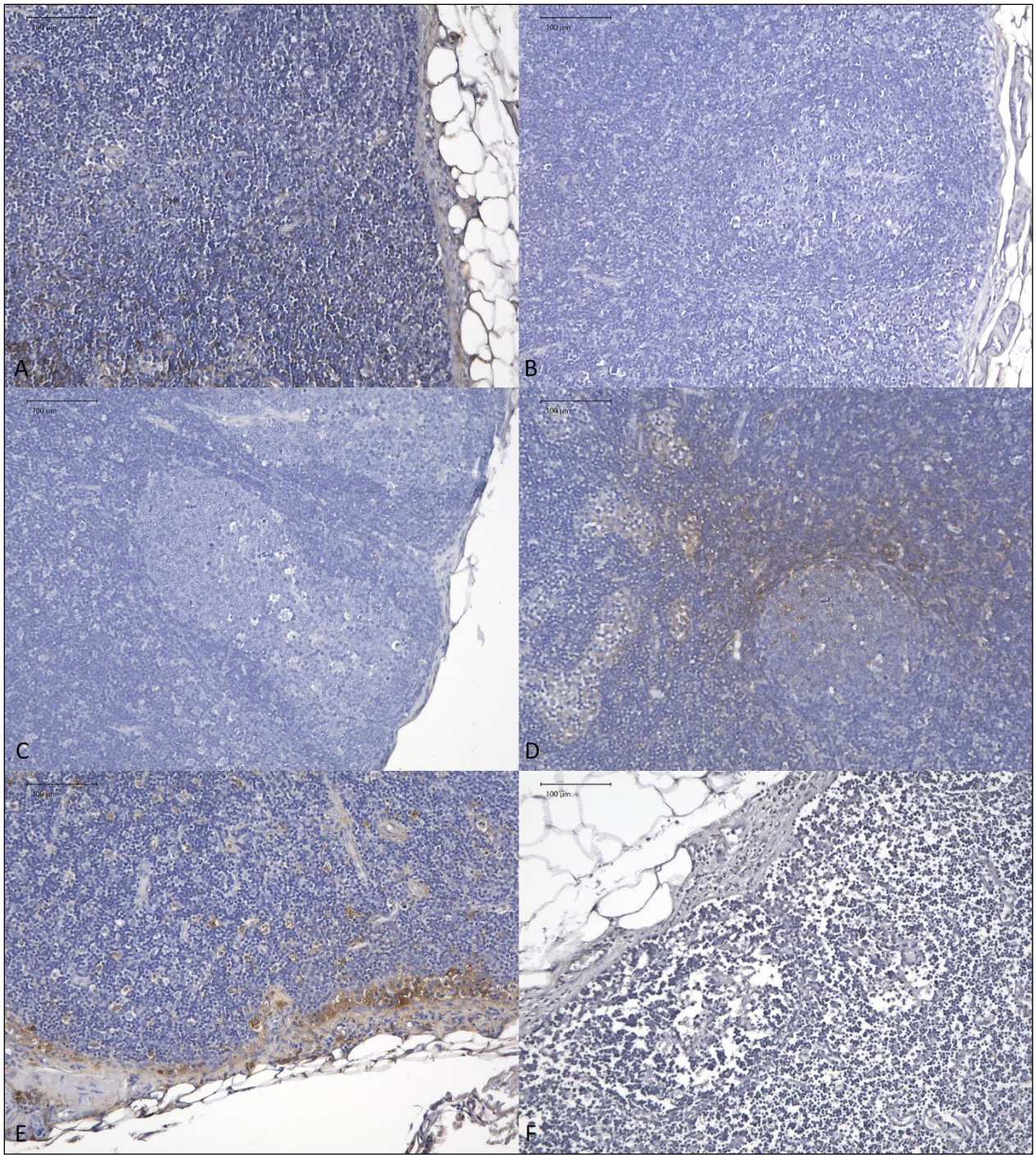


**Figure 22. Mesenteric lymph node FGF21 IHC**. (A-D) clinically healthy cats, (E) cat with pancreatitis, (F) cat with hepatic lipidosis

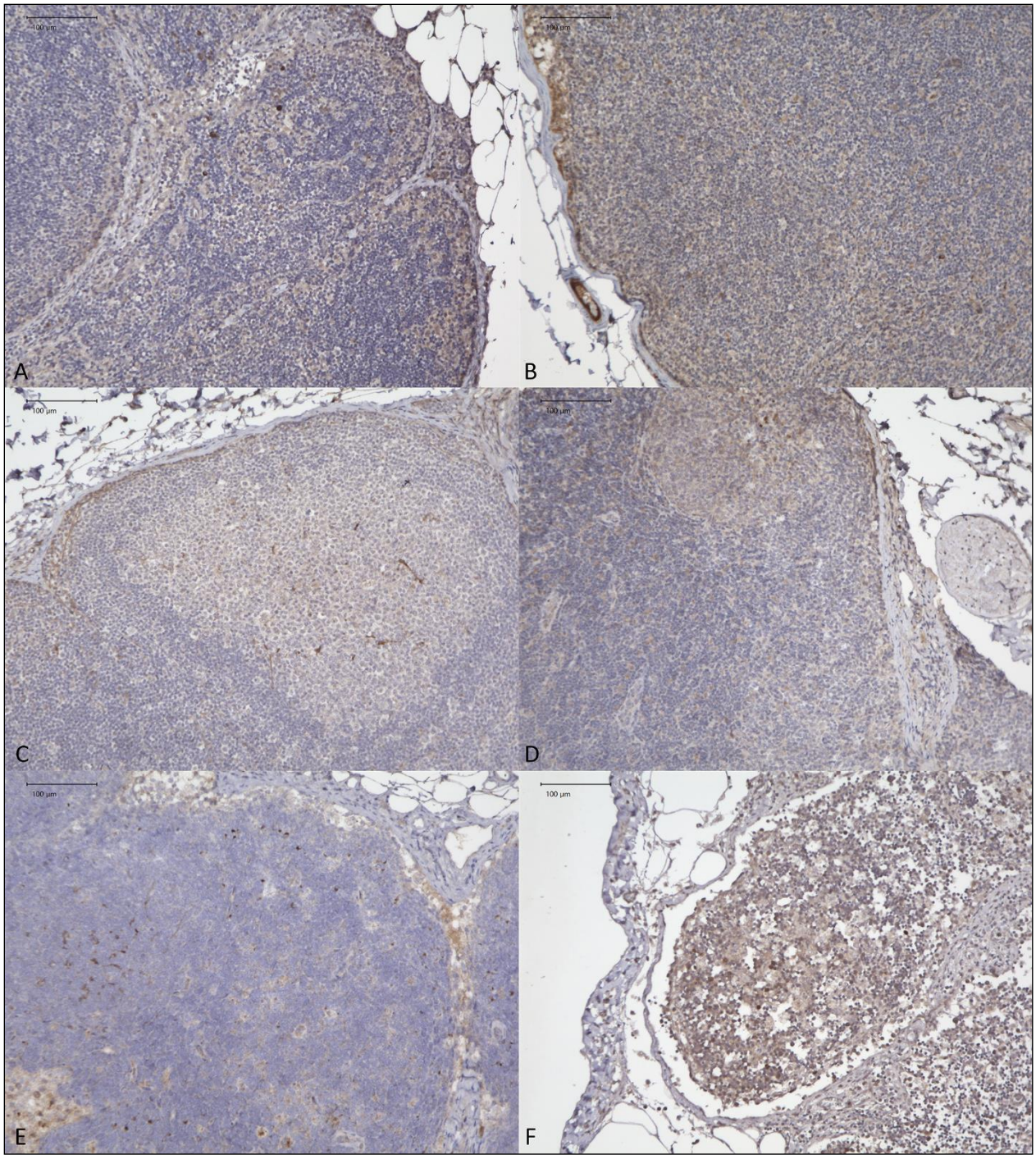


**Figure 23**. **Mesenteric lymph node KLB IHC**. (A-D) clinically healthy cats, (E) cat with pancreatitis, (F) cat with hepatic lipidosis.

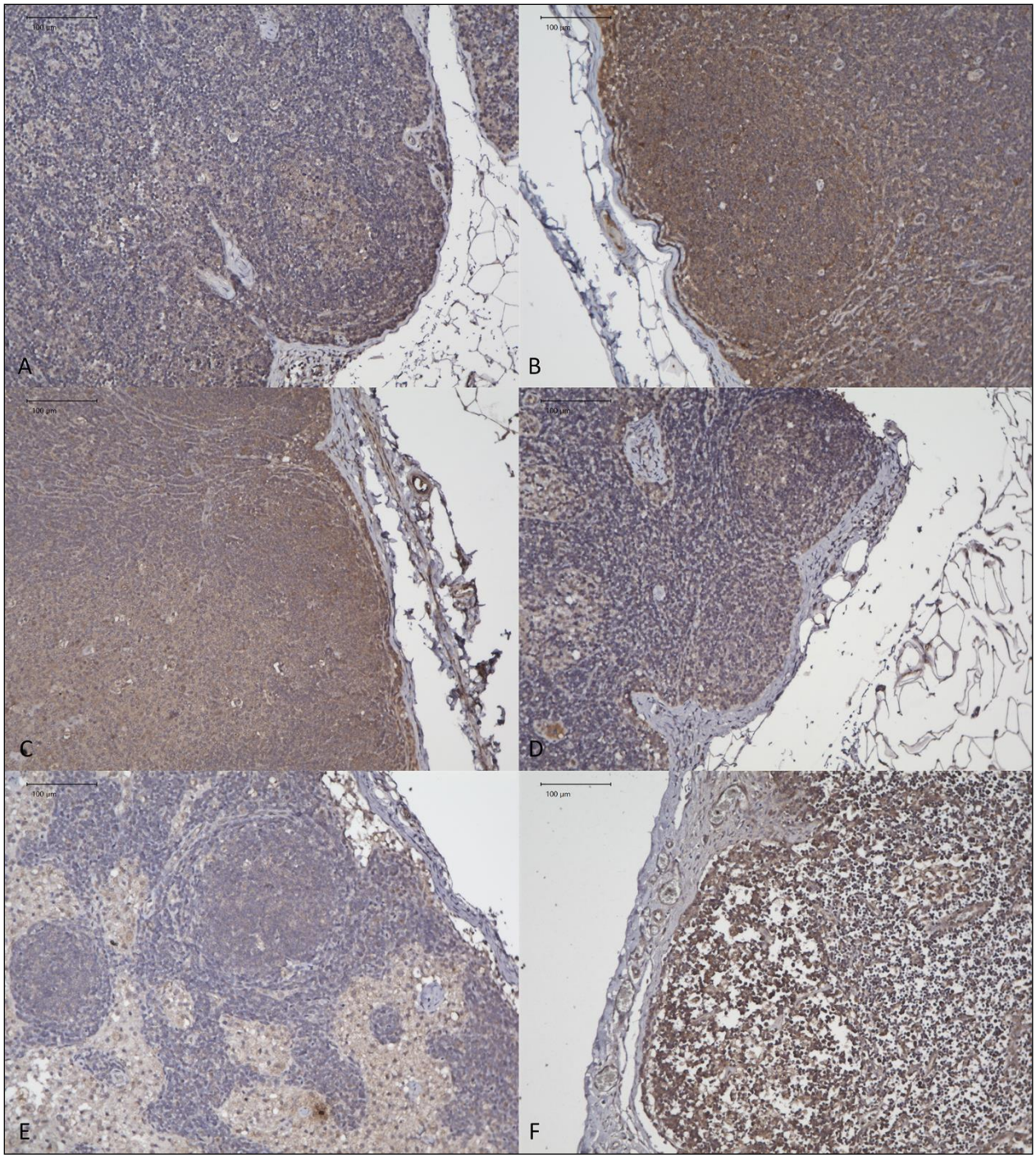


**Figure 24. Mesenteric lymph node FGFR1 IHC.** (A-D) clinically healthy cats, (E) cat with pancreatitis, (F) cat with hepatic lipidosis.

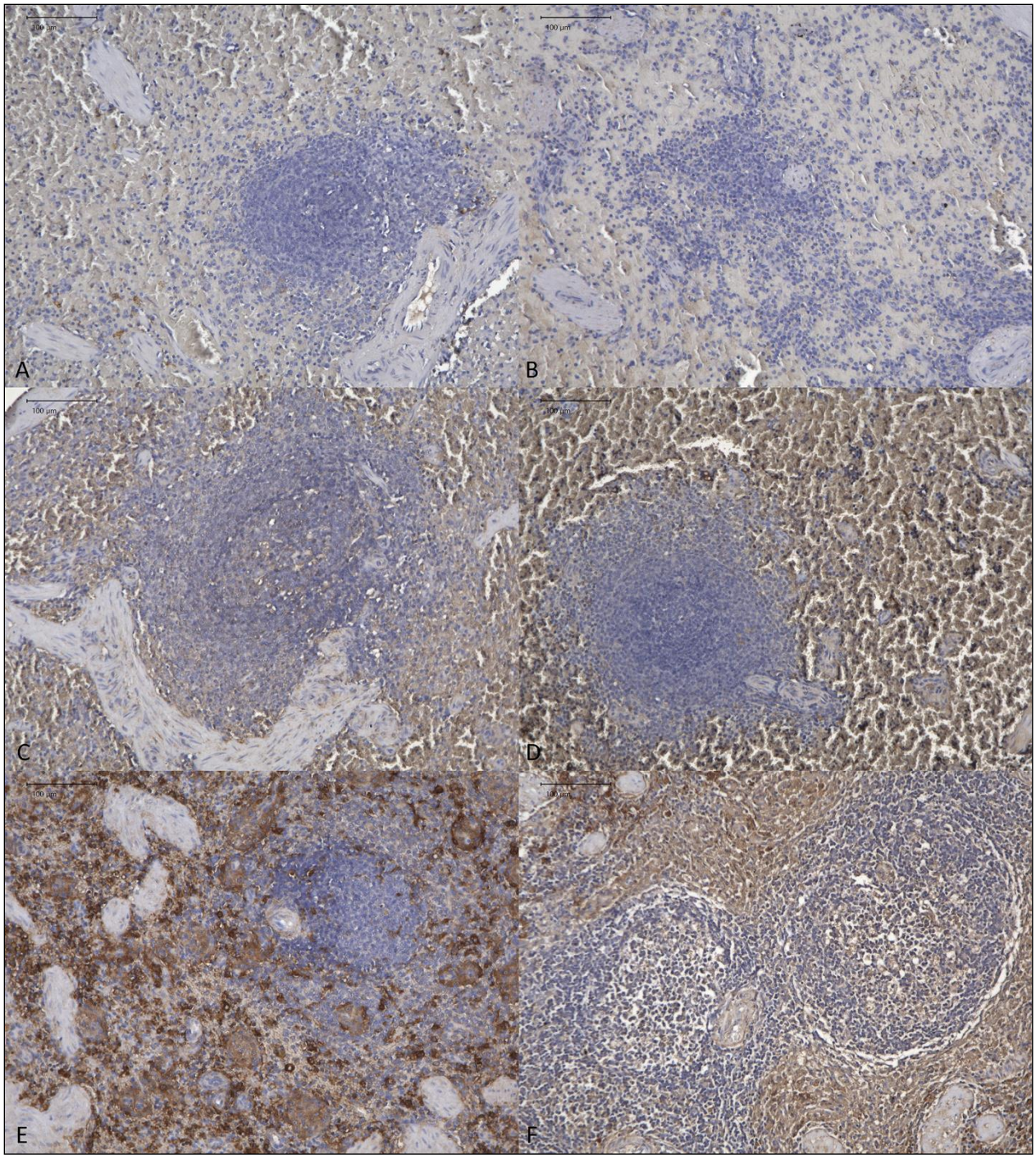


**Figure 25. Splenic FGF21 IHC**. (A-D) clinically healthy cats, (E) cat with pancreatitis, (F) cat with hepatic lipidosis.

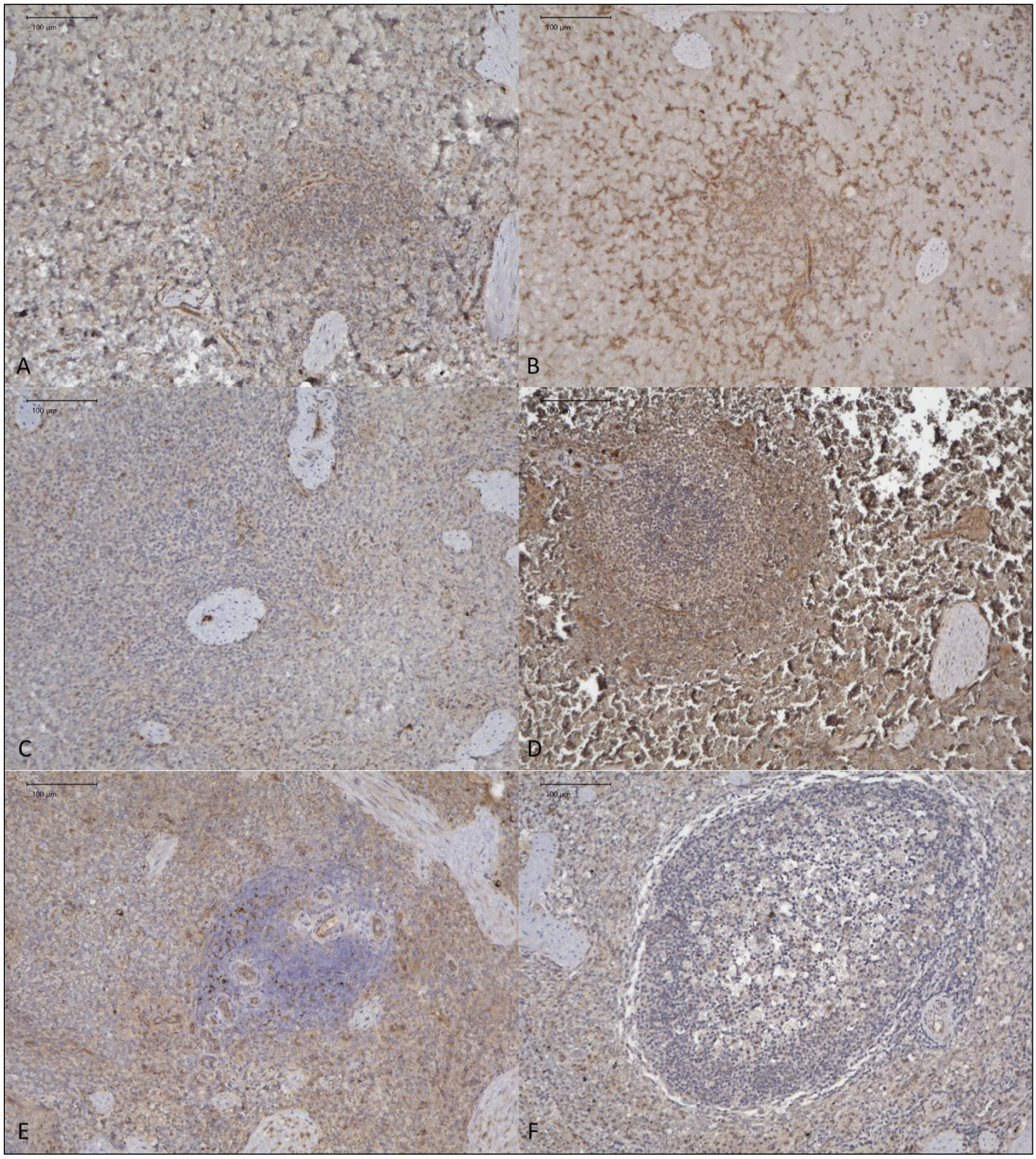


**Figure 26. Splenic KLB IHC.** (A-D) clinically healthy cats, (E) cat with pancreatitis, (F) cat with hepatic lipidosis.

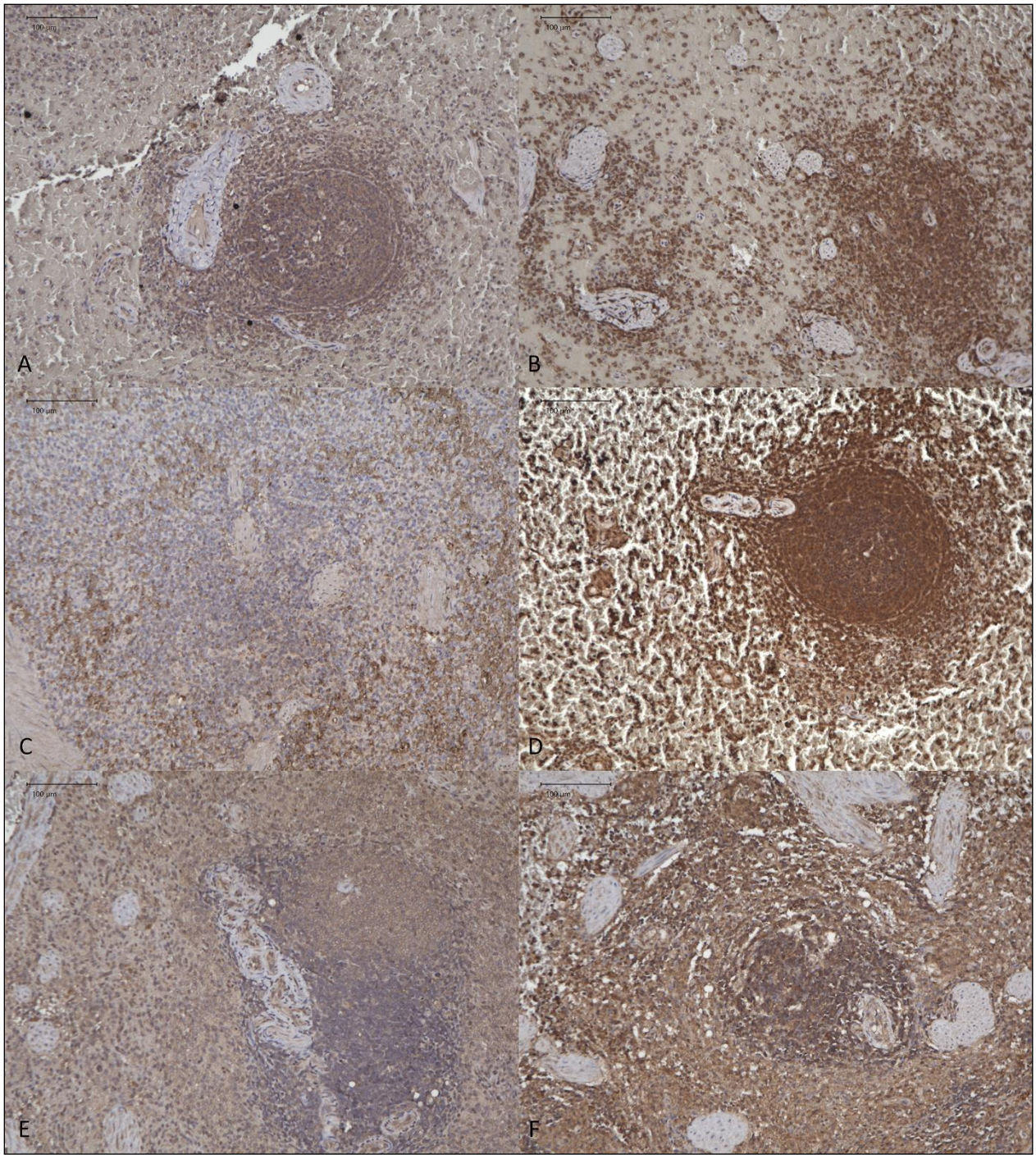


**Figure 27. Splenic FGFR1 IHC.** (A-D) clinically healthy cats, (E) cat with pancreatitis, (F) cat with hepatic lipidosis.

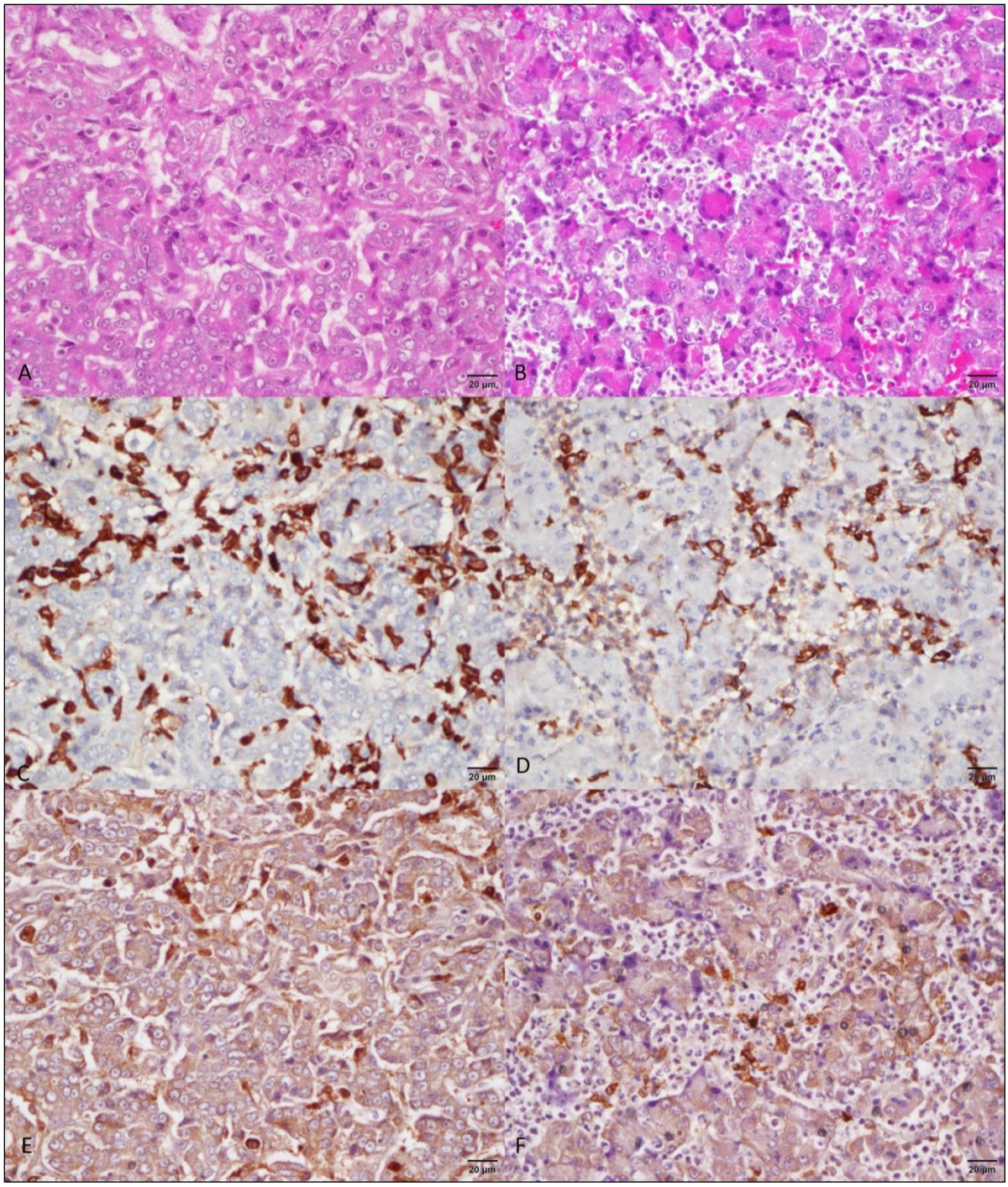


**Figure 28. Representative images from cats with pancreatitis.** H&E from (A) a hyperplastic nodule of a cat with chronic pancreatitis and (B) a cat with acute pancreatitis. (C) Iba1 IHC and (E) FGF21 from the same cat and near the same area of the pancreas as in (A). (D) Iba1 IHC and (F) FGF21 from the same cat and near the same area of the pancreas as in (B).

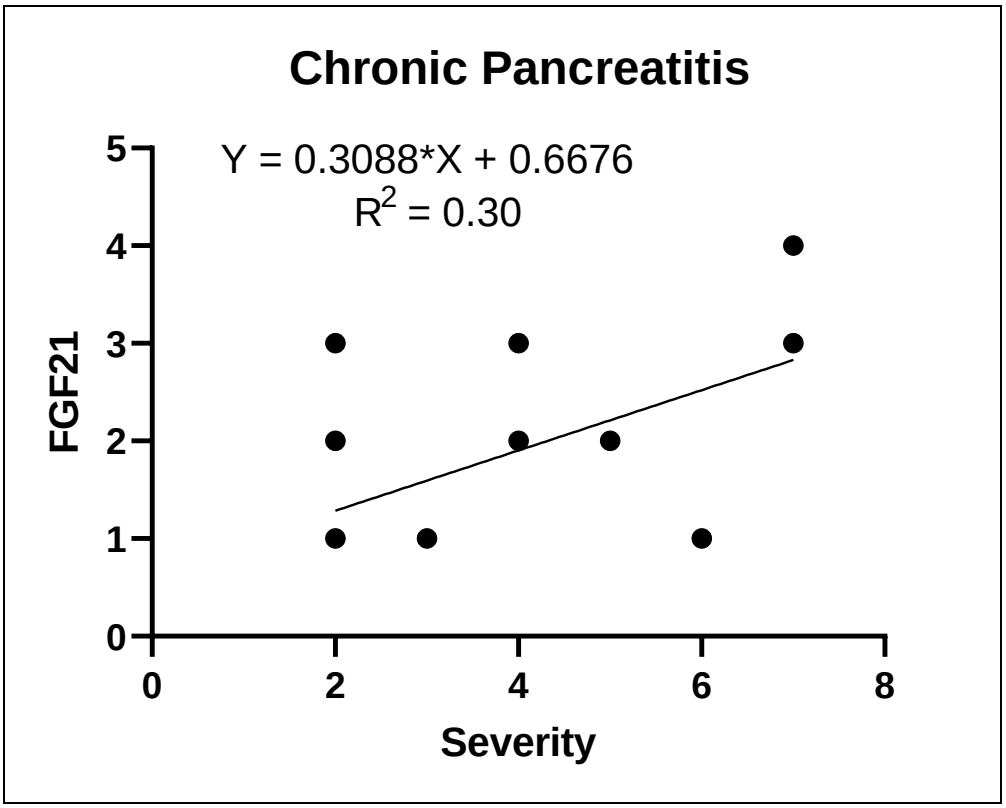


**Figure 29. Correlation of chronic pancreatitis severity with FGF21 staining score.**

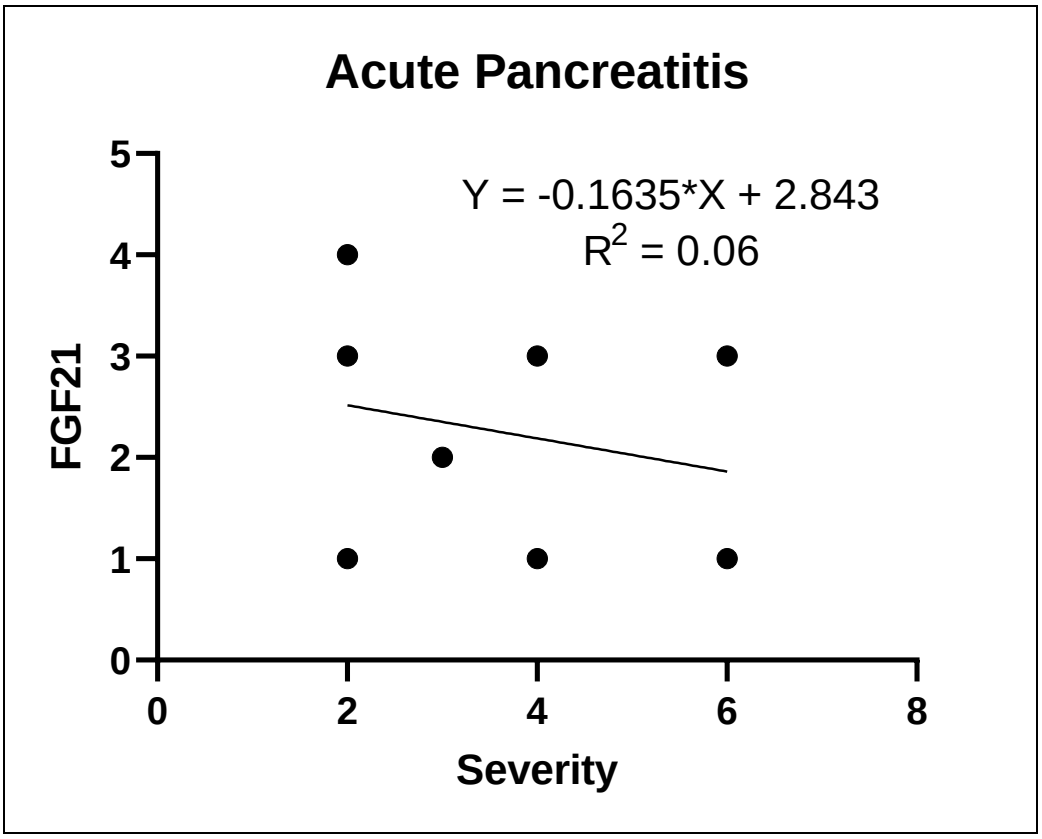


**Figure 30. Correlation of acute pancreatitis severity with FGF21 staining score.**

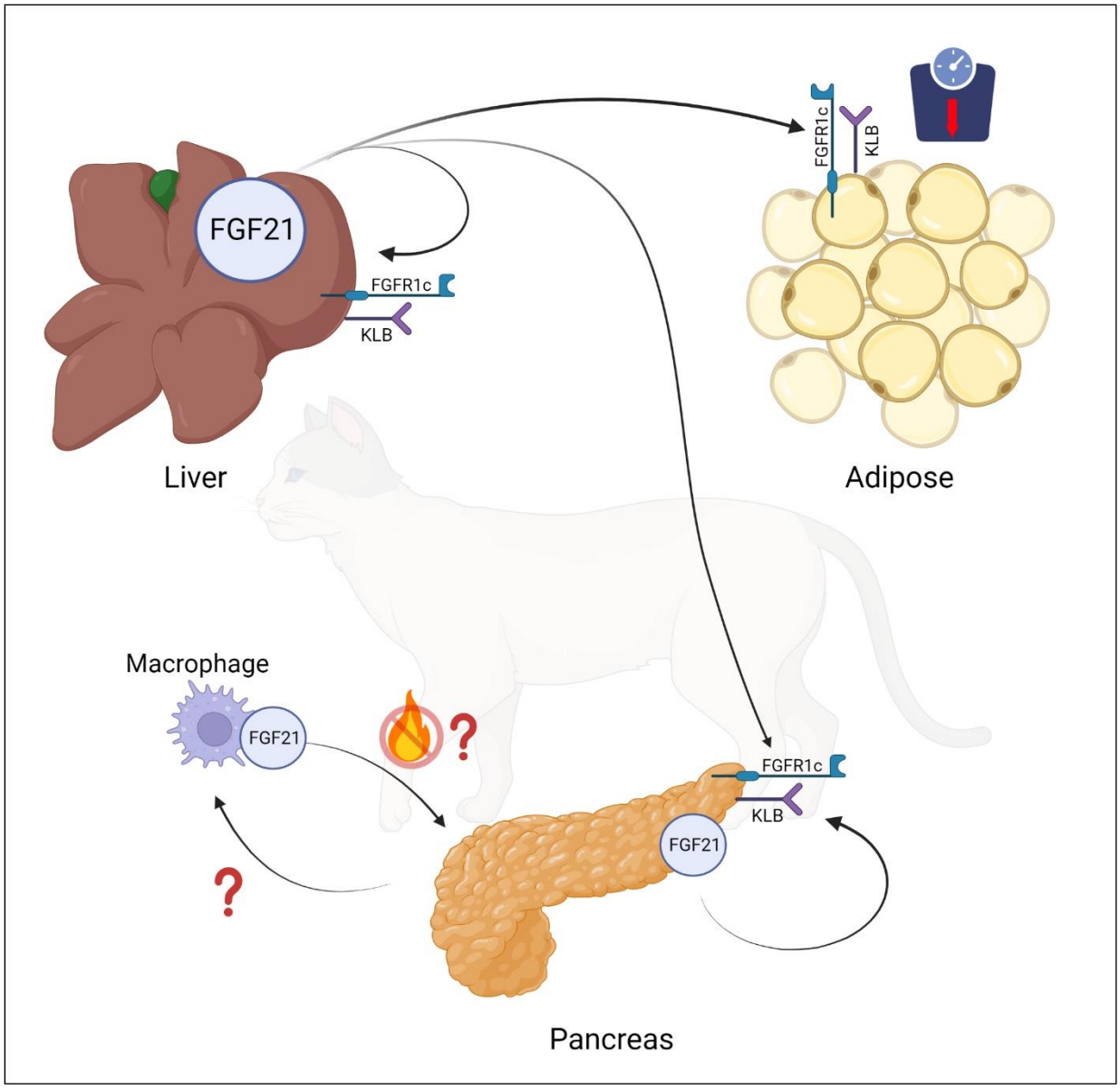


**Figure 31. Proposed FGF21 signaling pathway in the domestic cat.** FGF21 is produced in the liver and signals to the adipose tissue to induce lipolysis and weight loss. FGF21 has both endocrine and autocrine/paracrine signaling from the liver. The pancreas produces FGF21 and its receptors, KLB and FGFR1c, suggesting an autocrine/paracrine role. A subset of macrophages expresses FGF21 during pancreatitis, which may represent M2 polarization in an attempt to reduce inflammation.

# Chapter 4: Summary and Future Directions

The Fibroblast Growth Factor (FGF) family is composed of 23 different proteins within three phylogenetic categories: the canonical FGFs, the intracellular FGFs, and the group of interest to this dissertation, the endocrine FGFs (238).

Chapter 1 of this dissertation is a literature review of FGFs Of these, 18 signal to a group of tyrosine kinase receptors called fibroblast growth factor receptors (238). The endocrine group is composed of FGF15/19 (FGF15 is the rodent ortholog of mammalian FGF19), FGF21, and FGF23, which function as regulators of bile homeostasis, lipid and insulin homeostasis, and phosphate homeostasis, respectively (239). There are several current and potential applications for FGF endocrine family-targeting therapies to treat diseases such as X-linked hypophosphatemia, chronic liver disease, and obesity-related metabolic diseases (239). Numerous FGF21 analogs have been developed for pharmaceutical use and have undergone clinical trial testing of varying success (240). Domestic animals have overlapping clinical conditions with conditions targeted for FGF21 therapy. Despite this clinical overlap, FGF21 has not been as well studied in domestic animals as in humans, non-human primates, and rodents. Based on current research, FGF21 therapy may be suitable for animals with hepatic lipidosis or insulin-dependent diabetes mellitus (111, 131).

Chapter 2 of this dissertation explores the potential use of an FGF21 analog, LY2405319, in overweight and obese domestic cats. In this cross-sectional study, a colony of purpose-bred, male-neutered, 6-year-old cats was utilized. Over 14 days, cats were administered either the FGF21 mimetic or saline control. Cats treated with FGF21 had significant weight loss, a trend towards decreased intrahepatic triglyceride content, and a decrease in the sensitive marker of

lipid accumulation in cats, alkaline phosphatase (157). Despite reports in other animals, FGF21 treatment in cats did not lead to changes in basal glucose or insulin, changes indirect measures of insulin resistance, or circulating lipid parameters. This suggests that the FGF21 pathway is metabolically unique in the domestic cat compared to humans and laboratory animals. Importantly, no cats exhibited significant side effects from FGF21 administration. Therefore, although FGF21 pathway targeting therapy may not be beneficial for cats with insulin resistance or type II diabetes mellitus, it can still be safely adapted for other uses in the cat. As there was a trend towards hepatic lipid decrease in the treated cats, despite a hepatic lipid increase in the control cats, there may be a future for FGF21 in cats with the clinical syndrome feline hepatic lipidosis, a life-threatening condition of liver failure caused by overabundant hepatic triglyceride accumulation. Unfortunately, beyond treating the primary cause of feline hepatic lipidosis, there is no specific treatment other than supportive therapies (241). Investigating changes in hepatic triglyceride content with FGF21 therapy in cats with a marked amount of hepatic lipid accumulation, as in feline hepatic lipidosis (242), instead of a chronically mildly elevated level, as in overweight and obese cats (140), may yield massive breakthroughs for the management and treatment of feline hepatic lipidosis.

Chapter 3 of this dissertation delves into finding the unique FGF21 pathway differences that lead to weight loss without changes in insulin, glucose, or lipid homeostasis with FGF21 mimetic therapy in the domestic cat. Additionally, as there is evidence in rodent studies of FGF21 being capable of resolving cerulein-induced pancreatitis, we wanted to see how FGF21 was affected in cats with spotaneously-occurring cases of pancreatitis. In agreement with other studies (83), we determined that a large amount of FGF21 mRNA and protein expression is found within the liver, specifically the hepatocyte. Additionally, FGF21 mRNA with more

sporadic protein expression is found in the pancreas. However, contray to findings in rodents (207), in the domestic cat, FGF21 mRNA and protein is inconsistently expressed in the both the subcutaneous (inguinal) and visceral (falciform) adipose tissues. Interestingly, many of the FGF21 glucose and insulin homestatic mechanisms and amelioation of lipotoxicity in rodents are thought to be due from the autocrine/paracrine actions of FGF21 leading to downstream mediation of adiponectin (97, 98). The lack of consistent FGF21 mRNA and protein in the feline adipose tissues may reflect a loss of autocrine and paracrine signaling of FGF21 in the adipose and, consequentially, the inability of the adipose tissues to mediate the metabolic changes of FGF21 in cats, as seen in rodents. Additionally, we found that a subset of macrophages in cases of spontaneous acute and chronic pancreatitis highly expressed FGF21. As FGF21 is implicated in anti-inflammatory processed by inducing M2 polarity (233), we theorized that this might be an endogenous attempt at reducing local inflammation in the pancreas. We propose that FGF21 could, theoretically, be used as an adjuvant therapy in cats with pancreatitis to reduce the localized inflammation and allow clinical veterinarians to the ability treat an underlying condition if identifiable (215).

Together this dissertatiopn is the first work to examine FGF2 in domestic cats. It strives to provide an overview of current research with FGF21 including in domestic animals, investigate howwe know about FGF21 treatment affects cats, and delve into the idiosyncracies of the FGF21 pathway. Hopefully, with this knowledge, FGF21 pathway targeting therapy will change feline clinical veterinary medicine for the good.

References

1. Wei EQ, Barnett AS, Pitt GS, Hennessey JA. Fibroblast Growth Factor Homologous Factors in the Heart: A Potential Locus for Cardiac Arrhythmias. *Trends in Cardiovascular Medicine* (2011) 21(7):199-203. doi: https://doi.org/10.1016/j.tcm.2012.05.010.

2. Wang C, Wang C, Hoch EG, Pitt GS. Identification of Novel Interaction Sites That Determine Specificity between Fibroblast Growth Factor Homologous Factors and Voltage-Gated Sodium Channels. *Journal of Biological Chemistry* (2011) 286(27):24253-63. doi: 10.1074/jbc.m111.245803.

3. Xie Y, Su N, Yang J, Tan Q, Huang S, Jin M, et al. Fgf/Fgfr Signaling in Health and Disease. *Signal Transduction and Targeted Therapy* (2020) 5(1):181. doi: 10.1038/s41392-020-00222-7.

4. Gong S-G. Isoforms of Receptors of Fibroblast Growth Factors. *Journal of Cellular Physiology* (2014) 229(12):1887-95. doi: 10.1002/jcp.24649.

5. Zhang X, Ibrahimi OA, Olsen SK, Umemori H, Mohammadi M, Ornitz DM. Receptor Specificity of the Fibroblast Growth Factor Family. *Journal of Biological Chemistry* (2006) 281(23):15694-700. doi: 10.1074/jbc.m601252200.

6. Beenken A, Mohammadi M. The Fgf Family: Biology, Pathophysiology and Therapy. *Nature Reviews Drug Discovery* (2009) 8(3):235-53. doi: 10.1038/nrd2792.

7. Kurosu H, Kuro-o M. Endocrine Fibroblast Growth Factors as Regulators of Metabolic Homeostasis. *BioFactors* (2009) 35(1):52-60. doi: https://doi.org/10.1002/biof.12.

8. Kuro-o M. The Klotho Proteins in Health and Disease. *Nature Reviews Nephrology* (2019) 15(1):27-44. doi: 10.1038/s41581-018-0078-3.

9. Fon Tacer K, Bookout AL, Ding X, Kurosu H, John GB, Wang L, et al. Research Resource: Comprehensive Expression Atlas of the Fibroblast Growth Factor System in Adult Mouse. *Molecular Endocrinology* (2010) 24(10):2050-64. doi: 10.1210/me.2010-0142.

10. Ho BB, Bergwitz C. Fgf23 Signalling and Physiology. *Journal of Molecular Endocrinology* (2021) 66(2):R23-R32. doi: 10.1530/jme-20-0178.

11. Erben RG. Physiological Actions of Fibroblast Growth Factor-23. *Frontiers in Endocrinology* (2018) 9. doi: 10.3389/fendo.2018.00267.

12. Erben RG. Pleiotropic Actions of Fgf23. *Toxicologic Pathology* (2017) 45(7):904-10. doi: 10.1177/0192623317737469.

13. Feng JQ, Ward LM, Liu S, Lu Y, Xie Y, Yuan B, et al. Loss of Dmp1 Causes Rickets and Osteomalacia and Identifies a Role for Osteocytes in Mineral Metabolism. *Nature Genetics* (2006) 38(11):1310-5. doi: 10.1038/ng1905.

14. Bonewald LF, Wacker MJ. Fgf23 Production by Osteocytes. *Pediatr Nephrol* (2013) 28(4):563-8. Epub 20120916. doi: 10.1007/s00467-012-2309-3.

15. Rowe PS. A Unified Model for Bone–Renal Mineral and Energy Metabolism. *Current Opinion in Pharmacology* (2015) 22:64-71. doi: https://doi.org/10.1016/j.coph.2015.03.006.

16. Guo L, Wang Y, Li S, Zhou L, Li D. Galnt3 Protects against Phosphate-Induced Calcification in Vascular Smooth Muscle Cells by Enhancing Active Fgf23 and Inhibiting the Wnt/B-Catenin Signaling Pathway. *Cellular Signalling* (2022) 100:110477. doi: https://doi.org/10.1016/j.cellsig.2022.110477.

17. Tagliabracci VS, Engel JL, Wiley SE, Xiao J, Gonzalez DJ, Nidumanda Appaiah H, et al. Dynamic Regulation of Fgf23 by Fam20c Phosphorylation, Galnac-T3 Glycosylation, and Furin

Proteolysis. *Proceedings of the National Academy of Sciences* (2014) 111(15):5520-5. doi: doi:10.1073/pnas.1402218111.

18. Xiao Z, Huang J, Cao L, Liang Y, Han X, Quarles LD. Osteocyte-Specific Deletion of Fgfr1 Suppresses Fgf23. *PLOS ONE* (2014) 9(8):e104154. doi: 10.1371/journal.pone.0104154.

19. Urakawa I, Yamazaki Y, Shimada T, Iijima K, Hasegawa H, Okawa K, et al. Klotho Converts Canonical Fgf Receptor into a Specific Receptor for Fgf23. *Nature* (2006) 444(7120):770-4. doi: 10.1038/nature05315.

20. Farrow EG, Davis SI, Summers LJ, White KE. Initial Fgf23-Mediated Signaling Occurs in the Distal Convoluted Tubule. *Journal of the American Society of Nephrology* (2009) 20(5):955-60. doi: 10.1681/asn.2008070783.

21. Agoro R, Ni P, Noonan ML, White KE. Osteocytic Fgf23 and Its Kidney Function. *Frontiers in Endocrinology* (2020) 11. doi: 10.3389/fendo.2020.00592.

22. Andrukhova O, Zeitz U, Goetz R, Mohammadi M, Lanske B, Erben RG. Fgf23 Acts Directly on Renal Proximal Tubules to Induce Phosphaturia through Activation of the Erk1/2–Sgk1 Signaling Pathway. *Bone* (2012) 51(3):621-8. doi: https://doi.org/10.1016/j.bone.2012.05.015.

23. Krajisnik T, Björklund P, Marsell R, Ljunggren Os, Åkerström Gr, Jonsson KB, et al. Fibroblast Growth Factor-23 Regulates Parathyroid Hormone and 1α-Hydroxylase Expression in Cultured Bovine Parathyroid Cells. *Journal of Endocrinology* (2007) 195(1):125-31. doi: 10.1677/joe-07-0267.

24. Kawakami K, Takeshita A, Furushima K, Miyajima M, Hatamura I, Kuro-o M, et al. Persistent Fibroblast Growth Factor 23 Signalling in the Parathyroid Glands for Secondary

Hyperparathyroidism in Mice with Chronic Kidney Disease. *Scientific Reports* (2017) 7(1):40534. doi: 10.1038/srep40534.

25. Emboss Needle Pairwise Sequence Alignment: EMBL's European Bioinformatics Institute (2023) [cited 2023 December 12]. Available from: https://www.ebi.ac.uk/Tools/psa/emboss_needle/.

26. Faul C, Amaral AP, Oskouei B, Hu M-C, Sloan A, Isakova T, et al. Fgf23 Induces Left Ventricular Hypertrophy. *The Journal of Clinical Investigation* (2011) 121(11):4393-408. doi: 10.1172/JCI46122.

27. Grabner A, Schramm K, Silswal N, Hendrix M, Yanucil C, Czaya B, et al. Fgf23/Fgfr4-Mediated Left Ventricular Hypertrophy Is Reversible. *Scientific Reports* (2017) 7(1):1993. doi: 10.1038/s41598-017-02068-6.

28. Schindeler A, Biggin A, Munns CF. Clinical Evidence for the Benefits of Burosumab Therapy for X-Linked Hypophosphatemia (Xlh) and Other Conditions in Adults and Children. *Frontiers in Endocrinology* (2020) 11. doi: 10.3389/fendo.2020.00338.

29. Carpenter TO, Whyte MP, Imel EA, Boot AM, Högler W, Linglart A, et al. Burosumab Therapy in Children with X-Linked Hypophosphatemia. *New England Journal of Medicine* (2018) 378(21):1987-98. doi: 10.1056/NEJMoa1714641.

30. Insogna KL, Briot K, Imel EA, Kamenický P, Ruppe MD, Portale AA, et al. A Randomized, Double-Blind, Placebo-Controlled, Phase 3 Trial Evaluating the Efficacy of Burosumab, an Anti-Fgf23 Antibody, in Adults with X-Linked Hypophosphatemia: Week 24 Primary Analysis. *Journal of Bone and Mineral Research* (2018) 33(8):1383-93. doi: https://doi.org/10.1002/jbmr.3475.

31. Chiang JYL. Bile Acid Metabolism and Signaling. *Comprehensive Physiology* (2013) 3:1191-212. doi: https://doi.org/10.1002/cphy.c120023.

32. Forman BM, Goode E, Chen J, Oro AE, Bradley DJ, Perlmann T, et al. Identification of a Nuclear Receptor That Is Activated by Farnesol Metabolites. *Cell* (1995) 81(5):687-93. doi: https://doi.org/10.1016/0092-8674(95)90530-8.

33. Houten SM, Volle DH, Cummins CL, Mangelsdorf DJ, Auwerx J. In Vivo Imaging of Farnesoid X Receptor Activity Reveals the Ileum as the Primary Bile Acid Signaling Tissue. *Molecular Endocrinology* (2007) 21(6):1312-23. doi: 10.1210/me.2007-0113.

34. Kliewer SA, Mangelsdorf DJ. Bile Acids as Hormones: The Fxr-Fgf15/19 Pathway. *Digestive Diseases* (2015) 33(3):327-31. doi: 10.1159/000371670.

35. Laffitte BA, Kast HR, Nguyen CM, Zavacki AM, Moore DD, Edwards PA. Identification of the DNA Binding Specificity and Potential Target Genes for the Farnesoid X-Activated Receptor*. *Journal of Biological Chemistry* (2000) 275(14):10638-47. doi: https://doi.org/10.1074/jbc.275.14.10638.

36. Zhang JH, Nolan JD, Kennie SL, Johnston IM, Dew T, Dixon PH, et al. Potent Stimulation of Fibroblast Growth Factor 19 Expression in the Human Ileum by Bile Acids. *American Journal of Physiology-Gastrointestinal and Liver Physiology* (2013) 304(10):G940-G8. doi: 10.1152/ajpgi.00398.2012.

37. Inagaki T, Choi M, Moschetta A, Peng L, Cummins CL, McDonald JG, et al. Fibroblast Growth Factor 15 Functions as an Enterohepatic Signal to Regulate Bile Acid Homeostasis. *Cell Metabolism* (2005) 2(4):217-25. doi: https://doi.org/10.1016/j.cmet.2005.09.001.

38. Stroeve JHM, Brufau G, Stellaard F, Gonzalez FJ, Staels B, Kuipers F. Intestinal Fxr-Mediated Fgf15 Production Contributes to Diurnal Control of Hepatic Bile Acid Synthesis in

Mice. *Laboratory Investigation* (2010) 90(10):1457-67. doi: https://doi.org/10.1038/labinvest.2010.107.

39. Lundåsen T, Gälman C, Angelin B, Rudling M. Circulating Intestinal Fibroblast Growth Factor 19 Has a Pronounced Diurnal Variation and Modulates Hepatic Bile Acid Synthesis in Man. *Journal of Internal Medicine* (2006) 260(6):530-6. doi: https://doi.org/10.1111/j.1365-2796.2006.01731.x.

40. Zweers SJLB, Booij KAC, Komuta M, Roskams T, Gouma DJ, Jansen PLM, et al. The Human Gallbladder Secretes Fibroblast Growth Factor 19 into Bile: Towards Defining the Role of Fibroblast Growth Factor 19 in the Enterobiliary Tract. *Hepatology* (2012) 55(2):575-83. doi: https://doi.org/10.1002/hep.24702.

41. Schaap FG, van der Gaag NA, Gouma DJ, Jansen PLM. High Expression of the Bile Salt-Homeostatic Hormone Fibroblast Growth Factor 19 in the Liver of Patients with Extrahepatic Cholestasis. *Hepatology* (2009) 49(4):1228-35. doi: https://doi.org/10.1002/hep.22771.

42. Wunsch E, Milkiewicz M, Wasik U, Trottier J, Kempińska-Podhorodecka A, Elias E, et al. Expression of Hepatic Fibroblast Growth Factor 19 Is Enhanced in Primary Biliary Cirrhosis and Correlates with Severity of the Disease. *Scientific Reports* (2015) 5(1):13462. doi: 10.1038/srep13462.

43. Ricardo, Jo, Lory A, Maxine, Cooper S, Warner A, et al. Antibody-Mediated Inhibition of the Fgfr1c Isoform Induces a Catabolic Lean State in Siberian Hamsters. *Current Biology* (2015) 25(22):2997-3003. doi: 10.1016/j.cub.2015.10.010.

44. Wu X, Ge H, Lemon B, Weiszmann J, Gupte J, Hawkins N, et al. Selective Activation of Fgfr4 by an Fgf19 Variant Does Not Improve Glucose Metabolism in <I>Ob/Ob</I> Mice.

*Proceedings of the National Academy of Sciences* (2009) 106(34):14379-84. doi: doi:10.1073/pnas.0907812106.

45. Talukdar S, Kharitonenkov A. Fgf19 and Fgf21: In Nash We Trust. *Molecular Metabolism* (2021) 46:101152. doi: https://doi.org/10.1016/j.molmet.2020.101152.

46. Ge H, Baribault H, Vonderfecht S, Lemon B, Weiszmann J, Gardner J, et al. Characterization of a Fgf19 Variant with Altered Receptor Specificity Revealed a Central Role for Fgfr1c in the Regulation of Glucose Metabolism. *PLOS ONE* (2012) 7(3):e33603. doi: 10.1371/journal.pone.0033603.

47. Morón-Ros S, Uriarte I, Berasain C, Avila MA, Sabater-Masdeu M, Moreno-Navarrete JM, et al. Fgf15/19 Is Required for Adipose Tissue Plasticity in Response to Thermogenic Adaptations. *Molecular Metabolism* (2021) 43:101113. doi: https://doi.org/10.1016/j.molmet.2020.101113.

48. Potthoff Matthew J, Boney-Montoya J, Choi M, He T, Sunny Nishanth E, Satapati S, et al. Fgf15/19 Regulates Hepatic Glucose Metabolism by Inhibiting the Creb-Pgc-1α Pathway. *Cell Metabolism* (2011) 13(6):729-38. doi: https://doi.org/10.1016/j.cmet.2011.03.019.

49. Kir S, Beddow SA, Samuel VT, Miller P, Previs SF, Suino-Powell K, et al. Fgf19 as a Postprandial, Insulin-Independent Activator of Hepatic Protein and Glycogen Synthesis. *Science* (2011) 331(6024):1621-4. doi: doi:10.1126/science.1198363.

50. Lin BC, Wang M, Blackmore C, Desnoyers LR. Liver-Specific Activities of Fgf19 Require Klotho Beta. *Journal of Biological Chemistry* (2007) 282(37):27277-84. doi: 10.1074/jbc.M704244200.

51. Miura S, Mitsuhashi N, Shimizu H, Kimura F, Yoshidome H, Otsuka M, et al. Fibroblast Growth Factor 19 Expression Correlates with Tumor Progression and Poorer Prognosis of Hepatocellular Carcinoma. *BMC Cancer* (2012) 12(1):56. doi: 10.1186/1471-2407-12-56.

52. Wu X, Ge H, Lemon B, Vonderfecht S, Weiszmann J, Hecht R, et al. Fgf19-Induced Hepatocyte Proliferation Is Mediated through Fgfr4 Activation. *Journal of Biological Chemistry* (2010) 285(8):5165-70. doi: https://doi.org/10.1074/jbc.M109.068783.

53. Wu A-L, Coulter S, Liddle C, Wong A, Eastham-Anderson J, French DM, et al. Fgf19 Regulates Cell Proliferation, Glucose and Bile Acid Metabolism Via Fgfr4-Dependent and Independent Pathways. *PLOS ONE* (2011) 6(3):e17868. doi: 10.1371/journal.pone.0017868.

54. Nicholes K, Guillet S, Tomlinson E, Hillan K, Wright B, Frantz GD, et al. A Mouse Model of Hepatocellular Carcinoma: Ectopic Expression of Fibroblast Growth Factor 19 in Skeletal Muscle of Transgenic Mice. *The American Journal of Pathology* (2002) 160(6):2295-307. doi: https://doi.org/10.1016/S0002-9440(10)61177-7.

55. French DM, Lin BC, Wang M, Adams C, Shek T, Hötzel K, et al. Targeting Fgfr4 Inhibits Hepatocellular Carcinoma in Preclinical Mouse Models. *PLOS ONE* (2012) 7(5):e36713. doi: 10.1371/journal.pone.0036713.

56. Desnoyers LR, Pai R, Ferrando RE, Hötzel K, Le T, Ross J, et al. Targeting Fgf19 Inhibits Tumor Growth in Colon Cancer Xenograft and Fgf19 Transgenic Hepatocellular Carcinoma Models. *Oncogene* (2008) 27(1):85-97. doi: 10.1038/sj.onc.1210623.

57. Raja A, Park I, Haq F, Ahn S-M. Fgf19–Fgfr4 Signaling in Hepatocellular Carcinoma. *Cells* (2019) 8(6):536.

58. Pai R, French D, Ma N, Hotzel K, Plise E, Salphati L, et al. Antibody-Mediated Inhibition of Fibroblast Growth Factor 19 Results in Increased Bile Acids Synthesis and Ileal

Malabsorption of Bile Acids in Cynomolgus Monkeys. *Toxicological Sciences* (2012) 126(2):446-56. doi: 10.1093/toxsci/kfs011.

59. Chan SL, Schuler M, Kang Y-K, Yen C-J, Edeline J, Choo SP, et al. A First-in-Human Phase 1/2 Study of Fgf401 and Combination of Fgf401 with Spartalizumab in Patients with Hepatocellular Carcinoma or Biomarker-Selected Solid Tumors. *Journal of Experimental & Clinical Cancer Research* (2022) 41(1):189. doi: 10.1186/s13046-022-02383-5.

60. Liu H, Zheng S, Hou X, Liu X, Du K, Lv X, et al. Novel Abs Targeting the N-Terminus of Fibroblast Growth Factor 19 Inhibit Hepatocellular Carcinoma Growth without Bile-Acid-Related Side-Effects. *Cancer Science* (2020) 111(5):1750-60. doi: https://doi.org/10.1111/cas.14353.

61. Schadt HS, Wolf A, Mahl JA, Wuersch K, Couttet P, Schwald M, et al. Bile Acid Sequestration by Cholestyramine Mitigates Fgfr4 Inhibition-Induced Alt Elevation. *Toxicological Sciences* (2018) 163(1):265-78. doi: 10.1093/toxsci/kfy031.

62. Fu L, John LM, Adams SH, Yu XX, Tomlinson E, Renz M, et al. Fibroblast Growth Factor 19 Increases Metabolic Rate and Reverses Dietary and Leptin-Deficient Diabetes. *Endocrinology* (2004) 145(6):2594-603. doi: 10.1210/en.2003-1671.

63. Harrison SA, Neff G, Guy CD, Bashir MR, Paredes AH, Frias JP, et al. Efficacy and Safety of Aldafermin, an Engineered Fgf19 Analog, in a Randomized, Double-Blind, Placebo-Controlled Trial of Patients with Nonalcoholic Steatohepatitis. *Gastroenterology* (2021) 160(1):219-31.e1. doi: https://doi.org/10.1053/j.gastro.2020.08.004.

64. Harrison SA, Rinella ME, Abdelmalek MF, Trotter JF, Paredes AH, Arnold HL, et al. Ngm282 for Treatment of Non-Alcoholic Steatohepatitis: A Multicentre, Randomised, Double-

Blind, Placebo-Controlled, Phase 2 Trial. *The Lancet* (2018) 391(10126):1174-85. doi: https://doi.org/10.1016/S0140-6736(18)30474-4.

65. Sanyal AJ, Ling L, Beuers U, DePaoli AM, Lieu HD, Harrison SA, et al. Potent Suppression of Hydrophobic Bile Acids by Aldafermin, an Fgf19 Analogue, across Metabolic and Cholestatic Liver Diseases. *JHEP Reports* (2021) 3(3):100255. doi: https://doi.org/10.1016/j.jhepr.2021.100255.

66. Niu J, Zhao J, Wu J, Qiao G, Gu J, Zhou C, et al. Curtailing Fgf19's Mitogenicity by Suppressing Its Receptor Dimerization Ability. *Proceedings of the National Academy of Sciences* (2020) 117(46):29025-34. doi: doi:10.1073/pnas.2010984117.

67. Yie J, Hecht R, Patel J, Stevens J, Wang W, Hawkins N, et al. Fgf21 N- and C-Termini Play Different Roles in Receptor Interaction and Activation. *FEBS Letters* (2009) 583(1):19-24. doi: 10.1016/j.febslet.2008.11.023.

68. Foltz IN, Hu S, King C, Wu X, Yang C, Wang W, et al. Treating Diabetes and Obesity with an Fgf21-Mimetic Antibody Activating the βKlotho/Fgfr1c Receptor Complex. *Science Translational Medicine* (2012) 4(162):162ra53-ra53. doi: doi:10.1126/scitranslmed.3004690.

69. Planavila A, Redondo I, Hondares E, Vinciguerra M, Munts C, Iglesias R, et al. Fibroblast Growth Factor 21 Protects against Cardiac Hypertrophy in Mice. *Nature Communications* (2013) 4(1). doi: 10.1038/ncomms3019.

70. Kharitonenkov A, Shiyanova TL, Koester A, Ford AM, Micanovic R, Galbreath EJ, et al. Fgf-21 as a Novel Metabolic Regulator. *Journal of Clinical Investigation* (2005) 115(6):1627-35. doi: 10.1172/jci23606.

71. Fisher FM, Kleiner S, Douris N, Fox EC, Mepani RJ, Verdeguer F, et al. Fgf21 Regulates Pgc-1α and Browning of White Adipose Tissues in Adaptive Thermogenesis. *Genes & Development* (2012) 26(3):271-81. doi: 10.1101/gad.177857.111.

72. Potthoff MJ, Inagaki T, Satapati S, Ding X, He T, Goetz R, et al. Fgf21 Induces Pgc-1α and Regulates Carbohydrate and Fatty Acid Metabolism During the Adaptive Starvation Response. *Proceedings of the National Academy of Sciences* (2009) 106(26):10853-8. doi: 10.1073/pnas.0904187106.

73. Rusu PM, Chan AY, Heikenwalder M, Müller OJ, Rose AJ. Dietary Essential Amino Acid Restriction Promotes Hyperdipsia Via Hepatic Fgf21. *Nutrients* (2021) 13(5):1469. doi: 10.3390/nu13051469.

74. Song P, Zechner C, Hernandez G, Cánovas J, Xie Y, Sondhi V, et al. The Hormone Fgf21 Stimulates Water Drinking in Response to Ketogenic Diet and Alcohol. *Cell Metabolism* (2018) 27(6):1338-47.e4. doi: 10.1016/j.cmet.2018.04.001.

75. Fazeli PK, Lun M, Kim SM, Bredella MA, Wright S, Zhang Y, et al. Fgf21 and the Late Adaptive Response to Starvation in Humans. *Journal of Clinical Investigation* (2015) 125(12):4601-11. doi: 10.1172/jci83349.

76. Lundsgaard A-M, Fritzen AM, Sjøberg KA, Myrmel LS, Madsen L, Wojtaszewski JFP, et al. Circulating Fgf21 in Humans Is Potently Induced by Short Term Overfeeding of Carbohydrates. *Molecular Metabolism* (2017) 6(1):22-9. doi: https://doi.org/10.1016/j.molmet.2016.11.001.

77. Carmen G-Y, Víctor S-M. Signalling Mechanisms Regulating Lipolysis. *Cellular Signalling* (2006) 18(4):401-8. doi: https://doi.org/10.1016/j.cellsig.2005.08.009.

78. Srivastava S, Baxa U, Niu G, Chen X, L. Veech R. A Ketogenic Diet Increases Brown Adipose Tissue Mitochondrial Proteins and Ucp1 Levels in Mice. *IUBMB Life* (2013) 65(1):58-66. doi: 10.1002/iub.1102.

79. Zhao C, Liu Y, Xiao J, Liu L, Chen S, Mohammadi M, et al. Fgf21 Mediates Alcohol-Induced Adipose Tissue Lipolysis by Activation of Systemic Release of Catecholamine in Mice. *Journal of Lipid Research* (2015) 56(8):1481-91. doi: 10.1194/jlr.m058610.

80. Inagaki T, Dutchak P, Zhao G, Ding X, Gautron L, Parameswara V, et al. Endocrine Regulation of the Fasting Response by Pparα-Mediated Induction of Fibroblast Growth Factor 21. *Cell Metabolism* (2007) 5(6):415-25. doi: 10.1016/j.cmet.2007.05.003.

81. Pawlak M, Lefebvre P, Staels B. Molecular Mechanism of Pparα Action and Its Impact on Lipid Metabolism, Inflammation and Fibrosis in Non-Alcoholic Fatty Liver Disease. *Journal of Hepatology* (2015) 62(3):720-33. doi: https://doi.org/10.1016/j.jhep.2014.10.039.

82. Badman MK, Pissios P, Kennedy AR, Koukos G, Flier JS, Maratos-Flier E. Hepatic Fibroblast Growth Factor 21 Is Regulated by Pparα and Is a Key Mediator of Hepatic Lipid Metabolism in Ketotic States. *Cell Metabolism* (2007) 5(6):426-37. doi: 10.1016/j.cmet.2007.05.002.

83. Markan KR, Naber MC, Ameka MK, Anderegg MD, Mangelsdorf DJ, Kliewer SA, et al. Circulating Fgf21 Is Liver Derived and Enhances Glucose Uptake During Refeeding and Overfeeding. *Diabetes* (2014) 63(12):4057-63. doi: 10.2337/db14-0595.

84. Paul, Katafuchi T, Angie, Jang, Ruth, David, et al. Fibroblast Growth Factor-21 Regulates Pparγ Activity and the Antidiabetic Actions of Thiazolidinediones. *Cell* (2012) 148(3):556-67. doi: 10.1016/j.cell.2011.11.062.

85. Kim H, Mendez R, Zheng Z, Chang L, Cai J, Zhang R, et al. Liver-Enriched Transcription Factor Crebh Interacts with Peroxisome Proliferator-Activated Receptor A to Regulate Metabolic Hormone Fgf21. *Endocrinology* (2014) 155(3):769-82. doi: 10.1210/en.2013-1490.

86. Adams AC, Astapova I, Fisher FM, Badman MK, Kurgansky KE, Flier JS, et al. Thyroid Hormone Regulates Hepatic Expression of Fibroblast Growth Factor 21 in a Pparα-Dependent Manner. *Journal of Biological Chemistry* (2010) 285(19):14078-82. doi: 10.1074/jbc.c110.107375.

87. Yamashita H, Takenoshita M, Sakurai M, Bruick RK, Henzel WJ, Shillinglaw W, et al. A Glucose-Responsive Transcription Factor That Regulates Carbohydrate Metabolism in the Liver. *Proceedings of the National Academy of Sciences* (2001) 98(16):9116-21. doi: 10.1073/pnas.161284298.

88. Iroz A, Montagner A, Benhamed F, Levavasseur F, Polizzi A, Anthony E, et al. A Specific Chrebp and Pparα Cross-Talk Is Required for the Glucose-Mediated Fgf21 Response. *Cell Reports* (2017) 21(2):403-16. doi: 10.1016/j.celrep.2017.09.065.

89. De Sousa-Coelho AL, Relat J, Hondares E, Pérez-Martí A, Ribas F, Villarroya F, et al. Fgf21 Mediates the Lipid Metabolism Response to Amino Acid Starvation. *Journal of Lipid Research* (2013) 54(7):1786-97. doi: 10.1194/jlr.m033415.

90. Hondares E, Rosell M, Gonzalez FJ, Giralt M, Iglesias R, Villarroya F. Hepatic Fgf21 Expression Is Induced at Birth Via Pparα in Response to Milk Intake and Contributes to Thermogenic Activation of Neonatal Brown Fat. *Cell Metabolism* (2010) 11(3):206-12. doi: 10.1016/j.cmet.2010.02.001.

91. Sa-Nguanmoo P, Chattipakorn N, Chattipakorn SC. Potential Roles of Fibroblast Growth Factor 21 in the Brain. *Metabolic Brain Disease* (2016) 31(2):239-48. doi: 10.1007/s11011-015-9789-3.

92. Izumiya Y, Bina HA, Ouchi N, Akasaki Y, Kharitonenkov A, Walsh K. Fgf21 Is an Akt-Regulated Myokine. *FEBS Letters* (2008) 582(27):3805-10. doi: 10.1016/j.febslet.2008.10.021.

93. Chartoumpekis DV, Habeos IG, Ziros PG, Psyrogiannis AI, Kyriazopoulou VE, Papavassiliou AG. Brown Adipose Tissue Responds to Cold and Adrenergic Stimulation by Induction of Fgf21. *Molecular Medicine* (2011) 17(7-8):736-40. doi: 10.2119/molmed.2011.00075.

94. Collins S, Cao W, Robidoux J. Learning New Tricks from Old Dogs: B-Adrenergic Receptors Teach New Lessons on Firing up Adipose Tissue Metabolism. *Molecular Endocrinology* (2004) 18(9):2123-31. doi: 10.1210/me.2004-0193.

95. Hondares E, Iglesias R, Giralt A, Gonzalez FJ, Giralt M, Mampel T, et al. Thermogenic Activation Induces Fgf21 Expression and Release in Brown Adipose Tissue. *Journal of Biological Chemistry* (2011) 286(15):12983-90. doi: 10.1074/jbc.m110.215889.

96. Muise ES, Azzolina B, Kuo DW, El-Sherbeini M, Tan Y, Yuan X, et al. Adipose Fibroblast Growth Factor 21 Is up-Regulated by Peroxisome Proliferator-Activated Receptor Γ and Altered Metabolic States. *Molecular Pharmacology* (2008) 74(2):403-12. doi: 10.1124/mol.108.044826.

97. Lin Z, Tian H, Karen, Lin S, Ruby, Konishi M, et al. Adiponectin Mediates the Metabolic Effects of Fgf21 on Glucose Homeostasis and Insulin Sensitivity in Mice. *Cell Metabolism* (2013) 17(5):779-89. doi: 10.1016/j.cmet.2013.04.005.

98. Holland WL, Adams AC, Brozinick JT, Bui HH, Miyauchi Y, Kusminski CM, et al. An Fgf21-Adiponectin-Ceramide Axis Controls Energy Expenditure and Insulin Action in Mice. *Cell Metabolism* (2013) 17(5):790-7. doi: 10.1016/j.cmet.2013.03.019.

99. Chaurasia B, Summers SA. Ceramides – Lipotoxic Inducers of Metabolic Disorders. *Trends in Endocrinology & Metabolism* (2015) 26(10):538-50. doi: 10.1016/j.tem.2015.07.006.

100. Mashili FL, Austin RL, Deshmukh AS, Fritz T, Caidahl K, Bergdahl K, et al. Direct Effects of Fgf21 on Glucose Uptake in Human Skeletal Muscle: Implications for Type 2 Diabetes and Obesity. *Diabetes/Metabolism Research and Reviews* (2011) 27(3):286-97. doi: 10.1002/dmrr.1177.

101. Oost LJ, Kustermann M, Armani A, Blaauw B, Romanello V. Fibroblast Growth Factor 21 Controls Mitophagy and Muscle Mass. *Journal of Cachexia, Sarcopenia and Muscle* (2019) 10(3):630-42. doi: 10.1002/jcsm.12409.

102. Cheng P, Zhang F, Yu L, Lin X, He L, Li X, et al. Physiological and Pharmacological Roles of Fgf21 in Cardiovascular Diseases. *Journal of Diabetes Research* (2016) 2016:1-8. doi: 10.1155/2016/1540267.

103. Tanajak P, Sa-Nguanmoo P, Wang X, Liang G, Li X, Jiang C, et al. Fibroblast Growth Factor 21 (Fgf21) Therapy Attenuates Left Ventricular Dysfunction and Metabolic Disturbance by Improving Fgf21 Sensitivity, Cardiac Mitochondrial Redox Homoeostasis and Structural Changes in Pre-Diabetic Rats. *Acta Physiologica* (2016) 217(4):287-99. doi: 10.1111/apha.12698.

104. Singhal G, Fisher fM, Chee MJ, Tan TG, El Ouaamari A, Adams AC, et al. *Fibroblast Growth Factor 21 (Fgf21) Protects against High Fat Diet Induced Inflammation and Islet*

*Hyperplasia in Pancreas*. In: Sastre J, editor. PLOS ONE(2016). p. e0148252.doi: 10.1371/journal.pone.0148252.

105. Coate KC, Hernandez G, Thorne CA, Sun S, Le TDV, Vale K, et al. *Fgf21 Is an Exocrine Pancreas Secretagogue*. Cell Metabolism: Elsevier Inc. (2017). p. 472-80.doi: 10.1016/j.cmet.2016.12.004.

106. So WY, Cheng Q, Xu A, Lam KSL, Leung PS. Loss of Fibroblast Growth Factor 21 Action Induces Insulin Resistance, Pancreatic Islet Hyperplasia and Dysfunction in Mice. *Cell Death & Disease* (2015) 6(3):e1707-e. doi: 10.1038/cddis.2015.80.

107. Degirolamo C, Sabbà C, Moschetta A. Therapeutic Potential of the Endocrine Fibroblast Growth Factors Fgf19, Fgf21 and Fgf23. *Nature Reviews Drug Discovery* (2016) 15(1):51-69. doi: 10.1038/nrd.2015.9.

108. Zhang J, Li Y. Fibroblast Growth Factor 21 Analogs for Treating Metabolic Disorders. *Frontiers in Endocrinology* (2015) 6. doi: 10.3389/fendo.2015.00168.

109. Kharitonenkov A, Beals JM, Micanovic R, Strifler BA, Rathnachalam R, Wroblewski VJ, et al. *Rational Design of a Fibroblast Growth Factor 21-Based Clinical Candidate, Ly2405319*. In: Xu A, editor. PLoS ONE(2013). p. e58575.doi: 10.1371/journal.pone.0058575.

110. So WY, Leung PS. Fibroblast Growth Factor 21 as an Emerging Therapeutic Target for Type 2 Diabetes Mellitus. *Medicinal Research Reviews* (2016) 36(4):672-704. doi: 10.1002/med.21390.

111. Caixeta LS, Giesy SL, Krumm CS, Perfield JW, Butterfield A, Boisclair YR. Fibroblast Growth Factor-21 (Fgf21) Administration to Early-Lactating Dairy Cows. Ii. Pharmacokinetics, Whole-Animal Performance, and Lipid Metabolism. *Journal of Dairy Science* (2019) 102(12):11597-608. doi: 10.3168/jds.2019-16696.

112. Adams AC, Halstead CA, Hansen BC, Irizarry AR, Martin JA, Myers SR, et al. Ly2405319, an Engineered Fgf21 Variant, Improves the Metabolic Status of Diabetic Monkeys. *PLoS ONE* (2013) 8(6):e65763. doi: 10.1371/journal.pone.0065763.

113. Gaich G, Jenny, Fu H, Leonard, Mark, William, et al. The Effects of Ly2405319, an Fgf21 Analog, in Obese Human Subjects with Type 2 Diabetes. *Cell Metabolism* (2013) 18(3):333-40. doi: 10.1016/j.cmet.2013.08.005.

114. Huang J, Ishino T, Chen G, Rolzin P, Osothprarop TF, Retting K, et al. Development of a Novel Long-Acting Antidiabetic Fgf21 Mimetic by Targeted Conjugation to a Scaffold Antibody. *Journal of Pharmacology and Experimental Therapeutics* (2013) 346(2):270-80. doi: 10.1124/jpet.113.204420.

115. Weng Y, Chabot JR, Bernardo B, Yan Q, Zhu Y, Brenner MB, et al. Pharmacokinetics (Pk), Pharmacodynamics (Pd) and Integrated Pk/Pd Modeling of a Novel Long Acting Fgf21 Clinical Candidate Pf-05231023 in Diet-Induced Obese and Leptin-Deficient Obese Mice. *PLOS ONE* (2015) 10(3):e0119104. doi: 10.1371/journal.pone.0119104.

116. Talukdar S, Zhou Y, Li D, Rossulek M, Dong J, Somayaji V, et al. A Long-Acting Fgf21 Molecule, Pf-05231023, Decreases Body Weight and Improves Lipid Profile in Non-Human Primates and Type 2 Diabetic Subjects. *Cell Metabolism* (2016) 23(3):427-40. doi: 10.1016/j.cmet.2016.02.001.

117. Wei W, Dutchak PA, Wang X, Ding X, Wang X, Bookout AL, et al. Fibroblast Growth Factor 21 Promotes Bone Loss by Potentiating the Effects of Peroxisome Proliferator-Activated Receptor Γ. *Proceedings of the National Academy of Sciences* (2012) 109(8):3143-8. doi: 10.1073/pnas.1200797109.

118. Charoenphandhu N, Suntornsaratoon P, Krishnamra N, Sa-Nguanmoo P, Tanajak P, Wang X, et al. Fibroblast Growth Factor-21 Restores Insulin Sensitivity but Induces Aberrant Bone Microstructure in Obese Insulin-Resistant Rats. *Journal of Bone and Mineral Metabolism* (2017) 35(2):142-9. doi: 10.1007/s00774-016-0745-z.

119. Li X, Stanislaus S, Asuncion F, Niu Q-T, Chinookoswong N, Villasenor K, et al. Fgf21 Is Not a Major Mediator for Bone Homeostasis or Metabolic Actions of Pparα and Pparγ Agonists. *Journal of Bone and Mineral Research* (2017) 32(4):834-45. doi: 10.1002/jbmr.2936.

120. Jimenez V, Jambrina C, Casana E, Sacristan V, Muñoz S, Darriba S, et al. Fgf21 Gene Therapy as Treatment for Obesity and Insulin Resistance. *EMBO Molecular Medicine* (2018) 10(8):e8791. doi: 10.15252/emmm.201708791.

121. Charles ED, Neuschwander-Tetri BA, Pablo Frias J, Kundu S, Luo Y, Tirucherai GS, et al. Pegbelfermin (Bms-986036), Pegylated Fgf21, in Patients with Obesity and Type 2 Diabetes: Results from a Randomized Phase 2 Study. *Obesity* (2019) 27(1):41-9. doi: 10.1002/oby.22344.

122. Thompson KE, Guillot M, Graziano MJ, Mangipudy RS, Chadwick KD. Pegbelfermin, a Pegylated Fgf21 Analogue, Has Pharmacology without Bone Toxicity after 1-Year Dosing in Skeletally-Mature Monkeys. *Toxicology and Applied Pharmacology* (2021) 428:115673. doi: https://doi.org/10.1016/j.taap.2021.115673.

123. Sanyal A, Charles ED, Neuschwander-Tetri BA, Loomba R, Harrison SA, Abdelmalek MF, et al. Pegbelfermin (Bms-986036), a Pegylated Fibroblast Growth Factor 21 Analogue, in Patients with Non-Alcoholic Steatohepatitis: A Randomised, Double-Blind, Placebo-Controlled, Phase 2a Trial. *The Lancet* (2018) 392(10165):2705-17. doi: https://doi.org/10.1016/S0140-6736(18)31785-9.

124. Dong JQ, Rossulek M, Somayaji VR, Baltrukonis D, Liang Y, Hudson K, et al. Pharmacokinetics and Pharmacodynamics of Pf-05231023, a Novel Long-Acting Fgf21 Mimetic, in a First-in-Human Study. *British Journal of Clinical Pharmacology* (2015) 80(5):1051-63. doi: 10.1111/bcp.12676.

125. Stanislaus S, Hecht R, Yie J, Hager T, Hall M, Spahr C, et al. A Novel Fc-Fgf21 with Improved Resistance to Proteolysis, Increased Affinity toward B-Klotho, and Enhanced Efficacy in Mice and Cynomolgus Monkeys. *Endocrinology* (2017) 158(5):1314-27. doi: 10.1210/en.2016-1917.

126. Kaufman A, Abuqayyas L, Denney WS, Tillman EJ, Rolph T. Akr-001, an Fc-Fgf21 Analog, Showed Sustained Pharmacodynamic Effects on Insulin Sensitivity and Lipid Metabolism in Type 2 Diabetes Patients. *Cell Reports Medicine* (2020) 1(4):100057. doi: 10.1016/j.xcrm.2020.100057.

127. Chandler M, Cunningham S, Lund EM, Khanna C, Naramore R, Patel A, et al. *Obesity and Associated Comorbidities in People and Companion Animals: A One Health Perspective*. Journal of Comparative Pathology: Elsevier Ltd (2017). p. 296-309.doi: 10.1016/j.jcpa.2017.03.006.

128. Bobe G, Young JW, Beitz DC. Invited Review: Pathology, Etiology, Prevention, and Treatment of Fatty Liver in Dairy Cows*. *Journal of Dairy Science* (2004) 87(10):3105-24. doi: https://doi.org/10.3168/jds.S0022-0302(04)73446-3.

129. Kuzi S, Segev G, Kedar S, Yas E, Aroch I. Prognostic Markers in Feline Hepatic Lipidosis: A Retrospective Study of 71 Cats. *Veterinary Record* (2017) 181(19):512-. doi: 10.1136/vr.104252.

130. Xu P, Zhang Y, Jiang X, Li J, Song L, Khoso MH, et al. Canine Fibroblast Growth Factor 21 Ameliorates Hyperglycemia Associated with Inhibiting Hepatic Gluconeogenesis and Improving Pancreatic Beta-Cell Survival in Diabetic Mice and Dogs. *PLOS ONE* (2016) 11(5):e0155598. doi: 10.1371/journal.pone.0155598.

131. Jiang X, Liu S, Wang Y, Zhang R, Opoku YK, Xie Y, et al. Fibroblast Growth Factor 21: A Novel Long-Acting Hypoglycemic Drug for Canine Diabetes. *Naunyn-Schmiedeberg's Archives of Pharmacology* (2021) 394(5):1031-43. doi: 10.1007/s00210-020-02023-9.

132. Seita M, Noguchi H, Kubota Y, Kawamoto H, Nakaji S, Kobayashi N, et al. Development of Canine Models of Type 1 Diabetes with Partial Pancreatectomy and the Administration of Streptozotocin. *Cell Medicine* (2013) 6(1-2):25-31. doi: 10.3727/215517913x674289.

133. Araujo J, Paradis A, Mendes J, Petrik S, de Rivera C. Induction of Type I Diabetes Mellitus in Beagle Dogs Using Alloxan and Streptozotocin. *Current Protocols* (2022) 2(11):e580. doi: https://doi.org/10.1002/cpz1.580.

134. Caixeta LS, Giesy SL, Krumm CS, Perfield JW, Butterfield A, Schoenberg KM, et al. Effect of Circulating Glucagon and Free Fatty Acids on Hepatic Fgf21 Production in Dairy Cows. *American Journal of Physiology-Regulatory, Integrative and Comparative Physiology* (2017) 313(5):R526-R34. doi: 10.1152/ajpregu.00197.2017.

135. Schoenberg KM, Giesy SL, Harvatine KJ, Waldron MR, Cheng C, Kharitonenkov A, et al. Plasma Fgf21 Is Elevated by the Intense Lipid Mobilization of Lactation. *Endocrinology* (2011) 152(12):4652-61. doi: 10.1210/en.2011-1425.

136. Krumm CS, Giesy SL, Caixeta LS, Perfield JW, Sauerwein H, Moore BL, et al. Fibroblast Growth Factor-21 (Fgf21) Administration to Early-Lactating Dairy Cows. I. Effects

on Signaling and Indices of Insulin Action. *Journal of Dairy Science* (2019) 102(12):11586-96. doi: 10.3168/jds.2019-16695.

137. Lamb CL, Giesy SL, McGuckin MM, 2nd JWP, Butterfield A, Moniruzzaman M, et al. Fibroblast Growth Factor-21 Improves Insulin Action in Nonlactating Ewes. *American Journal of Physiology-Regulatory, Integrative and Comparative Physiology* (2022) 322(3):R170-R80. doi: 10.1152/ajpregu.00259.2021.

138. Allan FJ, Pfeiffer DU, Jones BR, Esslemont DHB, Wiseman MS. *A Cross-Sectional Study of Risk Factors for Obesity in Cats in New Zealand*. Preventive Veterinary Medicine(2000). p. 183-96.doi: 10.1016/S0167-5877(00)00147-1.

139. Gates M, Zito S, Harvey L, Dale A, Walker J. *Assessing Obesity in Adult Dogs and Cats Presenting for Routine Vaccination Appointments in the North Island of New Zealand Using Electronic Medical Records Data*. New Zealand Veterinary Journal: Taylor & Francis (2019). p. 126-33.doi: 10.1080/00480169.2019.1585990.

140. Clark MH, Larsen R, Lu W, Hoenig M. *Investigation of 1h Mrs for Quantification of Hepatic Triglyceride in Lean and Obese Cats*. Research in Veterinary Science(2013). p. 678-80.doi: 10.1016/j.rvsc.2013.04.004.

141. Nicoll RG, O'Brien RT, Jackson MW. *Qualitative Ultrasonography of the Liver in Obese Cats*. Veterinary Radiology and Ultrasound(1998). p. 47-50.doi: 10.1111/j.1740-8261.1998.tb00324.x.

142. Ogawa Y, Kurosu H, Yamamoto M, Nandi A, Rosenblatt KP, Goetz R, et al. *Betaklotho Is Required for Metabolic Activity of Fibroblast Growth Factor 21*. Proceedings of the National Academy of Sciences(2007). p. 7432-7.doi: 10.1073/pnas.0701600104.

143. Salgado JV, Goes MA, Salgado Filho N. Fgf21 and Chronic Kidney Disease. *Metabolism* (2021) 118:154738. doi: 10.1016/j.metabol.2021.154738.

144. Lee JH, Kang YE, Chang JY, Park KC, Kim HW, Kim JT, et al. An Engineered Fgf21 Variant, Ly2405319, Can Prevent Non-Alcoholic Steatohepatitis by Enhancing Hepatic Mitochondrial Function. *American Journal of Translational Research* (2016) 8(11):4750-63. Epub 20161115.

145. Ma X, Brinker E, Graff EC, Cao W, Gross AL, Johnson AK, et al. *Whole-Genome Shotgun Metagenomic Sequencing Reveals Distinct Gut Microbiome Signatures of Obese Cats*. In: Cheng D, editor. Microbiology Spectrum: American Society for Microbiology (2022).doi: 10.1128/spectrum.00837-22.

146. Maifeld A, Bartolomaeus H, Löber U, Avery EG, Steckhan N, Markó L, et al. *Fasting Alters the Gut Microbiome Reducing Blood Pressure and Body Weight in Metabolic Syndrome Patients*. Nature Communications(2021). p. 1970.doi: 10.1038/s41467-021-22097-0.

147. Martin A, Ecklu-Mensah G, Ha CWY, Hendrick G, Layman DK, Gilbert J, et al. *Gut Microbiota Mediate the Fgf21 Adaptive Stress Response to Chronic Dietary Protein-Restriction in Mice*. Nature Communications: Springer US (2021). p. 3838.doi: 10.1038/s41467-021-24074-z.

148. Luo Y, Decato BE, Charles ED, Shevell DE, McNaney C, Shipkova P, et al. *Pegbelfermin Selectively Reduces Secondary Bile Acid Concentrations in Patients with Non-Alcoholic Steatohepatitis*. JHEP Reports: The Author(s) (2022). p. 100392.doi: 10.1016/j.jhepr.2021.100392.

149. Lee DH. Imaging Evaluation of Non-Alcoholic Fatty Liver Disease: Focused on Quantification. *Clinical and Molecular Hepatology* (2017) 23(4):290-301. doi: 10.3350/cmh.2017.0042.

150. Hamilton G, Yokoo T, Bydder M, Cruite I, Schroeder ME, Sirlin CB, et al. In Vivo Characterization of the Liver Fat (1)H Mr Spectrum. *NMR Biomed* (2011) 24(7):784-90. Epub 20101212. doi: 10.1002/nbm.1622.

151. Szczepaniak LS, Nurenberg P, Leonard D, Browning JD, Reingold JS, Grundy S, et al. *Magnetic Resonance Spectroscopy to Measure Hepatic Triglyceride Content: Prevalence of Hepatic Steatosis in the General Population*. American Journal of Physiology-Endocrinology and Metabolism(2005). p. E462-E8.doi: 10.1152/ajpendo.00064.2004.

152. Heger M, Marsman HA, Bezemer R, Cloos MA, van Golen RF, van Gulik TM. *Non-Invasive Quantification of Triglyceride Content in Steatotic Rat Livers by 1h-Mrs*. Academic Radiology(2011). p. 1582-92.doi: 10.1016/j.acra.2011.08.014.

153. Szczepaniak LS, Babcock EE, Schick F, Dobbins RL, Garg A, Burns DK, et al. *Measurement of Intracellular Triglyceride Stores by H Spectroscopy: Validation in Vivo*. American Journal of Physiology-Endocrinology and Metabolism(1999). p. E977-E89.doi: 10.1152/ajpendo.1999.276.5.E977.

154. Deffieux T, Gennisson J-L, Bousquet L, Corouge M, Cosconea S, Amroun D, et al. Investigating Liver Stiffness and Viscosity for Fibrosis, Steatosis and Activity Staging Using Shear Wave Elastography. *Journal of Hepatology* (2015) 62(2):317-24. doi: https://doi.org/10.1016/j.jhep.2014.09.020.

155. Silva LDCMD, Oliveira JTD, Tochetto S, Oliveira CPMSD, Sigrist R, Chammas MC. Ultrasound Elastography in Patients with Fatty Liver Disease. *Radiologia Brasileira* (2020) 53(1):47-55. doi: 10.1590/0100-3984.2019.0028.

156. Park S, Choi J, Kim K, Oh D, Yoon J, Choi M. Point Shear Wave Elastography of the Liver in Healthy Adult Cats. *American Journal of Veterinary Research* (2021) 82(4):286-91. doi: 10.2460/ajvr.82.4.286.

157. Bain PJ. *Liver*. In: Latimer KS, editor. Duncan and Prasse's Veterinary Laboratory Medicine. West Sussex: John Wiley & Sons, Inc. (2011). p. 211 - 30.

158. Zini E, Moretti S, Tschuor F, Reusch CE. Evaluation of a New Portable Glucose Meter Designed for the Use in Cats. *Schweizer Archiv fur Tierheilkunde* (2009) 151:448-51. doi: 10.1024/0036-7281.151.9.448.

159. Strage EM, Holst BS, Nilsson G, Jones B, Lilliehöök I. *Validation of an Enzyme-Linked Immunosorbent Assay for Measurement of Feline Serum Insulin*. Veterinary Clinical Pathology(2012). p. 518-28.doi: 10.1111/j.1939-165x.2012.00476.x.

160. Appleton DJ, Rand JS, Sunvold GD. *Basal Plasma Insulin and Homeostasis Model Assessment (Homa) Are Indicators of Insulin Sensitivity in Cats*. Journal of Feline Medicine and Surgery(2005). p. 183-93.doi: 10.1016/j.jfms.2004.12.002.

161. Strage EM, Ley CJ, Forkman J, Öhlund M, Stadig S, Bergh A, et al. *Homeostasis Model Assessment, Serum Insulin and Their Relation to Body Fat in Cats*. BMC Veterinary Research: BMC Veterinary Research (2021). p. 1-10.doi: 10.1186/s12917-020-02729-1.

162. Ter Horst KW, Van Galen KA, Gilijamse PW, Hartstra AV, De Groot PF, Van Der Valk FM, et al. Methods for Quantifying Adipose Tissue Insulin Resistance in Overweight/Obese Humans. *International Journal of Obesity* (2017) 41(8):1288-94. doi: 10.1038/ijo.2017.110.

163. Ma X, Brinker E, Cao W, Graff EC, Wang X. Effect of Mineral Oil as a Lubricant to Collect Feces from Cats for Microbiome Studies. *Journal of Veterinary Internal Medicine* (2022) 36(6):1974-80. doi: 10.1111/jvim.16556.

164. Li H. *Aligning Sequence Reads, Clone Sequences and Assembly Contigs with Bwa-Mem*. (2013). p. 1-3.doi: 10.48550/arXiv.1303.399.

165. Li H, Handsaker B, Wysoker A, Fennell T, Ruan J, Homer N, et al. *The Sequence Alignment/Map Format and Samtools*. Bioinformatics(2009). p. 2078-9.doi: 10.1093/bioinformatics/btp352.

166. Dixon P. *Vegan, a Package of R Functions for Community Ecology*. Journal of Vegetation Science(2003). p. 927-30.doi: 10.1111/j.1654-1103.2003.tb02228.x.

167. McKnight PE, Najab J. *Mann-Whitney U Test*. The Corsini Encyclopedia of Psychology. Hoboken, NJ, USA: John Wiley & Sons, Inc. (2010).doi: 10.1002/9780470479216.corpsy0524.

168. Anderson MJ. *Permutational Multivariate Analysis of Variance.* Department of Statistics, University of Auckland, Auckland(2005). p. 32-46.

169. McKight PE, Najab J. *Kruskal-Wallis Test*. The Corsini Encyclopedia of Psychology. Hoboken, NJ, USA: John Wiley & Sons, Inc. (2010).doi: 10.1002/9780470479216.corpsy0491.

170. JD S, AJ B, A D, D R. *Qvalue: Q-Value Estimation for False Discovery Rate Control*. R package version 2300(2022).

171. Naressi A, Couturier C, Devos JM, Janssen M, Mangeat C, Beer Rd, et al. *Java-Based Graphical User Interface for the Mrui Quantitation Package*. Magma: Magnetic Resonance Materials in Physics, Biology, and Medicine(2001). p. 141-52.doi: 10.1007/BF02668096.

172. Vanhamme L, Van Den Boogaart A, Van Huffel S. *Improved Method for Accurate and Efficient Quantification of Mrs Data with Use of Prior Knowledge*. Journal of Magnetic Resonance(1997). p. 35-43.doi: 10.1006/jmre.1997.1244.

173. Longo R, Pollesello P, Ricci C, Masutti F, Kvam BJ, Bercich L, et al. *Proton Mr Spectroscopy in Quantitative in Vivo Determination of Fat Content in Human Liver Steatosis*. Journal of Magnetic Resonance Imaging(1995). p. 281-5.doi: 10.1002/jmri.1880050311.

174. Suda T, Kanefuji T, Abe A, Nagayama I, Hoshi T, Morita S, et al. *A Cut-Off Value of Shear Wave Speed to Distinguish Nonalcoholic Steatohepatitis Candidates*. Medicine(2019). p. e13958.doi: 10.1097/MD.0000000000013958.

175. Thanaboonnipat C, Sutayatram S, Buranakarl C, Choisunirachon N. *Renal Shear Wave Elastography and Urinary Procollagen Type Iii Amino-Terminal Propeptide (Upiiinp) in Feline Chronic Kidney Disease*. BMC Veterinary Research: BMC Veterinary Research (2019). p. 54.doi: 10.1186/s12917-019-1801-4.

176. Cui A, Li J, Ji S, Ma F, Wang G, Xue Y, et al. *The Effects of B1344, a Novel Fibroblast Growth Factor 21 Analog, on Nonalcoholic Steatohepatitis in Nonhuman Primates*. Diabetes(2020). p. 1611-23.doi: 10.2337/db20-0209.

177. Thompson WC, Zhou Y, Talukdar S, Musante CJ. *Pf-05231023, a Long-Acting Fgf21 Analogue, Decreases Body Weight by Reduction of Food Intake in Non-Human Primates*. Journal of Pharmacokinetics and Pharmacodynamics: Springer US (2016). p. 411-25.doi: 10.1007/s10928-016-9481-1.

178. Andersen B, Straarup EM, Heppner KM, Takahashi DL, Raffaele V, Dissen GA, et al. *Fgf21 Decreases Body Weight without Reducing Food Intake or Bone Mineral Density in High-*

*Fat Fed Obese Rhesus Macaque Monkeys*. International Journal of Obesity: Springer US (2018). p. 1151-60.doi: 10.1038/s41366-018-0080-7.

179. Coskun T, Bina HA, Schneider MA, Dunbar JD, Hu CC, Chen Y, et al. *Fibroblast Growth Factor 21 Corrects Obesity in Mice*. Endocrinology(2008). p. 6018-27.doi: 10.1210/en.2008-0816.

180. Véniant MM, Komorowski R, Chen P, Stanislaus S, Winters K, Hager T, et al. *Long-Acting Fgf21 Has Enhanced Efficacy in Diet-Induced Obese Mice and in Obese Rhesus Monkeys*. Endocrinology(2012). p. 4192-203.doi: 10.1210/en.2012-1211.

181. Søndergaard E, Espinosa De Ycaza AE, Morgan-Bathke M, Jensen MD. How to Measure Adipose Tissue Insulin Sensitivity. *The Journal of Clinical Endocrinology & Metabolism* (2017) 102(4):1193-9. doi: 10.1210/jc.2017-00047.

182. Lewis JE, Samms RJ, Cooper S, Luckett JC, Perkins AC, Adams AC, et al. *Reduced Adiposity Attenuates Fgf21 Mediated Metabolic Improvements in the Siberian Hamster*. Scientific Reports(2017). p. 4238.doi: 10.1038/s41598-017-03607-x.

183. Camporez JPG, Jornayvaz FR, Petersen MC, Pesta D, Guigni BA, Serr J, et al. *Cellular Mechanisms by Which Fgf21 Improves Insulin Sensitivity in Male Mice*. Endocrinology(2013). p. 3099-109.doi: 10.1210/en.2013-1191.

184. Fisher FM, Maratos-Flier E. Understanding the Physiology of Fgf21. *Annual Review of Physiology* (2016) 78(1):223-41. doi: 10.1146/annurev-physiol-021115-105339.

185. Queen NJ, Bates R, Huang W, Xiao R, Appana B, Cao L. Visceral Adipose Tissue-Directed Fgf21 Gene Therapy Improves Metabolic and Immune Health in Btbr Mice. *Molecular Therapy - Methods & Clinical Development* (2021) 20:409-22. doi: https://doi.org/10.1016/j.omtm.2020.12.011.

186. BonDurant LD, Ameka M, Naber MC, Markan KR, Idiga SO, Acevedo MR, et al. *Fgf21 Regulates Metabolism through Adipose-Dependent and -Independent Mechanisms*. Cell Metabolism: Elsevier Inc. (2017). p. 935-44.e4.doi: 10.1016/j.cmet.2017.03.005.

187. Szczepańska E, Gietka-Czernel M. Fgf21: A Novel Regulator of Glucose and Lipid Metabolism and Whole-Body Energy Balance. *Hormone and Metabolic Research* (2022) 54(04):203-11. doi: 10.1055/a-1778-4159.

188. Van De Velde H, Janssens GPJ, De Rooster H, Polis I, Peters I, Ducatelle R, et al. The Cat as a Model for Human Obesity: Insights into Depot-Specific Inflammation Associated with Feline Obesity. *British Journal of Nutrition* (2013) 110(7):1326-35. doi: 10.1017/s0007114513000226.

189. Okada Y, Kobayashi M, Sawamura M, Arai T. Comparison of Visceral Fat Accumulation and Metabolome Markers among Cats of Varying Bcs and Novel Classification of Feline Obesity and Metabolic Syndrome. *Frontiers in Veterinary Science* (2017) 4. doi: 10.3389/fvets.2017.00017.

190. Fettman MJ, Stanton CA, Banks LL, Hamar DW, Johnson DE, Hegstad RL, et al. Effects of Neutering on Bodyweight, Metabolic Rate and Glucose Tolerance of Domestic Cats. *Research in Veterinary Science* (1997) 62(2):131-6. doi: https://doi.org/10.1016/S0034-5288(97)90134-X.

191. Abbott RD, Borowsky FE, Quinn KP, Bernstein DL, Georgakoudi I, Kaplan DL. Non-Invasive Assessments of Adipose Tissue Metabolism in Vitro. *Annals of Biomedical Engineering* (2016) 44(3):725-32. doi: 10.1007/s10439-015-1438-9.

192. Nagarajan SR, Paul-Heng M, Krycer JR, Fazakerley DJ, Sharland AF, Hoy AJ. Lipid and Glucose Metabolism in Hepatocyte Cell Lines and Primary Mouse Hepatocytes: A Comprehensive Resource for in Vitro Studies of Hepatic Metabolism. *American Journal of*

*Physiology-Endocrinology and Metabolism* (2019) 316(4):E578-E89. doi: 10.1152/ajpendo.00365.2018.

193. Stockholm SL, Scott MA. *Fundamentals of Veterinary Clinical Pathology*. 2nd ed. Ames, Iowa, USA: Blackwell Publishing (2008).

194. Wong VW-S, Wong GL-H, Tse C-H, Chan HL-Y. *Prevalence of the Tm6sf2 Variant and Non-Alcoholic Fatty Liver Disease in Chinese*. Journal of Hepatology: European Association for the Study of the Liver (2014). p. 708-9.doi: 10.1016/j.jhep.2014.04.047.

195. Kleinert M, Müller TD. *A New Fgf21 Analog for the Treatment of Fatty Liver Disease*. Diabetes(2020). p. 1605-7.doi: 10.2337/dbi20-0025.

196. Van Werven JR, Marsman HA, Nederveen AJ, ten Kate FJ, van Gulik TM, Stoker J. *Hepatic Lipid Composition Analysis Using 3.0-T Mr Spectroscopy in a Steatotic Rat Model*. Magnetic Resonance Imaging: Elsevier Inc. (2012). p. 112-21.doi: 10.1016/j.mri.2011.07.028.

197. Hernandez G, Luo T, Javed TA, Wen L, Kalwat MA, Vale K, et al. Pancreatitis Is an Fgf21-Deficient State That Is Corrected by Replacement Therapy. *Science Translational Medicine* (2020) 12(525):eaay5186. doi: doi:10.1126/scitranslmed.aay5186.

198. Johnson CL, Weston JY, Chadi SA, Fazio EN, Huff MW, Kharitonenkov A, et al. Fibroblast Growth Factor 21 Reduces the Severity of Cerulein-Induced Pancreatitis in Mice. *Gastroenterology* (2009) 137(5):1795-804. doi: 10.1053/j.gastro.2009.07.064.

199. Akol KG, Washabau RJ, Saunders HM, Hendrick MJ. Acute Pancreatitis in Cats with Hepatic Lipidosis. *Journal of Veterinary Internal Medicine* (1993) 7(4):205-9. doi: 10.1111/j.1939-1676.1993.tb01008.x.

200. Swift NC, Marks SL, Maclachlan NJ, Norris CR. Evaluation of Serum Feline Trypsin-Like Immunoreactivity for the Diagnosis of Pancreatitis in Cats. *Journal of the American Veterinary Medical Association* (2000) 217(1):37-42. doi: 10.2460/javma.2000.217.37.

201. Hall RL, Bender HS. *Muscle*. In: Latimer KS, editor. Duncan and Prasse's Veterinary Laboratory Medicine. Fifth ed. West Sussex: Wiley-Blackwell (2011). p. 283 - 94.

202. Keipert S, Ost M, Johann K, Imber F, Jastroch M, van Schothorst EM, et al. *Skeletal Muscle Mitochondrial Uncoupling Drives Endocrine Cross-Talk through the Induction of Fgf21 as a Myokine*. American Journal of Physiology-Endocrinology and Metabolism(2014). p. E469-E82.doi: 10.1152/ajpendo.00330.2013.

203. Kim K, Lee J, So J, Jang Y-s, Jung M, Kang K, et al. Feasibility and Reliability of Two-Dimensional Shear-Wave Elastography of the Liver of Clinically Healthy Cats. *Frontiers in Veterinary Science* (2020) 7. doi: 10.3389/fvets.2020.614750.

204. Castera L, Friedrich-Rust M, Loomba R. Noninvasive Assessment of Liver Disease in Patients with Nonalcoholic Fatty Liver Disease. *Gastroenterology* (2019) 156(5):1264-81.e4. doi: 10.1053/j.gastro.2018.12.036.

205. van den Ingh TSGAM, Cullen JM, Twedt DC, Van Winkle T, Desmet VJ, Rothuizen J. Morphological Classification of Biliary Disorders of the Canine and Feline Liver. *Wsava Standards for Clinical and Histological Diagnosis of Canine and Feline Liver Diseases*. Society of Comparative Hepathology (2021).

206. Guerra JM, Daniel AGT, Cardoso NC, Grandi F, Queiroga F, Cogliati B. *Congenital Hepatic Fibrosis and Polycystic Kidney Disease Not Linked to C >a Mutation in Exon 29 of Pkd1 in a Persian Cat*. Journal of Feline Medicine and Surgery Open Reports(2015). p. 205511691561919.doi: 10.1177/2055116915619191.

207. Itoh N. Fgf21 as a Hepatokine, Adipokine, and Myokine in Metabolism and Diseases. *Frontiers in Endocrinology* (2014) 5. doi: 10.3389/fendo.2014.00107.

208. Brinker EJ, Towns TJ, Watanabe R, Ma X, Bashir A, Cole RC, et al. Direct Activation of the Fibroblast Growth Factor-21 Pathway in Overweight and Obese Cats. *Frontiers in Veterinary Science* (2023) 10. doi: 10.3389/fvets.2023.1072680.

209. Spann RA, Morrison CD, den Hartigh LJ. The Nuanced Metabolic Functions of Endogenous Fgf21 Depend on the Nature of the Stimulus, Tissue Source, and Experimental Model. *Frontiers in Endocrinology* (2022) 12. doi: 10.3389/fendo.2021.802541.

210. Kliewer SA, Mangelsdorf DJ. A Dozen Years of Discovery: Insights into the Physiology and Pharmacology of Fgf21. *Cell Metabolism* (2019) 29(2):246-53. doi: 10.1016/j.cmet.2019.01.004.

211. Hotta Y, Nakamura H, Konishi M, Murata Y, Takagi H, Matsumura S, et al. Fibroblast Growth Factor 21 Regulates Lipolysis in White Adipose Tissue but Is Not Required for Ketogenesis and Triglyceride Clearance in Liver. *Endocrinology* (2009) 150(10):4625-33. doi: 10.1210/en.2009-0119.

212. Yano K, Yamaguchi K, Seko Y, Okishio S, Ishiba H, Tochiki N, et al. Hepatocyte-Specific Fibroblast Growth Factor 21 Overexpression Ameliorates High-Fat Diet-Induced Obesity and Liver Steatosis in Mice. *Laboratory Investigation* (2022) 102(3):281-9. doi: https://doi.org/10.1038/s41374-021-00680-9.

213. Bazelle J, Watson P. Is It Being Overdiagnosed? Feline Pancreatitis. *Veterinary Clinics of North America: Small Animal Practice* (2020) 50(5):1107-21. doi: 10.1016/j.cvsm.2020.06.006.

214. De Cock HEV, Forman MA, Farver TB, Marks SL. Prevalence and Histopathologic Characteristics of Pancreatitis in Cats. *Veterinary Pathology* (2007) 44(1):39-49. doi: 10.1354/vp.44-1-39.

215. Forman MA, Steiner JM, Armstrong PJ, Camus MS, Gaschen L, Hill SL, et al. Acvim Consensus Statement on Pancreatitis in Cats. *Journal of Veterinary Internal Medicine* (2021) 35(2):703-23. doi: 10.1111/jvim.16053.

216. Ye J, Coulouris G, Zaretskaya I, Cutcutache I, Rozen S, Madden TL. Primer-Blast: A Tool to Design Target-Specific Primers for Polymerase Chain Reaction. *BMC Bioinformatics* (2012) 13(1):134. doi: 10.1186/1471-2105-13-134.

217. Pfaffl MW. A New Mathematical Model for Relative Quantification in Real-Time Rt–Pcr. *Nucleic Acids Research* (2001) 29(9):e45-e. doi: 10.1093/nar/29.9.e45.

218. Sayers EW, Bolton EE, Brister JR, Canese K, Chan J, Comeau Donald C, et al. Database Resources of the National Center for Biotechnology Information. *Nucleic Acids Research* (2021) 50(D1):D20-D6. doi: 10.1093/nar/gkab1112.

219. Shrader S, Lai S, Cline K, Moon R. Gliomatosis Cerebri in the Brain of a Cat. *Veterinary Sciences* (2016) 3(3):13.

220. Graff EC, Cochran JN, Kaelin CB, Day K, Gray-Edwards HL, Watanabe R, et al. Pea15 Loss of Function and Defective Cerebral Development in the Domestic Cat. *PLOS Genetics* (2020) 16(12):e1008671. doi: 10.1371/journal.pgen.1008671.

221. Cullen JM, Stalker MJ. Chapter 2 - Liver and Biliary System. In: Maxie MG, editor. *Jubb, Kennedy & Palmer's Pathology of Domestic Animals: Volume 2 (Sixth Edition)*. W.B. Saunders (2016). p. 258-352.e1.

222. Prayson RA. *Neurpathology Review*. Totowa, NJ: Humana Press (2008). 252 p.

223. Nygaard EB, Møller CL, Kievit P, Grove KL, Andersen B. Increased Fibroblast Growth Factor 21 Expression in High-Fat Diet-Sensitive Non-Human Primates (Macaca Mulatta). *International Journal of Obesity* (2014) 38(2):183-91. doi: 10.1038/ijo.2013.79.

224. Lundåsen T, Hunt MC, Nilsson L-M, Sanyal S, Angelin B, Alexson SEH, et al. Pparα Is a Key Regulator of Hepatic Fgf21. *Biochemical and Biophysical Research Communications* (2007) 360(2):437-40. doi: https://doi.org/10.1016/j.bbrc.2007.06.068.

225. Fisher fM, Estall JL, Adams AC, Antonellis PJ, Bina HA, Flier JS, et al. Integrated Regulation of Hepatic Metabolism by Fibroblast Growth Factor 21 (Fgf21) in Vivo. *Endocrinology* (2011) 152(8):2996-3004. doi: 10.1210/en.2011-0281.

226. Kharitonenkov A, Wroblewski VJ, Koester A, Chen Y-F, Clutinger CK, Tigno XT, et al. The Metabolic State of Diabetic Monkeys Is Regulated by Fibroblast Growth Factor-21. *Endocrinology* (2007) 148(2):774-81. doi: 10.1210/en.2006-1168.

227. Kuroda M, Muramatsu R, Maedera N, Koyama Y, Hamaguchi M, Fujimura H, et al. Peripherally Derived Fgf21 Promotes Remyelination in the Central Nervous System. *Journal of Clinical Investigation* (2017) 127(9):3496-509. doi: 10.1172/jci94337.

228. Pan Y, Wang B, Zheng J, Xiong R, Fan Z, Ye Y, et al. Pancreatic Fibroblast Growth Factor 21 Protects against Type 2 Diabetes in Mice by Promoting Insulin Expression and Secretion in a Pi3k/Akt Signaling-Dependent Manner. *Journal of Cellular and Molecular Medicine* (2019) 23(2):1059-71. doi: 10.1111/jcmm.14007.

229. Wente W, Efanov AM, Brenner M, Kharitonenkov A, Köster A, Sandusky GE, et al. *Fibroblast Growth Factor-21 Improves Pancreatic B-Cell Function and Survival by Activation of Extracellular Signal–Regulated Kinase 1/2 and Akt Signaling Pathways*. Diabetes(2006). p. 2470-8.doi: 10.2337/db05-1435.

230. Zini E, Lunardi F, Zanetti R, Heller RS, Coppola LM, Ferro S, et al. Endocrine Pancreas in Cats with Diabetes Mellitus. *Veterinary Pathology* (2016) 53(1):136-44. doi: 10.1177/0300985815591078.

231. Pierezan F, Mansell J, Ambrus A, Hoffmann AR. Immunohistochemical Expression of Ionized Calcium Binding Adapter Molecule 1 in Cutaneous Histiocytic Proliferative, Neoplastic and Inflammatory Disorders of Dogs and Cats. *Journal of Comparative Pathology* (2014) 151(4):347-51. doi: https://doi.org/10.1016/j.jcpa.2014.07.003.

232. Kang K, Xia A, Meng F, Chunyu J, Sun X, Ren G, et al. Fgf21 Alleviates Chronic Inflammatory Injury in the Aging Process through Modulating Polarization of Macrophages. *International Immunopharmacology* (2021) 96:107634. doi: https://doi.org/10.1016/j.intimp.2021.107634.

233. Yu Y, He J, Li S, Song L, Guo X, Yao W, et al. Fibroblast Growth Factor 21 (Fgf21) Inhibits Macrophage-Mediated Inflammation by Activating Nrf2 and Suppressing the Nf-Kb Signaling Pathway. *International Immunopharmacology* (2016) 38:144-52. doi: https://doi.org/10.1016/j.intimp.2016.05.026.

234. Hu F, Lou N, Jiao J, Guo F, Xiang H, Shang D. Macrophages in Pancreatitis: Mechanisms and Therapeutic Potential. *Biomedicine & Pharmacotherapy* (2020) 131:110693. doi: https://doi.org/10.1016/j.biopha.2020.110693.

235. Xue J, Sharma V, Hsieh MH, Chawla A, Murali R, Pandol SJ, et al. Alternatively Activated Macrophages Promote Pancreatic Fibrosis in Chronic Pancreatitis. *Nature Communications* (2015) 6(1):7158. doi: 10.1038/ncomms8158.

236. Pérez S, Rius-Pérez S. Macrophage Polarization and Reprogramming in Acute Inflammation: A Redox Perspective. *Antioxidants* (2022) 11(7):1394. doi: 10.3390/antiox11071394.

237. Barros MHM, Hauck F, Dreyer JH, Kempkes B, Niedobitek G. Macrophage Polarisation: An Immunohistochemical Approach for Identifying M1 and M2 Macrophages. *PLOS ONE* (2013) 8(11):e80908. doi: 10.1371/journal.pone.0080908.

238. Ornitz DM, Itoh N. The Fibroblast Growth Factor Signaling Pathway. *WIREs Developmental Biology* (2015) 4(3):215-66. doi: https://doi.org/10.1002/wdev.176.

239. Itoh N, Ohta H, Konishi M. Endocrine Fgfs: Evolution, Physiology, Pathophysiology, and Pharmacotherapy. *Frontiers in Endocrinology* (2015) 6. doi: 10.3389/fendo.2015.00154.

240. Geng L, Lam KSL, Xu A. The Therapeutic Potential of Fgf21 in Metabolic Diseases: From Bench to Clinic. *Nature Reviews Endocrinology* (2020) 16(11):654-67. doi: 10.1038/s41574-020-0386-0.

241. Webb CB. Hepatic Lipidosis: Clinical Review Drawn from Collective Effort. *Journal of Feline Medicine and Surgery* (2018) 20(3):217-27. doi: 10.1177/1098612x18758591.

242. Valtolina C, Favier RP. *Feline Hepatic Lipidosis*. Veterinary Clinics of North America: Small Animal Practice: Elsevier Inc (2017). p. 683-702.doi: 10.1016/j.cvsm.2016.11.014.